Reviews in Mineralogy & Geochemistry
Vol. 72 pp. 171-225, 2010

Diffusion of H, C, and O Components in Silicate Melts

Youxue Zhang

Department of Geological Sciences
University of Michigan
Ann Arbor, Michigan 48109-1005, U.S.A.

youxue@umich.edu

Huaiwei Ni

Bayerisches Geoinstitut
University of Bayreuth
D-95440 Bayreuth, Germany

INTRODUCTION

Silicate melts are complicated in structure and composition. Hence, diffusion in a melt (in this chapter, a melt includes both liquid and glass) can be very complicated due to the presence of many components, each of which can be present in different species, as well as various kinds of diffusion, such as self-diffusion, tracer diffusion, interdiffusion, effective binary diffusion and multi-component diffusion. In this chapter, the diffusion of H, C and O components is reviewed. H may be in the form of H_2O molecules (hereafter referred to as H_2O_m), OH groups (hereafter referred to as OH), H_2 molecules (hereafter referred to as H_2), and other species. H_2O_m and OH will be collectively referred to as the H_2O component, or the hydrous component. C may be present as CO_2 molecules (hereafter referred to as $CO_{2,molec}$), CO_3^{2-} groups (hereafter referred to as CO_3^{2-}), and other species (such as CO and CH_4). CO_2 molecules and CO_3^{2-} groups will be collectively referred to as total CO_2 ($CO_{2,total}$) or the CO_2 component. O may be present in the form of network oxygen (such as bridging oxygen, non-bridging oxygen, and free O^{2-}), H_2O_m, OH, $CO_{2,molec}$, CO_3^{2-}, O_2 molecules (hereafter referred to as O_2), etc. H_2O and CO_2 are the major volatile components in melts and their diffusion plays a critical role in bubble growth (e.g., Proussevitch and Sahagian 1998; Gardner et al. 2000; Liu and Zhang 2000; Wang et al. 2009), magma degassing (e.g., Bottinga and Javoy 1990; Navon and Lyakhovsky 1998; Proussevitch and Sahagian 1998), magma fragmentation (Zhang 1999a), volcanic eruptions (e.g., Proussevitch and Sahagian 1996), and welding of erupted volcanic particles (e.g., Sparks et al. 1999). Hence, understanding H_2O and CO_2 diffusion is important in terms of volcanic hazard mitigation and global volatile budgets. Diffusion of H_2O may also play a role during diffusive and convective growth and dissolution of hydrous minerals (e.g., Chen and Zhang 2008, 2009; Zhang 2008). In glass industry, H_2O diffusion is important to glass stability and strength (e.g., Doremus 1973). On the other hand, oxygen is the most abundant element in silicate melts, and its diffusion controls many reactions and transport properties of melts and is related to the melt structure. The diffusion of H_2O, CO_2 and oxygen is assessed together because of the following: (1) The diffusion of these three components is all affected by the presence of multiple species. Hence, the diffusion belongs to the same category of multi-species diffusion. (2) To understand oxygen diffusion, it is often necessary to understand the diffusion of the individual oxygen species including especially H_2O (as well as other oxygen-bearing species such as bridging oxygen, non-bridging oxygen, free O^{2-}, O_2 molecules, OH, CO_2 and CO_3^{2-}). (3) As the major volatile components in silicate melts,

1529-6466/10/0072-0005$10.00 DOI: 10.2138/rmg.2010.72.5

H_2O diffusion and CO_2 diffusion often must be considered together. For completeness of this review, molecular H_2 and O_2 diffusion is also included. Below, we first review H_2O (including OH) and molecular H_2 diffusion, then CO_2, and finally oxygen diffusion (including molecular O_2 diffusion). Other possible species of H, C, and O include CO and CH_4. However, in natural silicate melts, no data are available for the diffusion of these species, and the concentrations of these species are low, meaning that they are unlikely to play a major role in the transport of H, C and O in natural silicate melts.

DIFFUSION OF THE H_2O COMPONENT

A review covering H_2O diffusion was published recently (Zhang et al. 2007). Nonetheless, major progress has been made since then. As will be seen below, syntheses of experimental data to formulate more general models in several silicate melts have been carried out since 2007. Because H_2O speciation is the key in understanding the complicated behavior of H_2O diffusion, we first discuss both the equilibrium and kinetic aspects of H_2O speciation to prepare for the discussion of H_2O diffusion.

H_2O speciation: equilibrium and kinetics

In natural silicate melts, H is present in the oxidized form as the hydrous component. Dissolved H_2O in silicate melts is present in at least two species: one is H_2O_m, and the other is OH (Stolper 1982a,b). Total H_2O content will be referred as H_2O_t. Under highly reducing conditions, there may also be molecular hydrogen (H_2) that may transport the hydrogen component. In natural and experimental melts, the presence of H_2 has not been detected yet. H_2 diffusion will be discussed in a later section.

H_2O_m and OH can interconvert through the following reaction in melts (Stolper 1982a,b):

$$H_2O_m(\text{melt}) + O(\text{melt}) \rightleftharpoons 2OH(\text{melt}) \quad (1)$$

where O means an anhydrous oxygen ion, ionic charge is ignored, and the phase is indicated inside the parentheses. The two hydrous species, H_2O_m and OH, can be detected easily by near-infrared (NIR) spectroscopy (Stolper 1982a; Cherniak et al. 2010, this volume). To convert IR peak heights or areas to H_2O_m and OH concentrations requires independent calibration to determine molar absorptivities. The equilibrium constant of the above reaction can be written as:

$$K = \frac{[OH]_e^2}{[H_2O_m]_e[O]_e} \quad (2)$$

where brackets mean activities approximated by mole fractions, and the subscript "e" means at stable or metastable equilibrium. The mole fractions are calculated as:

$$[H_2O_t] = \frac{\frac{C_w}{18.015}}{\frac{C_w}{18.015} + \frac{(100 - C_w)}{W}} \quad (3)$$

$$[H_2O_m] = \frac{C_1}{C_w}[H_2O_t]$$

$$[OH] = 2([H_2O_t] - [H_2O_m])$$

$$[O] = 1 - [H_2O_m] - [OH]$$

where C_w is wt% of H_2O_t (at 2 wt%, $C_w = 2$), C_1 is wt% of H_2O_m, and W is the molar mass of the dry melt on a single oxygen basis (Stolper 1982a; Zhang 1999b; see Table 1). The composition

Table 1. Chemical composition (wt%) of melts for H_2O diffusion studies.

ID	Composition	SiO_2	TiO_2	Al_2O_3	FeO	MnO	MgO	CaO	Na_2O	K_2O	P_2O_5	*W*	Ref
1	Rhyolite 1	76.59	0.08	12.67	1.00		0.03	0.52	3.98	4.88		32.55	a-c
2	AOQ	76.14		13.53					4.65	5.68		32.60	d
3	Rhyolite 2	77.30	0.10	13.00	0.50		0.1	0.5	3.8	4.7		32.39	e
4	MAC	72.26	0.04	15.83	0.61	0.06	0.02	0.22	4.14	3.66		32.37	f
5	NSL	75.45	0.19	10.05	4.29	0.12	0	0.17	5.27	4.56		33.26	f
6	CBS rhyolite	76.38	0.20	10.32	4.37				5.11	4.66		33.19	g
7	Dacite 1	65.03	0.67	16.63	4.16		1.96	5.10	3.95	2.70		33.84	h-j
8	Dacite 2	67.54	0.77	15.74	4.28	0.12	1.43	4.40	3.58	2.15		33.49	i-k
9	Andesite 1	57.21	0.84	17.50	7.58	0.11	4.27	7.59	3.31	1.60		34.98	j
10	Andesite 2	62.54	0.70	16.74	5.55	0.10	2.97	6.48	3.20	1.69		34.13	k
11	Haploandesite	62.20		20.10	0.03	0.02	2.32	10.11	4.30	0.98	0.02	33.57	l
12	Trachyte	59.90	0.39	18.00	0.89	0.12	3.86	2.92	4.05	8.35	0.21	34.55	m
13	Basalt 1	50.60	1.88	13.90	12.5	0.23	6.56	11.4	2.64	0.17	0.21	36.59	n
14	Basalt 2	46.12	1.50	16.11	10.84	0.20	7.60	13.32	3.56	0.76		37.15	k

The compositions are listed on the anhydrous basis. *W* is weight of the dry melt per mole of oxygen (g/mol) assuming all Fe is ferrous. (Including ferric Fe would lower *W* values slightly.) For simplicity in treatment, small difference in *W* between similar compositions is ignored in literature. For example, for compositions 1-4, $W = 32.49$; for compositions 5 and 6, $W = 33.24$ (Wang et al. 2009 used a slightly different value of 33.14 by considering Fe_2O_3), etc. MAC is a peraluminous rhyolite; NSL and CBS rhyolite are peralkaline rhyolites.

References: a. Shaw (1974), Delaney and Karsten (1982), Karsten et al. (1982), and Zhang et al. (1991a); b. Zhang and Behrens (2000); Behrens et al. (2007); c. Ni and Zhang (2008); d. Nowak and Behrens (1997); e. Okumura and Nakashima (2004); f. Behrens and Zhang (2009); g. Wang et al. (2009); h. Liu et al. (2004b); i. Ni et al. (2009b); j. Behrens et al. (2004); k. Okumura and Nakashima (2006); l. Ni et al. (2009a); m. Freda et al. (2003); n. Zhang and Stolper (1991).

and W for some melts are listed in Table 1. The temperature dependence of K takes the following form (e.g., Zhang et al. 1997a):

$$\ln K = A + B/T \tag{4}$$

where A and B are constants related to the standard state entropy and enthalpy of Reaction (1).

The equilibrium speciation of rhyolite, dacite and andesite melts has been investigated. Before an understanding of equilibrium speciation, it is necessary to understand (i) the kinetics on how long it would take to reach equilibrium (e.g., Zhang et al. 1991a, 1995, 1997b, 2000; Withers et al. 1999; Liu et al. 2004a; Hui et al. 2008), and (ii) the kinetic effect on the species concentrations during cooling (Dingwell and Webb 1990; Zhang 1994) so as to understand whether species concentrations can be preserved upon quench. These have been reviewed in Zhang (1999b), Zhang et al. (2007) and Hui et al. (2008) and only a brief summary is given below. Speciation data include both quench data and *in situ* data. Both the quench data and *in situ* data suffered from problems in the early stages as shown below. The experimental studies of H_2O speciation are probably the most debated experimental topics concerning H_2O in silicate melts, with two major issues (the quench effect on quench experiments, and the temperature dependence of molar absorptivities on *in situ* IR analyses) summarized below.

Quench effect. The equilibrium speciation data obtained by the quench technique before 1990 (e.g., Silver and Stolper 1989; Stolper 1989; Silver et al. 1990) at temperatures above ~1000 K suffered from the quench effect. The data obtained at significantly lower temperatures in these papers are generally acceptable. The time for Reaction (1) to reach equilibrium decreases as temperature and H_2O_t increase. When the experimental temperature is high (typically ~1000 K, but depending on H_2O_t and cooling rate), it often takes less than a second (shorter at higher H_2O_t) for Reaction (1) to reach equilibrium. That is, there is continuous reaction as the sample cools down. To facilitate discussion, we define quotient Q as:

$$Q = \frac{[OH]^2}{[H_2O_m][O]} \tag{5}$$

The expression of Q is the same as that of K except that K is restricted to the case when equilibrium is reached. If $Q > K$, the reaction goes to the left to form H_2O_m. Otherwise, it goes to the right to form OH. For a sample cooled to room temperature, the measured species concentration can be used to calculate Q, which is the apparent equilibrium constant K_{ae} of this sample (it is called "apparent equilibrium" since the sample did not exactly reach equilibrium at the corresponding temperature). This apparent equilibrium constant corresponds to an apparent equilibrium temperature (T_{ae}) as follows,

$$\ln Q = A + \frac{B}{T_{ae}} \tag{6}$$

That is, the apparent equilibrium temperature is the temperature calculated from the quotient Q assuming Q were the same as K even though equilibrium is not reached at any temperature (comparing Eqns. 4 and 6). During cooling at various quench rates, the variation of Q and T_{ae} as a function of temperature is illustrated in Figure 1 (Zhang 1994, 2008; Zhang et al. 1997b, 2000).

Starting from a high temperature, if cooling rate is high, the resulting T_{ae} after cooling down is also high, and vice versa. Even at a high cooling rate, species concentrations may change upon cooling. For a rhyolite melt containing 2.5 wt% H_2O_t equilibrated at a temperature of 1000 K and cooled down at 70 K/s, the resulting T_{ae} is only about 800 K (Zhang et al. 2000), rather than the experimental equilibrium temperature of 1000 K. Dingwell and Webb (1990) were the first to analyze this problem using the concept of cooling-rate-dependent glass transition temperature, and assumed that the apparent equilibrium temperature for Reaction (1) is similar to the glass transition temperature, which was verified later (e.g., Zhang et al.

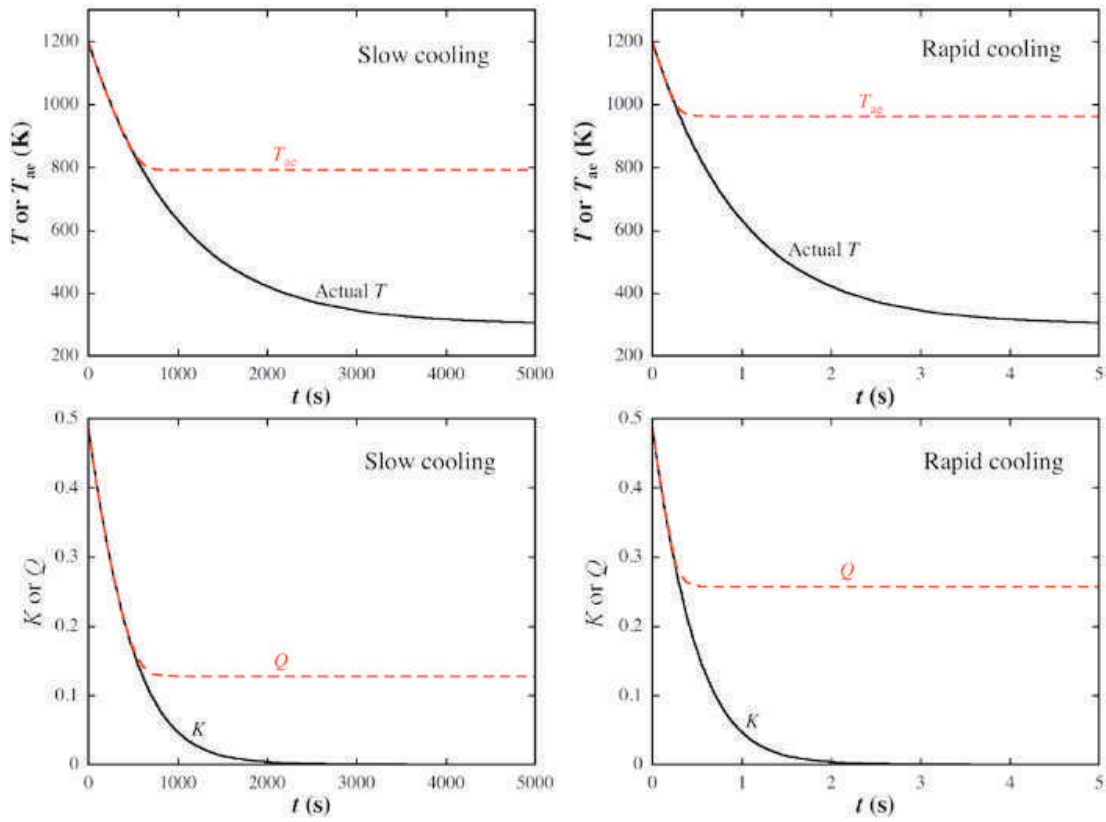

Figure 1. Schematic evolution of Q and T_{ae} for rapid cooling and slow cooling of a hypothetical reaction.

1997b, 2003; Behrens and Nowak 2003; Hui et al. 2008). Because the temperature was high for many early experiments using the quench method, equilibrium H_2O speciation was not fully quenchable even with the fastest achievable quench rate. That is, the reported data did not reflect true speciation at the experimental temperature; only T_{ae} can be obtained. On the other hand, when the experimental temperature is low enough (usually below 900 K, but depending on H_2O_t and quench rate), reaction during quench is negligible and T_{ae} is roughly the same as the experimental temperature. However, the experimental temperature cannot be too low (such as < 600 K) either, otherwise it would require too long a duration to reach equilibrium. Based on the above considerations, the appropriate temperature range for quench method is typically 650-900 K (which are referred to as intermediate temperatures).

Dependence of molar absorptivities on temperature. The first *in situ* IR measurements indicated that the molar absorptivities depend on temperature (e.g., Keppler and Bagdassarov 1993). However, for some years afterwards, temperature effects were not considered in interpreting *in situ* IR speciation data (Nowak and Behrens 1995; Shen and Keppler 1995; Sowerby and Keppler 1999) and the results were inconsistent with speciation data quenched from intermediate temperatures (e.g., Zhang et al. 1991a, 1995; Ihinger et al. 1999). To resolve the inconsistency, two groups with different views collaborated (Zhang and Behrens 1998; Withers et al. 1999). They demonstrated that (i) molar absorptivities vary with temperature even below the glass transition, which led to an apparent change in species concentrations as well as inaccuracy of K values in Nowak and Behrens (1995), Shen and Keppler (1995), and Sowerby and Keppler (1999); and (ii) after accounting for the temperature effect of the molar absorptivities, the speciation data from quench experiments from intermediate temperatures and those from *in situ* experiments are consistent, as also demonstrated by other studies (Zhang 1999b; Withers and Behrens 1999; Nowak and Behrens 2001; Behrens and Nowak 2003).

However, the two data sets cover different temperatures (with only small overlap) and seem to indicate a slightly different standard state enthalpy change for Reaction (1).

Summary of speciation data. After two vigorous debates discussed above, one on the quench effect, and the other on the *in situ* measurements, it is now known that the quench method can be used to obtain reliable speciation data when the experimental temperature is low enough (usually below ~900 K, but the exact temperature depends on H_2O_t and quench rate, and must be determined experimentally for a given system), and the *in situ* method can also be used to obtain reliable speciation data when the temperature dependence of the molar absorptivities is accounted for. In addition, the speciation constant as a function of temperature may be inferred by estimation of the glass transition temperature from viscosity models and assuming the glass transition temperature is the apparent equilibrium temperature (Dingwell and Webb 1990; Zhang et al. 2003); referred to as the fictive temperature method hereafter. Subsequently, speciation in the following melts have been investigated further: albite and some synthetic sodium-calcium aluminosilicate melts (Ohlhorst et al. 2000), AOQ ($Qz_{28}Ab_{38}Or_{34}$ where Qz means quartz, Ab means albite and Or means orthoclase, and the values indicate wt%) melt (Nowak and Behrens 2001; Behrens and Nowak 2003), dacite melt (Liu et al. 2004a), andesite melt (Botcharnikov et al. 2006), NS4 ($Na_2O{\cdot}4SiO_2$, or $Na_2Si_4O_9$) and NS6 ($Na_2O{\cdot}6SiO_2$, or $Na_2Si_6O_{13}$) melts (Behrens and Yamashita 2008), high-pressure rhyolite melts (Hui et al. 2008), and haploandesite melt (Ni et al. 2009a). The precision of the speciation data depends on the method (the 2σ precision in $\ln K$ is often about 0.025 for the quench method, 0.1 for the *in situ* method, and 0.1 to 0.5 for the fictive temperature method). The accuracy, on the other hand, depends on the accuracy of the infrared calibration for species concentrations, which is not well characterized. For example, even for rhyolite glass, which has been studied most extensively (Newman et al. 1986; Zhang et al. 1997a; Withers and Behrens 1999), the possible variation of molar absorptivities with H_2O_t and quench rate is still not accurately known. Studies on hydrous speciation in Fe-rich melts such as dacite melt have another difficulty: the high iron concentration leads to significant and broad absorption bands that overlap with hydrous species bands in the NIR. What makes the problem worse is the variation of the shape and intensity of the iron-related bands before and after heating. Hence, many authors have opted to investigate iron-free analogs of natural silicate melts.

With the above preamble and precaution, some speciation data are shown and compared in Figure 2. The pressure effect on speciation is examined by Hui et al. (2008); K may increase or decrease with pressure, but the effect is not very large and not included in Figure 2. From Figure 2, several observations can be made: (i) K in sodium silicates (NS4 and NS6) is much greater than in natural aluminosilicate melts and their analogs (as well as albite melt), supporting the suggestion of formation of NaOH clusters (Kohn et al. 1989), especially in the absence of Al; (ii) K in a natural rhyolite is similar to that in haplorhyolite (AOQ); the similarity also holds for natural andesite and haploandesite; (iii) K increases with temperature (meaning Reaction (1) is an endothermic process); (iv) K increases slightly from rhyolite to dacite to andesite melts, which means that K values do not simply increase with Na_2O because the Na_2O (as well as the K_2O) content decreases from rhyolite to dacite to andesite melts. The speciation models (Zhang et al. 1997a; Liu et al. 2004a; Ni et al. 2009a) that are often used in diffusion studies (Zhang and Behrens 2000; Behrens et al. 2007; Ni and Zhang, 2008; Behrens and Zhang 2009; Wang et al. 2009; Ni et al. 2009a,b) are:

$$K_{rhyolite} = \exp\left(1.876 - \frac{3110}{T}\right) \tag{7a}$$

$$K_{dacite} = \exp\left(1.49 - \frac{2634}{T}\right) \tag{7b}$$

$$K_{haploandesite} = \exp\left(1.55 - \frac{2453}{T}\right) \tag{7c}$$

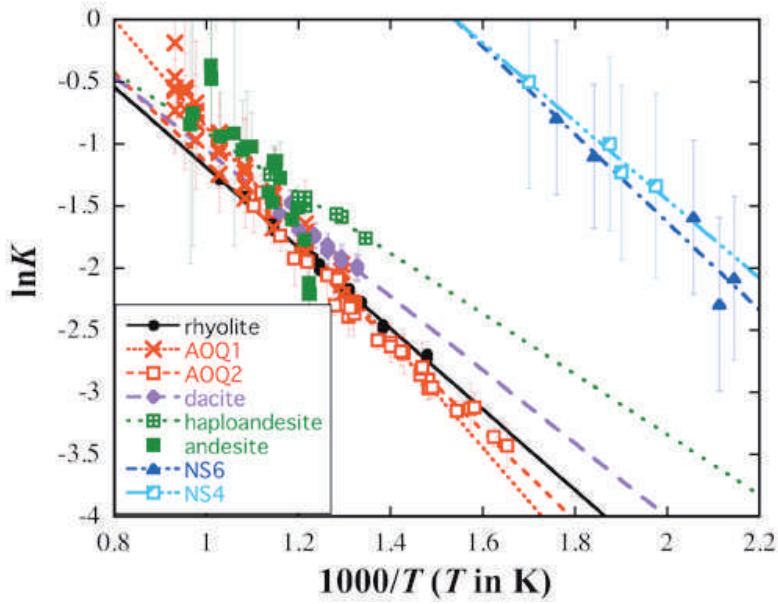

Figure 2. Speciation data (with 2σ errors) and regression lines in different melts at ≤ 0.8 GPa. For rhyolite melts, the data are also limited to $H_2O_t \leq 3$ wt% because the given calibration (Zhang et al. 1997a) is best applied to $H_2O_t \leq 3$ wt%. Error bars for ln*K* in rhyolite and haploandesite melts are smaller than the size of the symbols. Data sources: rhyolite melt using the quench method: Zhang et al. (1997a); Ihinger et al. (1999); Hui et al. (2008); AOQ1: AOQ melt (Table 1) using the *in situ* method (Nowak and Behrens 2001); AOQ2: AOQ melt using the fictive temperature method (Behrens and Nowak 2003); dacite melt using the quench method: Liu et al. (2004a); haploandesite melt using the quench method: Ni et al. (2009a); andesite melt using the fictive temperature method: Botcharnikov et al. (2006); NS4 ($Na_2O{\cdot}4SiO_2$) and NS6 ($Na_2O{\cdot}6SiO_2$) melts using the fictive temperature method: Behrens and Yamashita (2008).

Other expressions of equilibrium constants are available (e.g., Ihinger et al. 1999; Nowak and Behrens 2001; Hui et al. 2008), but they have not been much used in diffusion studies either because they are new, or because they are complicated, or because of the need to maintain internal consistency with other studies. Using different *K* values would impact the retrieval of the diffusivities of individual H_2O species but only negligibly the retrieval of $D_{H_2O_t}$ because the latter is essentially constrained by the length and shape of an H_2O_t concentration profile.

More detailed studies of hydrous species reaction kinetics have been carried out through isothermal experiments or controlled cooling rate experiments (Zhang et al. 1995, 1997b, 2000; Liu et al. 2004a; Hui et al. 2008). However, in treating H_2O diffusion, for simplicity, quasi-equilibrium is often assumed for the species reaction, and complicated kinetics are not incorporated. Hence, the kinetics is not discussed in detail here.

The variations of H_2O_m and OH concentrations with H_2O_t for a fixed equilibrium constant *K* are shown in Figure 3. It can be seen that H_2O_m is not proportional to H_2O_t (that is, the X_m/X curve in Fig. 3 is not a horizontal line). Instead, at low H_2O_t, H_2O_m is roughly proportional to the square of H_2O_t (in other words, H_2O_m/H_2O_t ratio is proportional to H_2O_t), meaning a more rapid increase of H_2O_m concentration as H_2O_t increases. Below about 0.2 wt% H_2O_t, almost all H_2O_t is OH (which does not mean that OH would play a main role in H_2O diffusion, as will be clear later in this chapter). This behavior arises from the stoichiometric coefficient 2 for OH in Reaction (1), which means the square of OH concentration is proportional to H_2O_m concentration, leading to the complicated relation between H_2O_m and H_2O_t concentrations as well as the complicated behavior of H_2O_t diffusion.

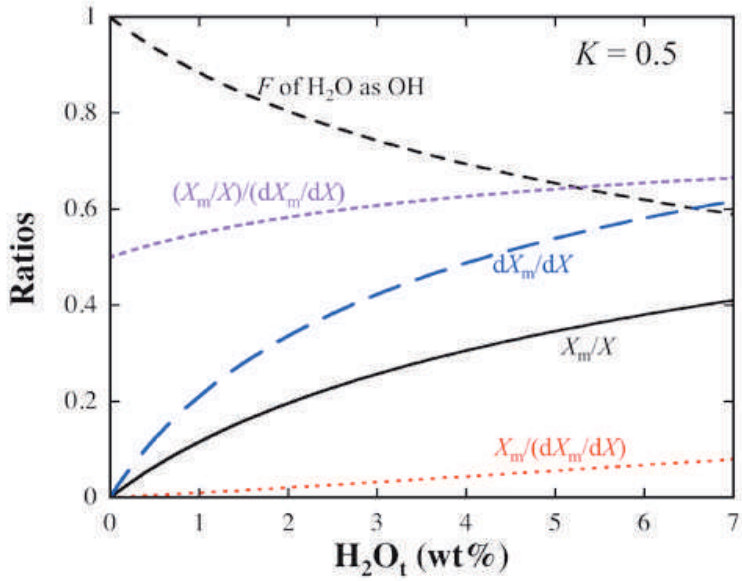

Figure 3. Species fractions, dX_m/dX, $X_m/(dX_m/dX)$ and $(X_m/X)/(dX_m/dX)$ versus H_2O_t at a fixed K of 0.5 where $X_m = [H_2O_m]$ and $X = [H_2O_t]$. $X_m/X = [H_2O_m]/[H_2O_t]$ (fraction of molecular H_2O). F is fraction of OH. $D_{H_2O_t}$ and $D_{H_2O_m}$ are related through dX_m/dX; $D_{^{18}O}$ and $D_{H_2O_t}$ are related through $X_m/(dX_m/dX)$; and ^2H-^1H self-diffusivity in hydrous melts and $D_{H_2O_t}$ (chemical diffusivity) are related through $(X_m/X)/(dX_m/dX)$.

H_2O diffusion literature

Technological improvements and theoretical modeling were the keys in the development of H_2O diffusion studies. Most H_2O diffusion experiments can be characterized as follows: hydration of an originally homogeneous and almost water-free sample by exposure to water vapor or fluid, dehydration of an initially homogeneous hydrous glass by exposure to dry N_2 or Ar, and diffusion couple (two samples with different water contents juxtaposed against each other). In the early years of H_2O diffusion studies in silicate melts, diffusion profiles could not be measured, so either the bulk H_2O mass loss from dehydration or mass gain from hydration was determined by weight change or mass spectrometry or infrared spectroscopy, from which the diffusivity was inferred (e.g., Shaw 1974). Later, advancements in ion microprobe analyses (Coles and Long 1974; Hofmann 1974) allowed the microanalytical determination of H_2O diffusion profiles (Delaney and Karsten 1981), but species concentrations could not be determined. Afterwards, advancement in infrared spectroscopy (Stolper 1982a,b; Acocella et al. 1984) led to the measurement of concentration profiles of both H_2O_m and OH species (Zhang et al. 1991a). Coupled speciation and diffusion studies (Zhang et al. 1991a) helped establish the basic mechanism of H_2O diffusion. Later studies, especially those at high temperatures, used only H_2O_t concentration profiles from micro-IR to model H_2O diffusion because species concentrations cannot be quenched from high temperatures.

In the glass and materials science literature, H_2O diffusion studies began in the 1960's. The studies were limited to low H_2O concentrations, with H_2O_t typically no more than 0.1 wt% (e.g., Drury and Roberts 1963; Cockram et al. 1969; Burn and Roberts 1970; Lanford et al. 1979; Houser et al. 1980; Tsong et al. 1980; Nogami and Tomozawa 1984a,b; and the recent review by Shelby 2008). The average OH concentration (proportional to H_2O_t) in a thin wafer upon heat treatment is monitored by IR and the diffusivity is obtained from the diffusive mass loss equation for a thin wafer (Crank 1975):

$$F = \frac{4\sqrt{D}}{\sqrt{\pi}L}\sqrt{t} \tag{8}$$

where F is the fractional mass loss (H_2O_t loss divided by initial H_2O_t), L is the thickness of the wafer, t is time, and D is apparent diffusivity (more specifically, D is diffusion-out diffusivity of H_2O_t, denoted as D_{out}, see below). It is often observed that D_{out} is proportional to H_2O_t, from which it was suggested that the diffusing species is H_2O_m (because the H_2O_m concentration is proportional to the square of the H_2O_t concentration: a rigorous explanation can be found below in Eqn. 11) (Doremus 1969, 1973; Ernsberger 1980; Smets and Lommen 1983; Nogami and Tomozawa 1984a,b), but other explanations included the interdiffusion of hydronium H_3O^+ and cations (e.g., Cockram et al. 1969; Doremus 1975; Lanford et al. 1979; Houser et al. 1980; Tsong et al. 1980), or the depolymerization of the silicate network (e.g., Haller 1963; Roberts and Roberts 1966; Delaney and Karsten 1981). These other explanations gradually become less cited as later direct measurements of species concentration profiles and modeling showed that assuming H_2O_m as the diffusing species can model the detailed diffusion profiles almost perfectly.

Shaw (1974) was the first to investigate H_2O diffusion in a geologically relevant silicate melt. He determined total mass gain due to hydration, and inferred that H_2O_t diffusivity depends strongly on H_2O_t content. Jambon (1979) carried out dehydration experiments and measured the mass loss from the sample. This study was later corrected by Jambon et al. (1992): because of an error in the estimated initial H_2O_t in the sample (0.38 wt% in Jambon 1979 versus the correct 0.114 wt% in Jambon et al. 1992), the diffusion-out H_2O_t diffusivity was corrected upward by a factor of 11.

Delaney and Karsten (1981) and Karsten et al. (1982) were the first to measure H_2O concentration profiles using the ion microprobe after hydration experiments. The profiles were fit by numerical solutions assuming some dependence of $D_{H_2O_t}$ on H_2O_t. Good fits were obtained for $D_{H_2O_t} = D_0\exp(bC_w)$ where C_w is the H_2O_t concentration and D_0 and b are two fitting parameters. Hence, it was assumed that $D_{H_2O_t}$ depends exponentially on H_2O_t. However, the expression does not work at low H_2O_t (such as below 0.5 wt%) because it implies that $D_{H_2O_t}$ approaches a constant as C_w approaches zero, but prior experimental data in the glass science literature showed that $D_{H_2O_t}$ is proportional to C_w even down to very low C_w. Lapham et al. (1984) used a similar technique and compared diffusion of ^1H_2O and ^2H_2O (or D_2O) in rhyolite melts using ion microprobe measurements. Their data apparently showed that the ^1H_2O diffusivity was 2 times the ^2H_2O diffusivity. However, a later publication from the same laboratory (Stanton et al. 1985) retracted this claim and found no measurable difference between ^2H_2O and ^1H_2O diffusivities.

Wasserburg (1988) analyzed the role of H_2O speciation in H_2O diffusion. Zhang et al. (1991a) were the first to utilize FTIR to measure concentration profiles of both H_2O_m and OH species in dehydration studies of natural obsidian, at 676-823 K, 0.1 MPa, and ≤ 1.7 wt% H_2O_t. By considering the interconversion reaction between H_2O_m and OH and the diffusion of both H_2O_m and OH in concert, they concluded that OH diffusivity is negligible compared to H_2O_m diffusivity (i.e., H_2O_m is the diffusing species), and H_2O_m diffusivity is roughly independent of H_2O_t in the samples studied. At low H_2O_t, a constant H_2O_m diffusivity leads to proportionality between the H_2O_t diffusivity and H_2O_t content, consistent with the glass science literature. The much higher diffusivity of H_2O_m than OH is understandable because H_2O_m is a neutral molecule hence its diffusion does not require breaking strong bonds, whereas OH is bonded to other cations (Si^{4+}, Al^{3+}, Na^+, etc) and its motion requires breaking strong bonds in the silicate structure. In terms of particle size, H_2O_m is similar or slightly smaller than OH (Shannon 1976; Zhang and Xu 1995). Zhang et al. (1991a) also distinguished H_2O_t diffusivities during diffusion-out (dehydration) versus diffusion-in (hydration) experiments (Moulson and Roberts 1961). Because of the dependence of $D_{H_2O_t}$ on H_2O_t content, the diffusion-in diffusivity is 1.78 times the diffusion-out diffusivity when $D_{H_2O_t}$ is proportional to H_2O_t under otherwise identical conditions (see also Wang et al. 1996). Zhang and Stolper (1991) investigated H_2O diffusion in basalt melt at 1573-1773 K, 1.0 GPa, and ≤0.42 wt% H_2O_t, and found that the H_2O_t

diffusivity is roughly proportional to H_2O_t, consistent with H_2O_m being the diffusing species and the H_2O_m diffusivity being independent of H_2O_t. Jambon et al. (1992) re-interpreted their earlier dehydration data and found that (i) the data are consistent with Zhang et al. (1991a) and (ii) disequilibrium in Reaction (1) can significantly affect $D_{H_2O_t}$.

Nowak and Behrens (1997) carried out diffusion couple experiments and investigated H_2O diffusion in a synthetic rhyolite melt (AOQ) at 1073-1473 K, 0.05-0.5 GPa, and ≤ 9.0 wt% H_2O_t. They demonstrated that the H_2O_t diffusivity at H_2O_t > 3 wt% increases exponentially with H_2O_t, implying that the H_2O_m diffusivity cannot be constant but must increase with H_2O_t content at H_2O_t > 3 wt%. They fit $\log D_{H_2O_t}$ as a polynomial function of H_2O_t. Zhang and Behrens (2000) studied H_2O diffusion in rhyolite melts at 673-1473 K, 0.0001-0.81 GPa, and ≤ 7.7 wt% H_2O_t. They confirmed the observations of Nowak and Behrens (1997) and found that the diffusion profiles can be accurately modeled by assuming H_2O_m is the diffusing species and $D_{H_2O_m}$ increases exponentially with H_2O_t, $D_{H_2O_m} = D_0 e^{aX}$, where X is mole fraction of H_2O_t, D_0 is the $D_{H_2O_m}$ value as X approaches zero, and a is a parameter characterizing how rapidly $D_{H_2O_m}$ increases with H_2O_t. The exponential increase means that at low H_2O_t, $D_{H_2O_m}$ increases only slowly with H_2O_t and can be treated roughly as a constant (e.g., for a = 25 and from 0 to 1 wt% H_2O_t, e^{aX} varies from 1 to 1.56, only slightly outside the experimental uncertainty of diffusivity determinations at high temperatures), consistent with the observations of Zhang et al. (1991a). The exponential increase is also consistent with the diffusivities of neutral molecular species such as Ar (Behrens and Zhang 2001) and CO_2 (Watson et al. 1982; Watson 1991).

Later experimental studies in general followed the framework established in Zhang et al. (1991a), Zhang and Stolper (1991), and Zhang and Behrens (2000). Freda et al. (2003) investigated H_2O diffusion in a trachyte melt at 1334-1601 K, 1 GPa, and ≤ 2.0 wt% H_2O_t. Okumura and Nakashima (2004, 2006) developed the *in situ* FTIR measurements of H_2O loss due to dehydration to obtain diffusivities, and reported results on rhyolite melts at ≤ 4.1 wt% H_2O_t and on dacite, andesite and basalt melts at ≤ 1.1 wt% H_2O_t. Their method works well for rapidly obtaining diffusion data but cannot resolve how $D_{H_2O_t}$ depends on H_2O_t. Liu et al. (2004b) explored H_2O diffusion in dacite melts by dehydration experiments at 824-910 K, ≤ 0.15 GPa, and ≤ 2.5 wt% H_2O_t. Behrens et al. (2004) studied H_2O diffusion in dacite and andesite melts at 1458-1858 K, 0.5-1.5 GPa, and ≤ 6.3 wt% H_2O_t; some of their data are consistent with concentration-independent $D_{H_2O_t}$. Behrens et al. (2007) obtained some H_2O diffusion data in rhyolite melts in a study comparing oxygen and H_2O diffusion. Ni and Zhang (2008) further resolved the pressure effect on H_2O diffusion in rhyolite melts and constructed a general H_2O diffusivity model over a large range of T, P and H_2O_t. Behrens and Zhang (2009) and Wang et al. (2009) quantified H_2O diffusion in peralkaline rhyolite melts. Ni et al. (2009a,b) examined H_2O diffusion in dacite and haploandesite melts. All the melt compositions that have been studied for H_2O diffusion are listed in Table 1.

H_2O diffusion, theory and data summary

Strictly speaking, silicate melts are multicomponent systems, and H_2O diffusion should fall into the category of multicomponent diffusion. However, the anhydrous melt composition generally does not vary along a diffusion profile in the typical design of the experiments, and addition of H_2O mainly causes a dilution effect. Therefore, H_2O diffusion in the literature is treated as effective binary diffusion, or the first kind of effective binary diffusion defined by Zhang (2010, this volume) and Zhang et al. (2010, this volume).

Because $D_{H_2O_t}$ depends on H_2O_t concentration, the general equation for one-dimensional diffusion is as follows:

$$\frac{\partial X}{\partial t} = \frac{\partial}{\partial x}\left(D_{H_2O_t} \frac{\partial X}{\partial x} \right) \tag{9}$$

where t is time, x is distance, $D_{H_2O_t}$ is the diffusivity (effective binary diffusivity) of H_2O_t, and $X = [H_2O_t]$ (see Eqn. 3a). The above diffusion equation can be solved given how $D_{H_2O_t}$ varies with H_2O_t, and boundary and initial conditions. For hydration and dehydration experiments, the equilibrium surface concentration and the initial concentration (usually uniform) are the boundary and initial conditions, respectively. For diffusion couple experiments, no boundary condition is needed and the initial concentrations in the two starting halves are the initial condition. If $D_{H_2O_t}$ were independent of H_2O_t (or X), then the diffusion profile could be fit by an error function solution. However, this is rarely the case: the variation of $D_{H_2O_t}$ with H_2O_t turns out to be complicated.

Experimental results in the glass and geological literature show that when H_2O_t is sufficiently low (≤ 2 wt%, but depending on temperature), $D_{H_2O_t}$ is proportional to H_2O_t (or proportional to X in Eqn. 9). Such an equation can be solved numerically (e.g., Crank 1975) and the solution has been applied to fit diffusion profiles. If a profile can be fit within experimental uncertainty (e.g., Fig. 4), then the proportionality relation is assumed to describe how $D_{H_2O_t}$ varies with H_2O_t.

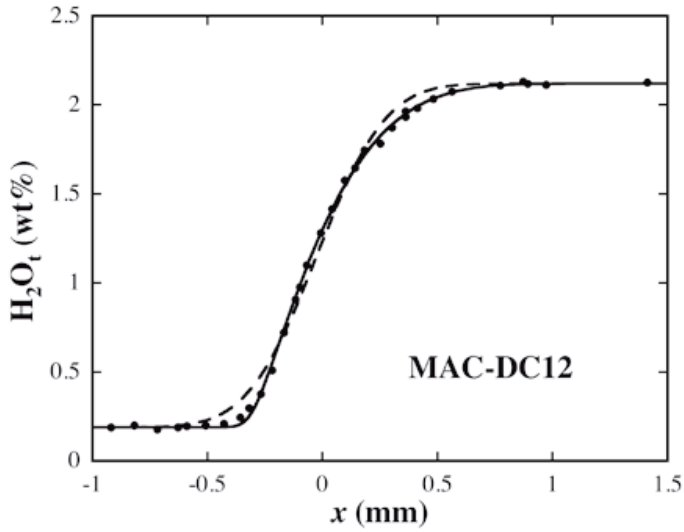

Figure 4. Experimental H_2O_t diffusion profile (points) in a peraluminous rhyolite melt and two fits. The dashed curve is an error function fit (assuming $D_{H_2O_t}$ is independent of H_2O_t). The solid curve is a fit assuming $D_{H_2O_t}$ is proportional to H_2O_t. The solid curve agrees well with experimental data. From Behrens and Zhang (2009).

At high H_2O_t (such as >3 wt%, especially at relatively low temperatures such as 800 K), the proportionality relation often does not work well (Nowak and Behrens 1997; Zhang and Behrens 2000; Liu et al. 2004b; Ni and Zhang 2008; Ni et al. 2009a,b; Wang et al. 2009). One example is given in Figure 5. Hence, more complicated relations are proposed to describe how $D_{H_2O_t}$ varies with H_2O_t. Based on our knowledge of H_2O speciation, the general and mechanistic approach is to consider the diffusion of both species:

$$\frac{\partial X}{\partial t} = \frac{\partial}{\partial x}\left(D_{H_2O_m} \frac{\partial X_m}{\partial x} + \frac{1}{2} D_{OH} \frac{\partial X_{OH}}{\partial x} \right) \tag{10}$$

where X_m is the mole fraction of H_2O_m, X_{OH} is the mole fraction of OH, and $D_{H_2O_m}$ and D_{OH} are the diffusivities of H_2O_m and OH. The factor 1/2 is due to the fact that one mole of H_2O_m reacts to form two moles of OH (Reaction 1).

Experimental data show $D_{OH} << D_{H_2O_m}$ in rhyolite melt so that diffusive flux due to OH diffusion can be ignored (Zhang et al. 1991a). (The small diffusivity of OH does not mean that OH profile is flat, because interconversion between OH and H_2O_m can change OH concentration.) Therefore, Equation (10) can be simplified as:

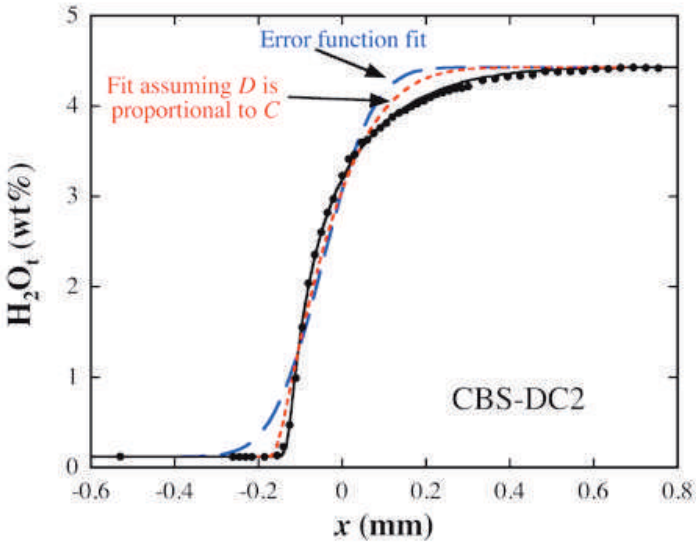

Figure 5. Experimental H_2O_t diffusion profile (points) in a peralkaline rhyolite melt and three fits. The long-dashed (blue in online version) curve is an error function fit (assuming $D_{H_2O_t}$ is independent of H_2O_t). The short-dashed (red in online version) curve is a fit assuming $D_{H_2O_t}$ is proportional to H_2O_t. The solid curve is a fit assuming $D_{H_2O_m} = D_0 e^{aX}$ (Eqn. 12). The solid curve agrees well with experimental data. From Wang et al. (2009).

$$\frac{\partial X}{\partial t} = \frac{\partial}{\partial x}\left(D_{H_2O_m} \frac{\partial X_m}{\partial x} \right) \tag{11}$$

The above equation means that $D_{H_2O_t} = D_{H_2O_m} dX_m/dX$ if equilibrium for Reaction (1) is reached at every point along a profile (dX_m/dX for $K = 0.5$ is shown in Fig. 3). (Equilibrium for Reaction (1) is necessary because without equilibrium the partial differential $\partial X_m/\partial X$ would depend on time and cannot be simplified to dX_m/dX.) At low H_2O_t (e.g., below 2 wt% but depending on the temperature), $D_{H_2O_m}$ is roughly independent of H_2O_t, and dX_m/dX is proportional to H_2O_t (Fig. 3), leading to $D_{H_2O_t}$ proportional to H_2O_t. However, at high H_2O_t, $D_{H_2O_m}$ must increase with H_2O_t (Nowak and Behrens 1997) and has been shown to increase exponentially with H_2O_t (Zhang and Behrens 2000; Liu et al. 2004b; Ni and Zhang 2008; Ni et al. 2009a,b; Wang et al. 2009):

$$D_{H_2O_m} = D_0 e^{aX} \tag{12}$$

where a is a fitting parameter that may vary with T and P. Numerous studies have found that a increases with decreasing temperature, indicating a stronger dependence of $D_{H_2O_m}$ on H_2O_t at lower temperatures. This finding is not surprising since at low T the presence of H_2O has a larger impact on melt properties such as viscosity (e.g., Zhang et al. 2003), which is not simply related to the formation of the number of OH but is also related to the larger effect of each OH and H_2O_m on the melt viscosity at low temperatures. The above approach can fit all H_2O_t profiles within experimental uncertainty (as well as species concentration profiles if the species concentrations can be preserved during quench), including those profiles that cannot be fit by assuming $D_{H_2O_t}$ is proportional to H_2O_t (Fig. 5). Furthermore, experiments using samples with different H_2O_t generally yield the same set of parameters D_0 and a, which further supports the validity of Equation (12). The exponential dependence of the diffusivity of H_2O_m as well as other neutral molecules (Watson 1991; Behrens and Zhang 2001) on H_2O_t concentration might be related to the dramatic change of melt structure, as evidenced by the significantly reduced melt viscosity caused by the addition of H_2O (e.g., Shaw 1974; Zhang et al. 2003).

If equilibrium for Reaction (1) is reached at every point along a profile, the general relation between $D_{H_2O_t}$ and $D_{H_2O_m}$ is (Wang et al. 2009):

$$D_{H_2O_t} = D_{H_2O_m} \frac{dX_m}{dX} = D_{H_2O_m}\left[1 - \frac{(0.5 - X)}{[X(1-X)((4/K)-1) + 0.25]^{1/2}}\right] \tag{13}$$

where K is the equilibrium constant of Reaction (1) and depends on temperature (to a lesser extent, on pressure or H_2O_t), and X and X_m are mole fractions of H_2O_t and H_2O_m on a single oxygen basis. Hence, if K is known or fixed, $D_{H_2O_t}$ can be calculated from $D_{H_2O_m}$ using the above equation. Figure 6 illustrates how $D_{H_2O_m}$ and $D_{H_2O_t}$ vary with H_2O_t concentration at given K and a. At low H_2O_t, $D_{H_2O_t}$ is approximately proportional to H_2O_t; while at higher H_2O_t, the relation transitions to exponential. For rhyolite, dacite and haploandesite melts, K is given by Equations (7a) to (7c). Diffusion data in various melts are summarized below.

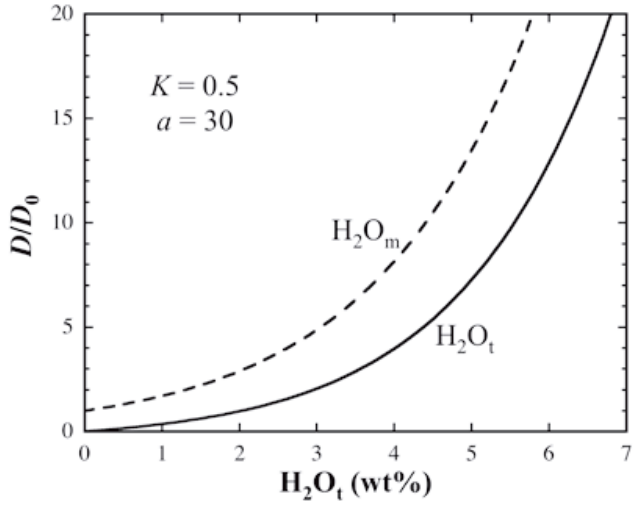

Figure 6. $D_{H_2O_m}$ and $D_{H_2O_t}$ as function of H_2O_t for a given set of K and a, calculated from Equations (12) and (13). The relation between $D_{H_2O_t}$ and H_2O_t shifts from quasi-proportional to quasi-exponential as H_2O_t increases. $D_{H_2O_t}$ is lower than $D_{H_2O_m}$.

If equilibrium for Reaction (1) is not reached (at relatively low temperatures and low H_2O_t), one would have to consider the kinetics of Reaction (1) and couple the kinetic equation with the diffusion equation 11 to solve the concentration profiles. Such full treatment has not been carried out yet, but experimental data have been noted where these conditions exist (Jambon et al. 1992; Zhang et al. 2007).

Metaluminous and peraluminous rhyolite melts. "Normal" metaluminous rhyolite melts including haplorhyolite melts (compositions 1-3 in Table 1) have been studied most extensively (Shaw 1974; Delaney and Karsten 1981; Karsten et al. 1982; Zhang et al. 1991a; Nowak and Behrens 1997; Zhang and Behrens 2000; Okumura and Nakashima 2004; Behrens et al. 2007; Ni and Zhang 2008). Figure 7 compares $D_{H_2O_t}$ in rhyolite melts at 1 wt% H_2O_t from various laboratories. It can be seen that the original diffusivity data from different laboratories are largely consistent at this H_2O_t when cast in the same way. Furthermore, there is a significant pressure effect on $D_{H_2O_t}$, especially at low temperature.

Ni and Zhang (2008) combined their new experimental data and literature data at 676-1900 K, 0-1.9 GPa, 0-8 wt% H_2O_t (reflecting the coverage of conditions by the experimental data), using K from Equation (7a), and obtained $D_{H_2O_m}$ (m^2/s) as follows:

$$D_{H_2O_m}^{\text{rhyolite}} = \exp\left(-14.26 + 1.888P - 37.26X - \frac{12939 + 3626P - 75884X}{T}\right) \qquad (14)$$

where T is in K, P is in GPa, and X is mole fraction of H_2O_t on a single oxygen basis. The H_2O_t diffusivity in peraluminous rhyolite melts (composition 4 in Table 1) at ≤ 0.5 GPa is indistinguishable from that in "normal" rhyolite melts and can be described by the above expression as well (Behrens and Zhang 2009). Hence, $D_{H_2O_t}$ for metaluminous and peraluminous rhyolite melts can be calculated from the above $D_{H_2O_m}$ using Equation (13) with K from Equation (7a). The 2σ uncertainty in $\ln D_{H_2O_t}$ is about 0.5 for this and other melts discussed below.

The above equation implies that $D_{H_2O_m}$ increases rapidly with H_2O_t at low temperatures but slowly at higher temperatures. Therefore, at higher temperatures, $D_{H_2O_t}$ is proportional to H_2O_t from zero to higher concentrations of H_2O_t. Because the proportionality equation is easy to apply and works well at low H_2O_t (which means ≤ 1 wt% at 773 K and ≤ 3 wt% at 1473 K), it is given below (Ni and Zhang 2008):

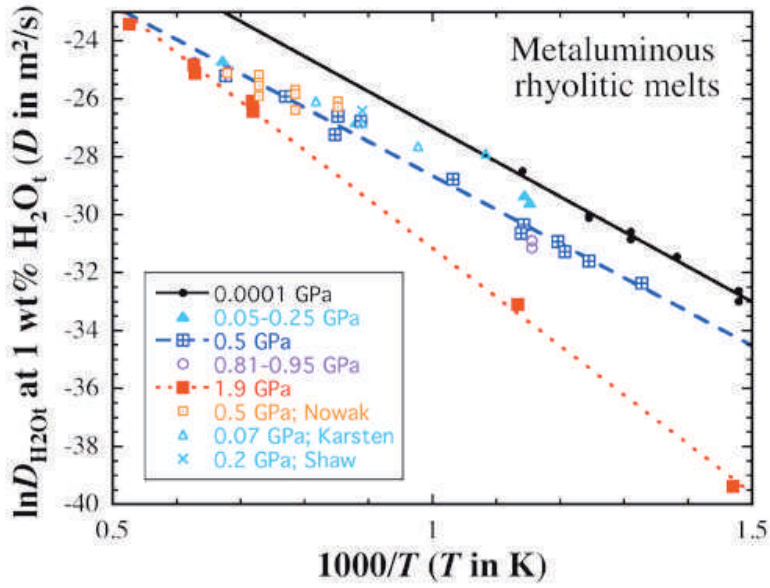

Figure 7. Comparison of experimental data on H_2O_t diffusivities in "normal" rhyolite melts at 1 wt% H_2O_t. Data sources: Data are from Zhang et al. (1991a), Zhang and Behrens (2000), and Ni and Zhang (2008), unless otherwise indicated as: Nowak and Behrens (1997); Karsten et al. (1982); Shaw (1974).

$$D_{H_2O_t}^{\text{rhyolite}} = C_w \exp\left(-18.10 + 1.888P - \frac{9699 + 3626P}{T}\right) \quad (15)$$

where T is in K, P is in GPa, and C_w is wt% of H_2O_t ($C_w = 1$ for 1 wt% H_2O_t).

Peralkaline rhyolite melts. Behrens and Zhang (2009) and Wang et al. (2009) investigated H_2O diffusion in peralkaline (PA) rhyolite melts (compositions 5 and 6 in Table 1) covering 789-1516 K, 0-1.4 GPa, 0-4.6 wt% H_2O_t. Behrens and Zhang (2009) investigated diffusion at low H_2O_t, and Wang et al. (2009) expanded the studied range of H_2O_t and pressure. Even though these studies are not numerous, the effort was coordinated and systematic so that the data are sufficient to allow the construction of a general model for $D_{H_2O_m}$ (and hence $D_{H_2O_t}$). Figure 8 compares the H_2O_t diffusivities in peralkaline rhyolite melts to metaluminous rhyolite melts. On average, $D_{H_2O_t}$ at 0.5 GPa and 1 wt% H_2O_t in peralkaline rhyolite melt is ~2 times that in metaluminous rhyolite melt. The effect of pressure on $D_{H_2O_t}$ in peralkaline rhyolite melts is smaller than that in metaluminous rhyolite melts. For example, $\ln D_{H_2O_t}$ decreases by ~1.6 as pressure increases from 0.0001 to 0.5 GPa for metaluminous rhyolite melts; but by only ~0.3 for peralkaline rhyolite melts. At various P-T conditions, the difference between $D_{H_2O_t}$ in peralkaline rhyolite melts and that in metaluminous rhyolite melts is often a factor of 2 or smaller.

Using results from both Behrens and Zhang (2009) and Wang et al. (2009), and K from Equation (7a), Wang et al. (2009) constructed the following expression for $D_{H_2O_m}$ (m^2/s):

$$D_{H_2O_m}^{\text{PA rhyolite}} = \exp\left(-12.79 - 27.87X - \frac{13939 + 1230P - 60559X}{T}\right) \quad (16)$$

where T is in K, P is in GPa, and X is mole fraction of H_2O_t on a single oxygen basis. $D_{H_2O_t}$ for peralkaline rhyolite melts can be calculated from the above $D_{H_2O_m}$ using Equation (13) with K from Equation (7a). The resulting $D_{H_2O_m}$ and $D_{H_2O_t}$ are slightly larger than that in "normal" rhyolite melts, but no more than a factor of 2. By combining the data in both Behrens and Zhang (2009) and Wang et al. (2009), a simple equation to calculate directly $D_{H_2O_t}$ at low H_2O_t (which means ≤ 1 wt% at 773 K and ≤ 3 wt% at 1473 K) is as follows:

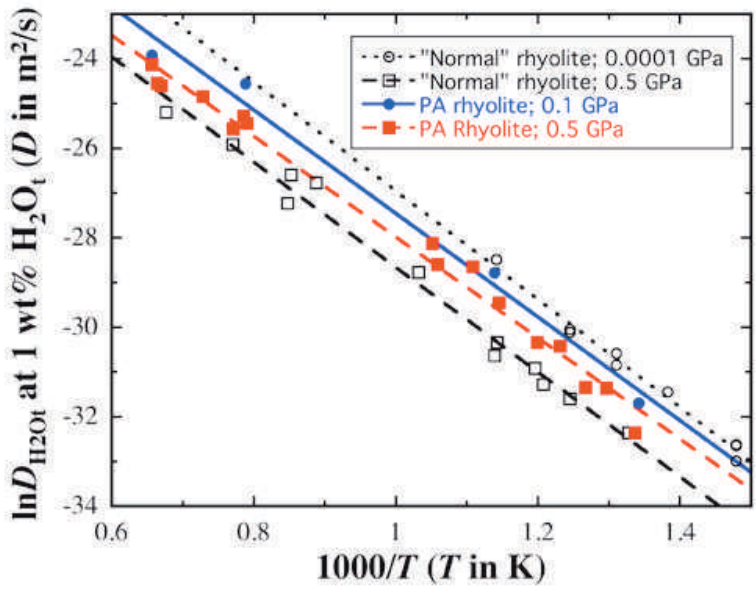

Figure 8. Comparison between H_2O_t diffusivities in peralkaline rhyolite melt at 0.5 GPa (filled circles) and those in metaluminous (or "normal") rhyolite melts at 0.0001 and 0.5 GPa (open circles and squares). Data sources for peralkaline rhyolite: Behrens and Zhang (2009) and Wang et al. (2009). See Figure 7 for data sources for metaluminous rhyolite.

$$D_{H_2O_t}^{\text{PA rhyolite}} = C_w \exp\left(-16.55 - \frac{10870 + 1101P}{T}\right) \tag{17}$$

where T is in K, P is in GPa, and C_w is wt% of H_2O_t.

Dacite melts. Liu et al. (2004b), Behrens et al. (2004), Okumura and Nakashima (2006), and Ni et al. (2009b) quantified H_2O diffusion in dacite melts (compositions 7 and 8 in Table 1), covering 786-1800 K, 0-1 GPa, 0-8 wt% H_2O_t. Liu et al. (2004b) and Okumura and Nakashima (2006) conducted dehydration experiments at intermediate temperature and low pressure; Behrens et al. (2004) carried out diffusion couple experiments at high temperature and high pressure; and Ni et al. (2009b) investigated H_2O diffusion at intermediate temperature and high pressure. All data have been combined to evaluate the effect of temperature, pressure and H_2O_t on H_2O diffusion. Figure 9 shows some experimental diffusion data and compares these with data in rhyolite melts. At 1 wt% H_2O_t, $D_{H_2O_t}$ in dacite melts is lower than that in rhyolite melts at < 1470 K. Furthermore, for both rhyolite and dacite melts, $D_{H_2O_t}$ decreases as pressure increases. As pressure increases from 0.0001 to 0.5 GPa, $\ln D_{H_2O_t}$ decreases by ~1.6 for rhyolite melt; but only by ~1.0 for dacite melts. That is, the pressure effect becomes smaller from rhyolite melt to dacite melt.

Using results from Liu et al. (2004b), Behrens et al. (2004) and Ni et al. (2009b), and K from Equation (7b), $D_{H_2O_m}$ at 786-1800 K, 0-1 GPa, and 0-8 wt% H_2O_t (reflecting conditions covered by the experimental data) can be expressed as (Ni et al. 2009b):

$$D_{H_2O_m}^{\text{dacite}} = \exp\left(-9.42 - 62.38X - \frac{19064 + 1477P - 108882X}{T}\right) \tag{18}$$

where T is in K, P is in GPa, and X is the mole fraction of H_2O_t on a single oxygen basis. $D_{H_2O_t}$ for dacite melts can be calculated from the above $D_{H_2O_m}$ using Equation (13) with K from Equation (7b). At ≤0.7 wt% H_2O_t at 773 K, and ≤ 6.2 wt% H_2O_t at 1673 K, $D_{H_2O_t}$ is proportional to H_2O_t and can be expressed as follows:

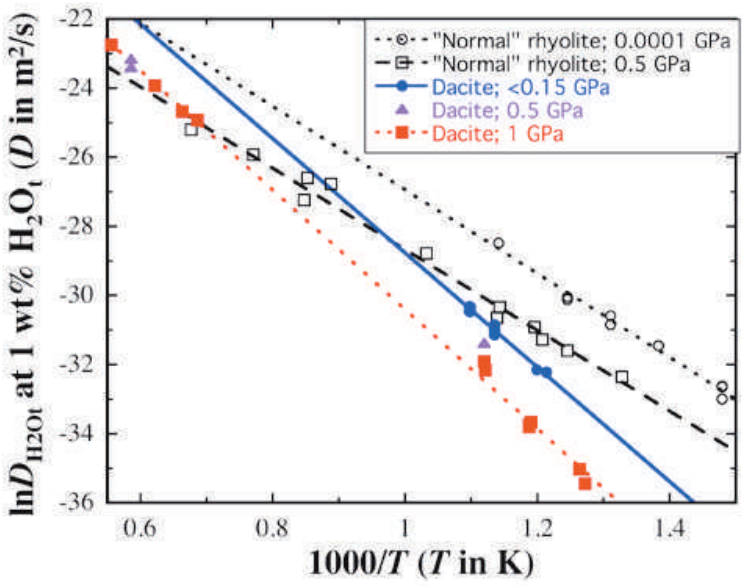

Figure 9. Comparison of $D_{H_2O_t}$ in dacite melts (solid circles, triangles and squares) and rhyolite melts (open circles and squares) at 1 wt% H_2O_t. Data sources for dacite melts: <0.15 GPa: Liu et al. (2004b); 0.5 GPa and 1 GPa: Behrens et al. (2004) and Ni et al. (2009b). Data sources for rhyolite melt: see Figure 7. The data of Okumura and Nakashima (2006) are not shown because there is a small systematic difference between their data and other data (Ni et al. 2009b).

$$D_{H_2O_t}^{\text{dacite}} = C_w \exp\left(-13.32 - \frac{15722 + 1466P}{T}\right) \quad (19)$$

where T is in K, P is in GPa, and C_w is wt% of H_2O_t. Note that the proportionality relation holds for a smaller H_2O_t range (≤ 0.7 wt%) in dacite than in rhyolite at intermediate temperatures such as 773 K, but for a larger H_2O_t range (≤ 5 wt%) in dacite than in rhyolite (≤ 3 wt%) at high temperatures such as 1473 K.

Andesite melts. There have been three studies (Behrens et al. 2004; Okumura and Nakashima 2006; Ni et al. 2009a) on andesite melts (compositions 9-11 in Table 1). However, the data are insufficient for the construction of a general model for $D_{H_2O_m}$ or $D_{H_2O_t}$. There is also a significant compositional difference (e.g., 5 wt% difference in SiO_2, 7 wt% difference in FeO) between the three andesites used in these studies. H_2O diffusion data are summarized in Figure 10.

Examining Figure 10, the pressure dependence of $D_{H_2O_t}$ at 1 wt% H_2O_t in andesite melts is small, at least at high temperature. For example, from 0.5 to 1.5 GPa at high temperature (triangular points), the variation of $D_{H_2O_t}$ is within uncertainty. Furthermore, the difference in $D_{H_2O_t}$ between haploandesite melt and normal andesite melt is small. Hence, we ignore the pressure dependence and compositional difference and fit all $D_{H_2O_t}$ data at low H_2O_t in three andesite melts to obtain the following equation:

$$D_{H_2O_t}^{\text{andesite}} = C_w \exp\left(-11.80 - \frac{18340}{T}\right) \quad (20)$$

where T is in K, D is in m^2/s, and C_w is wt% of H_2O_t. The above proportionality relation is applicable to ≤ 0.7 wt% H_2O_t at 773 K and ≤ 3.5 wt% H_2O_t at 1473 K. At temperatures ≥ 1573 K, there is ambiguity regarding how $D_{H_2O_t}$ depends on H_2O_t: whether $D_{H_2O_t}$ is proportional to H_2O_t or independent of H_2O_t (Behrens et al. 2004).

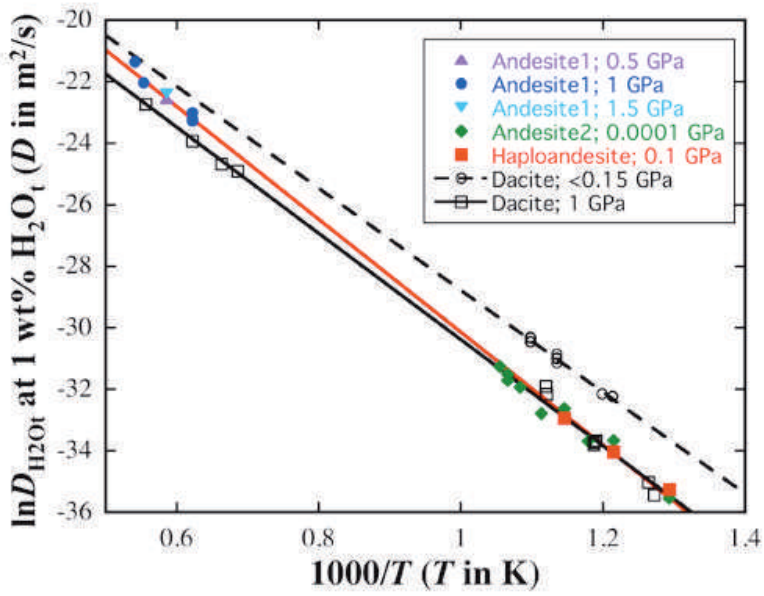

Figure 10. Comparison of $D_{H_2O_t}$ in andesite melts (solid circles, triangles, diamonds, and squares) and dacite melts (open circles and squares) at 1 wt% H_2O_t. Data sources for andesite melts: Andesite1: Behrens et al. (2004); Andesite2: Okumura and Nakashima (2006); Haploandesite: Ni et al. (2009a). Data sources for dacite melt: see Figure 9.

At intermediate temperatures and high H_2O_t, $D_{H_2O_t}$ increases strongly with H_2O_t and calculation of $D_{H_2O_t}$ is best through $D_{H_2O_m}$. For haploandesite melts (composition 11 in Table 1) at 743-873 K, 0.1 GPa, 0-2.5 wt% H_2O_t, using K from Equation (7c), $D_{H_2O_m}$ can be expressed as (Ni et al. 2009b):

$$D_{H_2O_m}^{\text{haploandesite}} = \exp\left(-12.27 - 13.91X - \frac{18172 - 73136X}{T}\right) \tag{21}$$

where T is in K and X is the mole fraction of H_2O_t on a single oxygen basis. $D_{H_2O_t}$ for haploandesite melts (also for Andesite 2 in Table 1, judging from similarity in $D_{H_2O_t}$ in the two melts in Fig. 10) can be calculated from the above $D_{H_2O_m}$ using Equation (13) with K from Equation (7c), but only under the limited conditions of 743-873 K, 0.1 GPa, 0-2.5 wt% H_2O_t.

For other silicate melts (such as basalt and trachyte), the equilibrium constant K for Reaction (1) has not been characterized. Hence, no $D_{H_2O_m}$ values or equations have been reported in the literature, and only $D_{H_2O_t}$ values and expressions under limited conditions are obtained. These are summarized below.

Basalt melts. For basalt melts (compositions 13 and 14 in Table 1), the investigations are limited (Zhang and Stolper 1991; Okumura and Nakashima 2006; Persikov et al. 2010) and the range of H_2O_t covered in experiments is only ≤ 1.1 wt%. Assuming $D_{H_2O_t}$ is proportional to H_2O_t and ignoring the pressure effect on the diffusivity (the validity of this assumption needs confirmation), Zhang et al. (2007) summarized the data and expressed $D_{H_2O_t}$ as follows at 673-1773 K, ≤ 1 GPa and ≤ 1.1 wt% H_2O_t:

$$D_{H_2O_t}^{\text{basalt}} = C_w \exp\left(-8.56 - \frac{19110}{T}\right) \tag{22}$$

where T is in K and C_w is wt% of H_2O_t. The recent high temperature data on a haplobasalt melt (62.2 wt% SiO_2, 10.5 wt% Al_2O_3, 6.8 wt% MgO; 14.2 wt% CaO and 6.3 wt% Na_2O) by Persikov et al. (2010) are about 0.17 times those on a MORB melt (composition 13 in Table 1)

by Zhang and Stolper (1991) when compared at 1 wt% H_2O_t assuming. It is not clear whether this difference is due to the significant compositional difference between the two melts, or due to the different H_2O_t concentration coverage, or due to experimental uncertainties.

Trachyte melts. For trachyte melt (composition 12 in Table 1), there has been only one study (Freda et al. 2003). The equilibrium constant K for Reaction (1) for trachyte melts has not been characterized. Assuming $D_{H_2O_t}$ is proportional to H_2O_t, Zhang et al. (2007) summarized the data and expressed $D_{H_2O_t}$ as follows at 1334-1601 K, 1 GPa and ≤ 2 wt% H_2O_t:

$$D_{H_2O_t}^{\text{trachyte}} = C_w \exp\left(-10.90 - \frac{17975}{T}\right) \tag{23}$$

where T is in K and C_w is wt% of H_2O_t. The H_2O diffusivity in trachyte melt is slightly (by a factor of about 3) higher than that in andesite melt with a similar SiO_2 content. Combining this observation with the small difference in the H_2O diffusivity between metaluminous rhyolite and peralkaline rhyolite, it appears that H_2O diffusivity in silicate melts depends primarily on the SiO_2 content, and the effects of other components, such as alkalinity, are minor (though still noticeable).

Self-diffusion of H_2O. The above discussion is on the chemical diffusion or effective binary diffusion of H_2O, when there is a chemical concentration (or chemical potential) gradient in H_2O. Limited data on the self-diffusion of H_2O, or exchange of ^2H_2O and ^1H_2O in a chemically homogeneous system (i.e., without H_2O chemical concentration gradients), are available (e.g., Nowak and Behrens 1997). The theoretical analysis by Zhang et al. (1991b) showed that the self-diffusivity of H_2O ($D_{^1H_2O\text{-}^2H_2O}$) can be written as follows if H_2O_m is the diffusing species:

$$D_{^1H_2O\text{-}\ ^2H_2O} = D_{H_2O_m}\frac{X_m}{X} = D_{H_2O_t}\frac{X_m / X}{dX_m / dX} \tag{24}$$

where X and X_m are mole fractions of H_2O_t and H_2O_m on a single oxygen basis. The ratio (X_m/X) can be calculated as follows (Eqn. 13 in Zhang 1999b):

$$\frac{X_m}{X} = \frac{8X}{8X + K(1-2X) + \sqrt{K^2(1-2X)^2 + 16KX(1-X)}} \tag{25}$$

where K is the equilibrium constant of Reaction (1). The calculation of dX_m/dX can be found from Equation (13). The values of $(X_m/X)/(dX_m/dX)$ are shown in Figure 3 for $K = 0.5$, and vary from 0.5 at 0 wt% H_2O_t to 0.67 at 7 wt% H_2O_t. Hence, at low H_2O_t, the D-H self-diffusivity $D_{^1H_2O\text{-}^2H_2O}$ is about 0.5 times $D_{H_2O_t}$ (Doremus 1969; Zhang et al. 1991b). At higher H_2O_t, $D_{^1H_2O\text{-}^2H_2O}$ is closer to $D_{H_2O_t}$ (such as 0.7 times $D_{H_2O_t}$). The data of Nowak and Behrens (1997) are consistent with the above results. This analysis shows that under some conditions, self-diffusivity is smaller than chemical diffusivity, although some studies showed that self-diffusivity is often greater than chemical (effective binary) diffusivity (Lesher 1990, 1994; Zhang 1993; Van der Laan et al. 1994).

All natural silicate melts. For rhyolite to andesite melts in the calc-alkaline series, Behrens et al. (2004) provided an expression of H_2O_t diffusivity at 1 wt% H_2O_t, Okumura and Nakashima (2006) related the H_2O_t diffusivity at 0.7 wt% H_2O_t to NBO/T (ratio of non-bridging oxygen to tetrahedrally coordinated cations) in the melt, and Ni et al. (2009a) presented a new diffusivity expression specifically for intermediate temperatures (700-900 K). In all three studies, a single parameter (silica content or NBO/T) is used to characterize the complicated melt composition variation, which is clearly a simplification.

H_2O_t diffusivities at 1 wt% H_2O_t in various melts are summarized in Figure 11. Continuing the effort of Behrens et al. (2004) and Ni et al. (2009a), we use H_2O_t diffusivity data from 116

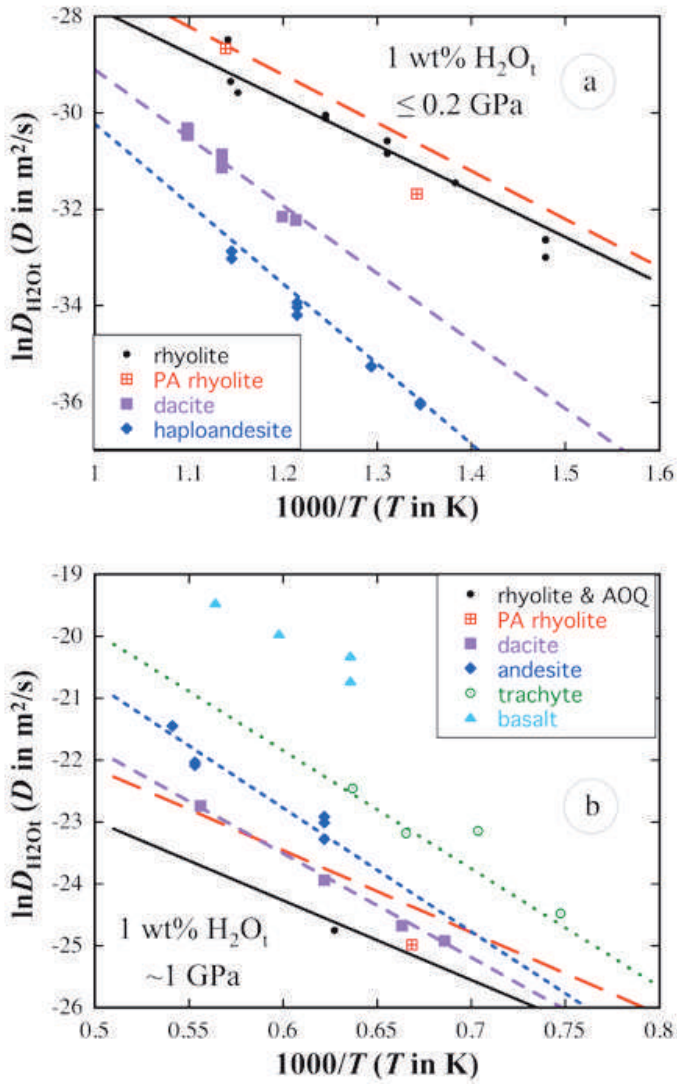

Figure 11. Comparison of H_2O_t diffusivity at 1 wt% H_2O_t in different melts at (a) intermediate temperatures and ≤ 0.2 GPa; and (b) high temperatures and 1 GPa. The trend from rhyolite to dacite to andesite is the opposite in the two cases. H_2O_t diffusivity is higher in peralkaline melts than in metaluminous and peraluminous melts. The lines (of the same color in the online version as the data points; solid line for rhyolite melt; long dashes for peralkaline rhyolite; medium dashes for dacite; short dashes for andesite; and dot line for trachyte) are calculated for the appropriate melt by Equation (26).

experiments by IR profiling method except for basalt melts, and arrive at the following general model for $D_{H_2O_t}$ at 1 wt% H_2O_t:

$$\ln D^{1\text{ wt\%}}_{H_2O_t} = 12.06 + 14.75\text{AI} - 42.22\text{Si} + 2.716P \times \text{Si} - \frac{42021 - 45407\text{Si} + (7409\text{Si} - 1593)P}{T} \quad (26)$$

where D is in m²/s, T is in K, P is in GPa, Si is the cation mole fraction of Si, and AI = Na+K-Al where Na, K and Al are cation mole fractions. One additional compositional parameter AI is used in the above fitting compared to the models of Behrens et al. (2004) and Ni et al. (2009a). The above expression reproduces all the literature data for rhyolite-peralkaline rhyolite-dacite-andesite-haploandesite-trachyte composition within a factor of 2, covering 676-1629 K and 0-1.9 GPa (Fig. 11). Equation (26) can also be used to estimate the H_2O_t diffusivity at <1 wt% H_2O_t at intermediate temperatures and ≤ 3 wt% H_2O_t at high temperatures with the aid of proportionality assumption. The data on basalt melt (Zhang and Stolper 1991) cannot be modeled well using a simple compositional dependence. The reason is not clear. The data of Okumura and Nakashima (2004, 2006) are not included in the fitting because they are not based on measured profiles.

To develop a more general expression of H_2O diffusivity in all natural silicate melts at both high and low H_2O_t for geological applications, more experimental data are necessary. The critical data include diffusion in basalt melts at high H_2O_t at both high and intermediate temperatures, and in andesite melts at high H_2O_t and intermediate temperatures. Furthermore, it is necessary to resolve the dependence of $D_{H_2O_t}$ on H_2O_t content in high-temperature andesite melts by careful experiments. More data on peralkaline melts from basanite to phonolite to further confirm that the effect of peralkalinity is small would also greatly help. For specific modeling involving a melt that is very different from studied melts (such as lunar basalt – Saal et al. 2008; Zhang 2009), it is essential to obtain at least a few data points to verify that the compositional difference does not lead to very different H_2O diffusivities.

Some clarifying points. Below are some additional points of clarification:

(1) Although we often say that $D_{H_2O_t}$ is proportional to H_2O_t at low H_2O_t (≤ a couple of percent), meaning that $D_{H_2O_t}$ approaches zero as H_2O_t approaches zero, it is just an approximation. In theory, $D_{H_2O_t}$ approaches D_{OH} as H_2O_t approaches zero ($d[H_2O_m]/d[H_2O_t]$ would be so small so that OH diffusion will dominate). That is, if species equilibrium is reached, $D_{H_2O_t}$ is linear with H_2O_t with a very small intercept D_{OH}, but D_{OH} is so small that it has not been resolved experimentally in natural melts discussed above. However, in a soda lime silicate melt (74 mol% SiO_2, 10 mol% CaO, and 16 mol% Na_2O) and a float melt (72.5 mo% SiO_2, 0.4 mol% Al_2O_3, 3.3 mol% MgO, 9.8 mol% CaO, and 13.7 mol% Na_2O), $D_{H_2O_t}$ is independent of H_2O_t concentration at 0.02 to 0.25 wt% H_2O_t (Behrens 2006), possibly indicating that the D_{OH} limit is reached, as well as fairly large D_{OH} values for these sodic melts.

(2) The proportionality relation at low H_2O_t and Equation (13) holds only when there is rough equilibrium between H_2O_m and OH for Reaction (1). Because the reaction rate constant increases with increasing temperature and H_2O_t, equilibrium is reached at relatively high temperature but not low temperature. For a given temperature, the proportionality applies at high H_2O_t but not very low H_2O_t; what can be considered as very low H_2O_t depends on the temperature. For example, Jambon et al. (1992) showed that for rhyolite melt, at 0.114 wt% H_2O_t and 783 K, Equation (13) and the proportionality relation do not hold. Therefore, regarding point (1), in many cases the proportionality relation may already be inapplicable before H_2O_t becomes so low that D_{OH} becomes important.

(3) H_2O_m diffusivity is a modeling parameter that depends on the accuracy of the equilibrium constant K, which in turn depends on the accuracy of the infrared calibration to measure species concentrations. On the other hand, H_2O_t diffusivity is constrained by the length and shape of the measured H_2O_t concentration profiles. Hence, if K values in a melt are improved in the future, one cannot simply use the new K values in the above equations in conjunction with $D_{H_2O_m}$ above to calculate $D_{H_2O_t}$ because the H_2O_m diffusivities themselves are based on the specific K values. That is, internal consistency must be maintained for accurate calculation of $D_{H_2O_t}$. The expressions of K values listed above should still be used to calculate $D_{H_2O_t}$ unless a new $D_{H_2O_m}$ expression is obtained by using the new K values.

(4) If different experimental methods are applied to characterize $D_{H_2O_t}$ as a function of H_2O_t content (i.e., using concentration profiles), the diffusivity values at given T-P-H_2O_t and melt composition conditions should be independent of the method (such as diffusion couple, dehydration, hydration, etc.) However, some methods can only obtain average diffusivities (e.g., mass loss or gain methods), and different averages may have different meanings, leading to different diffusivities. For example, under the same conditions, the average $D_{H_2O_t}$ value during dehydration experiments (during

which H_2O diffuses out) and that during hydration experiments (during which H_2O diffuses in) are different (Moulson and Roberts 1961; Zhang et al. 1991a; Wang et al. 1996; Zhang 1999b; Figure 3-33 in Zhang 2008). If the surface H_2O_t during hydration experiments is the same as the initial H_2O_t during dehydration experiments, and the minimum H_2O_t concentration is zero, and if $D_{H_2O_t}$ is proportional to H_2O_t, then (Zhang et al. 1991a; Wang et al. 1996):

$$D_{in} = 0.619 D_{X_s} \tag{27a}$$

$$D_{out} = 0.347 D_{X_i} \tag{27b}$$

$$D_{in} = 1.78 D_{out} \tag{27c}$$

where D_{X_i} is $D_{H_2O_t}$ at the initial H_2O_t content of the sample during dehydration, and D_{X_s} is $D_{H_2O_t}$ at the surface H_2O_t content of the sample during hydration. Ni and Zhang (2008) showed how to derive the general relation between D_{out} and D_{X_i}.

There have also been many studies on obsidian hydration near room temperatures (e.g., Friedman and Long, 1976; Cole an Chakraborty 2001; Riciputi et al. 2002; Anovitz et al. 2004, 2006, 2008). These studies are not discussed here because (i) they do not seem to fit neatly into the diffusion data trends by higher-temperature data, probably due to effects of disequilibrium that cannot be treated simply, and (ii) our focus here is on silicate melts at high temperatures to intermediate temperatures (e.g., > 600 K), not surface processes at room temperatures.

MOLECULAR H_2 DIFFUSION

In terrestrial magmas, hydrogen is typically oxidized and hence in the form of the hydrous component. Under extremely reducing conditions, the hydrogen component may be present in the elemental form as molecular H_2. Diffusion of molecular H_2 is different from that of H_2O and may play a role under very low f_{O_2}. In this section, diffusion of molecular H_2 is reviewed for completeness of coverage, and also for discussing the possible role of H_2 diffusion relative to H_2O diffusion in natural silicate melts.

H_2 has not been detected as a dissolved gas species in terrestrial silicate melt because it is easily oxidized in natural melts when there is ferric iron present. To understand H_2 diffusion, it is necessary to avoid H_2 oxidation so that pure molecular H_2 (that is, the ratio of H_2/H_2O is >> 1) diffusion can be characterized. Therefore, H_2 diffusion experiments must be conducted under very reducing conditions. Under such reducing conditions, iron in natural melts would be significantly reduced to metallic Fe, which would complicate the experiments. Hence, extensive and reliable H_2 as well as D_2 diffusion data are available only for pure silica glass. There are more data on D_2 diffusion (Lee et al. 1962; Lee 1963; Perkins and Begeal 1971; Shelby 1977) than on H_2 diffusion (Barrer 1941; Lee et al. 1962; Lee 1963; Shang et al. 2009).

Molecular H_2 diffusion data on other melts and glasses are limited and their reliability is uncertain. Chekhmir et al. (1985) tried to infer molecular H_2 diffusivity in albite melt based on reduction-induced color change (by reducing CO_2 to graphite). Gaillard et al. (2002, 2003a,b) investigated the kinetics of reduction of Fe^{3+} to Fe^{2+} by molecular H_2 in rhyolite melts, and tried to infer molecular H_2 diffusivity (Gillard et al. 2003b). Because the mechanisms of these complicated process (including solution, reactions and diffusion) are not well quantified (e.g., what the redox reaction kinetics are, whether the redox reaction plays a role in limiting the entire process, how the process depends on H_2 fugacity), it is not clear whether the inferred molecular H_2 diffusivity data are correct. The activation energy for "molecular H_2 diffusion" inferred by Chekhmir et al. (1985) is 113 kJ/mol (clearly too high, more likely reflect molecular H_2O diffusion), and by Gillard et al. (2003b) is about 40 kJ/mol (more reasonable). Even though

it is not clear whether the estimated H_2 diffusivities by Gaillard et al. (2003b) are correct, the method used by Gaillard et al. (2003a,b) has great potential because they were able to measure both molecular H_2 and OH bands by infrared spectroscopy (the H_2 peak at 415 mm^{-1} is weak in IR spectra but detectable), and it may hence be possible to treat the problem quantitatively in a similar fashion as in Zhang et al. (1991a) to understand both the redox reaction and diffusion. In the discussion below, we focus on H_2 and D_2 diffusion in silica glass (in the glass science literature, silica glass is sometimes referred to fused quartz, or even simply "quartz"), rather than the unverified semi-quantitative data by Chekhmir et al. (1985) and Gillard et al. (2003b).

Most experimental data on H_2 and D_2 diffusion in silica glass are based on permeation experiments, in which gas permeates from one side of a glass (in contact with hydrogen gas of, e.g., 90 kPa) to the other side (a vacuum line connected to a mass spectrometer). It takes some time for the gas to diffuse through the glass and reach a steady state. Hence, there is a pre-steady-state stage, during which the gas flux builds up; there is also a post-steady-state stage, during which the gas flux gradually decays to zero. Permeability (SI units: $mol \cdot m^{-1} \cdot s^{-1} \cdot Pa^{-1}$) is directly obtained from the experimental flux and pressure gradient (pressure difference in two chambers divided by the thickness of the glass wafer) at steady-state permeation. Diffusivity may be calculated either from the measured permeability and solubility, or from the non-steady state decay after the steady-state permeation terminates (or build-up at the beginning of the permeation experiments). Because absolute concentrations are difficult to measure accurately, the error in the solubility often dominates the error in the diffusivity if the solubility is needed to estimate the diffusivity. In addition, pre-existing OH in the silica glass may contribute to the permeation flux, and dissolved hydrogen molecules (including both H_2 and D_2) may react with silica to form bound hydrogen such as OH or SiH (Shelby 1994). Hence, experimental data must be carefully examined so that these effects are avoided. Shelby (1977) showed that once these effects are accounted for, D_2 (and H_2) diffusivities can be obtained consistently.

Even though several groups investigated H_2 permeation and diffusion in silica in 1910-1940, as summarized in Barrer (1941), these earlier data were often an order of magnitude off (Shang et al. 2009) and are not discussed here. Lee et al. (1962) measured the diffusivity of H_2 and D_2 and found the data at $T > 1073$ K are scattered and do not follow the trend defined by lower-temperature data. This was explained by a possible reaction of H_2 or D_2 with silica network at high temperature. They also found that the diffusivity determined at the decay stage of the permeation experiments is more reliable than that determined from the build-up stage, likely because the sample is more fully annealed at the decay stage. Lee (1963) investigated the effect of impurities in the silica glass and obtained new H_2 and D_2 diffusivity data at 600-1300 K. The effect of impurities including Al_2O_3 (ranging from 0.1 to 160 ppm) and OH (10 to 3000 ppm) in silica glass turned out to be small as long as care is taken to avoid possible reactions and to use only the steady state and post-steady-state data. The data in Lee et al. (1962) are not discussed further because the work was superseded by Lee (1963). Perkins and Begeal (1971) reported D_2 (and noble gas element) diffusivities in silica glass at 298-448 K. Shelby (1977) determined D_2 diffusivities in various silica glasses at 450-1000 K, and the differences were found to be no more than 0.17 log units (0.38 ln units) (these are highly reproducible experiments with internal precision better than 10% relative, or 0.04 log units). Shang et al. (2009) developed a new technique and obtained H_2 diffusivities at 296-523 K. All of these studies were conducted at low pressures (often less than one atmosphere pressure).

Figure 12 compares all the H_2 and D_2 diffusion data in Lee (1963), Perkins and Begeal (1971), Shelby (1977), and Shang et al. (2009). Data scatter is small; the maximum minus minimum at a given temperature is about 0.4 in ln$D$. At high temperatures, H_2 and D_2 diffusion was investigated by the same author (Lee 1963) on the same silica glass, and it was found that H_2 diffusivity is greater than D_2 diffusivity, as expected, but by only about 20%, not the theoretical 41% difference based on the square root of mass relation. The difference of 20% is

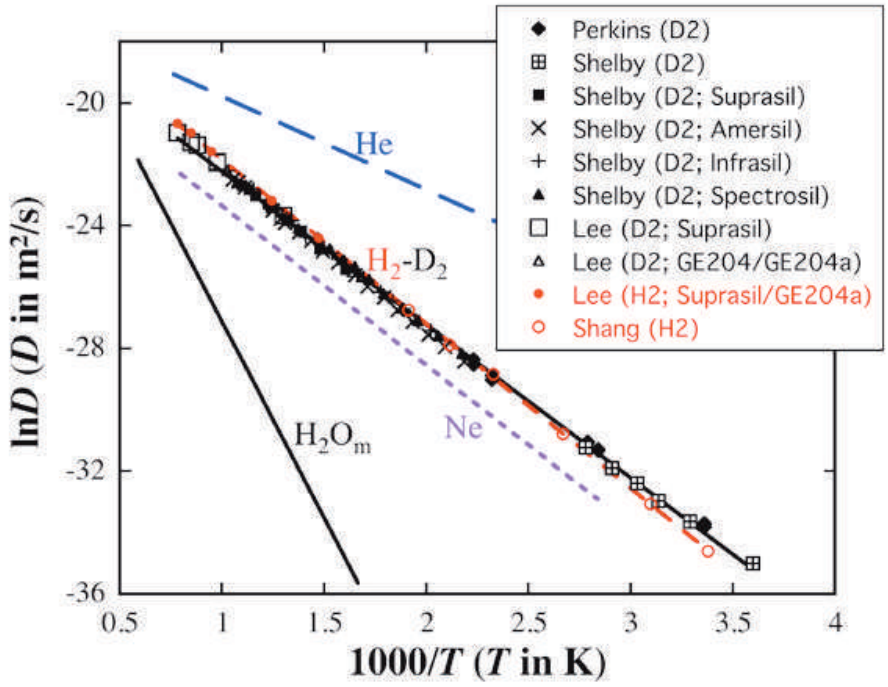

Figure 12. Diffusion data of H_2 and D_2 from literature (Lee 1963; Perkins and Begeal 1971; Shelby 1977; Shang et al. 2009). Data of Lee (1963) and Shelby (1977) are read from figures in these papers. Nominal errors on the data are smaller than the symbols. He and Ne diffusion data in silica glass (Swets et al. 1961; Frank et al. 1961; Perkins and Begeal 1971; Behrens 2010), and molecular H_2O_m diffusion in nominally dry rhyolite melt (Ni and Zhang 2008) are shown for comparison.

large enough to be distinguished in the same glass by the same author when self-consistency is high, but roughly within error when results from different silica glasses and different authors are compared. At lower temperatures (<500 K), H_2 diffusivity is apparently smaller than D_2 diffusivity, and the difference can reach 20% relative (except for one point at room temperature that deviates more). This difference is probably due to differences between various silica glasses (such as different OH content), and accuracy of the solubility models used. Because there are more data on D_2 diffusion and they are all obtained by similar permeation methods with more careful assessment of glass composition, the uncertainties on D_2 diffusivities are smaller.

Fitting H_2 and D_2 diffusion data (Shang et al. 2009; Shelby 1977) by the Arrhenian relation leads to:

$$D_{H_2}^{\text{silica melt}} = \exp\left(-(16.471 \pm 0.070) - \frac{(5363 \pm 33.4)}{T}\right) \tag{28}$$

$$D_{D_2}^{\text{silica melt}} = \exp\left(-(17.228 \pm 0.042) - \frac{(4996 \pm 21.8)}{T}\right) \tag{29}$$

where D is in m^2/s, T is in K, and errors are given at the 2σ level. The activation energy for H_2 or D_2 diffusion is low, of the order 41-45 kJ/mol.

However, the relation between D_2 diffusivity and temperature is slightly non-Arrhenian (e.g., Shelby 1977), which can be captured well by the following expression:

$$D_{D_2}^{\text{silica melt}} = T \cdot \exp\left(-(24.546 \pm 0.031) - \frac{(4480.5 \pm 16.1)}{T}\right) \tag{30}$$

where D is in m^2/s, and T is temperature in K. The above equation reproduces all experimental D_2 diffusion data in silica melt and glass within 24% (2σ error in ln$D$ is 0.20, which is mainly due to differences between different silica glasses). The implied Arrhenian activation energy from the above equation depends somewhat on temperature as $R(4480.5+T)$ based on the above equation where R is the universal gas constant and T is temperature in K. That is, the activation energy varies from 39.7 to 45.6 kJ/mol from 300 to 1000 K.

When compared with diffusivities of neutral noble gas molecules in silica melt (Swets al. 1961; Frank et al. 1961; Perkins and Begeal 1971), H_2 and D_2 diffusivities are between that of He and Ne (Fig. 12). Furthermore, the activation energy for H_2 and D_2 diffusion is similar to that for Ne diffusion and is greater than that for He diffusion.

Below, we evaluate the possible role of molecular H_2 diffusion to the diffusion of the hydrogen component (including H_2O_m and OH). In the presence of H_2, one-dimensional diffusion of total hydrogen component can be expressed as (following Zhang et al. 1991b):

$$\frac{\partial C_{\text{total H}}}{\partial t} = \frac{\partial}{\partial x}\left(D_{\text{H}_2} \frac{2\partial C_{\text{H}_2}}{\partial x} + D_{\text{H}_2\text{O}_\text{m}} \frac{2\partial C_{\text{H}_2\text{O}_\text{m}}}{\partial x} \right) \tag{31}$$

where C is concentration in mol/m^3, $C_{\text{total H}}$ is total H concentration (moles of H atoms per m^3), D_{H_2} and $D_{\text{H}_2\text{O}_\text{m}}$ are molecular H_2 and molecular H_2O diffusion coefficients, and OH diffusion is ignored as discussed earlier. The factor of 2 in the above equation is due to the fact that each H_2 molecule or H_2O_m molecule contains two H atoms and the hydrogen atoms are used to represent the hydrogen component. Comparing the above equation with

$$\frac{\partial C_{\text{total H}}}{\partial t} = \frac{\partial}{\partial x}\left(D_{\text{total H}} \frac{\partial C_{\text{total H}}}{\partial x} \right) \tag{32}$$

where $D_{\text{total H}}$ is the total H diffusivity, we obtain:

$$D_{\text{total H}} \frac{\partial C_{\text{total H}}}{\partial x} = D_{\text{H}_2} \frac{2\partial C_{\text{H}_2}}{\partial x} + D_{\text{H}_2\text{O}_\text{m}} \frac{2\partial C_{\text{H}_2\text{O}_\text{m}}}{\partial x} \tag{33}$$

Assuming local chemical equilibrium between various hydrogen species (including H_2, H_2O_m, and OH), then,

$$D_{\text{total H}} = 2D_{\text{H}_2} \frac{\partial C_{\text{H}_2}}{\partial C_{\text{total H}}} + 2D_{\text{H}_2\text{O}_\text{m}} \frac{\partial C_{\text{H}_2\text{O}_\text{m}}}{\partial C_{\text{total H}}} \tag{34}$$

Hence, the ratio of the molecular H_2 diffusion contribution to the molecular H_2O_m contribution is (again assuming local chemical equilibrium among species):

$$\text{Ratio} = \frac{D_{\text{H}_2}}{D_{\text{H}_2\text{O}_\text{m}}} \frac{\partial C_{\text{H}_2}}{\partial C_{\text{H}_2\text{O}_\text{m}}} = \frac{D_{\text{H}_2} C_{\text{H}_2}}{D_{\text{H}_2\text{O}_\text{m}} C_{\text{H}_2\text{O}_\text{m}}} \tag{35}$$

The last equal sign in the above equation holds if H_2 concentration is proportional to that of H_2O_m (e.g., uniform oxygen fugacity). If the ratio equals 1, the two species contribute equally. If the ratio is smaller than 1, molecular H_2O diffusion contributes dominantly. If the ratio is greater than 1, molecular H_2 diffusion contributes dominantly. The contribution of H_2 to total H diffusion depends on the concentration ratio of H_2/H_2O_m and the diffusivity ratio.

H_2/H_2O_m in a given melt depends on the H_2/H_2O ratio in the gas or fluid phase (which depends on oxygen fugacity f_{O_2}) and the solubility of H_2 and H_2O. First, we consider the oxidation reaction in the gas phase:

$$H_2O(g) \rightleftharpoons H_2(g) + ½\ O_2(g) \tag{36}$$

The equilibrium constant ($K_{H_2\text{-}H_2O}$) can be written as:

$$K_{H_2\text{-}H_2O} = \frac{f_{H_2} f_{O_2}^{1/2}}{f_{H_2O}} \tag{37}$$

where f stands for fugacity. Using thermodynamic data in Robie and Hemingway (1995), the equilibrium constant depends on temperature as follows:

$$K_{H_2\text{-}H_2O} = \exp\left(6.347 - \frac{29435}{T}\right) \text{bar}^{1/2} \tag{38}$$

where T is in K. At 298.15 K, $K_{H_2\text{-}H_2O} = 7.6\times10^{-41}$ bar$^{1/2}$; at 1800 K, $K_{H_2\text{-}H_2O} = 4.5\times10^{-5}$ bar$^{1/2}$. Hence, at a given f_{O_2}, f_{H_2}/f_{H_2O} ratio increases with temperature. Oxygen fugacity in natural magmas is often within 2 log units of Ni-NiO (NNO) buffer (Carmichael and Ghiorso 1990). Figure 13a shows f_{H_2}/f_{H_2O} ratio as a function of temperature along the NNO buffer (plus or minus 2 log units) using the thermodynamic data in Robie and Hemingway (1995) (the NIST-JANAF Thermodaynamic Data Table does not contain data on NiO). It can be seen that f_{H_2}/f_{H_2O} is often of the order 10^{-4} to 0.1 in the gas phase in equilibrium with natural melts. Note that the f_{H_2}/f_{H_2O} ratio is different from the H_2/H_2O_m concentration ratio in the melt, which also depends on the solubility of H_2 and H_2O.

To relate the fugacity ratio to the molar concentration ratio of dissolved H_2 to H_2O_m concentrations in a melt, it is necessary to know the solubility of both H_2 and H_2O_m (not H_2O_t). Note that resorting to solubility here does not necessarily mean the investigated melt is saturated with respect to molecular or H_2 or H_2O_m. No reliable data are available for both H_2 and H_2O_m solubility and diffusivity in any given melt. There are H_2 solubility and diffusivity data on

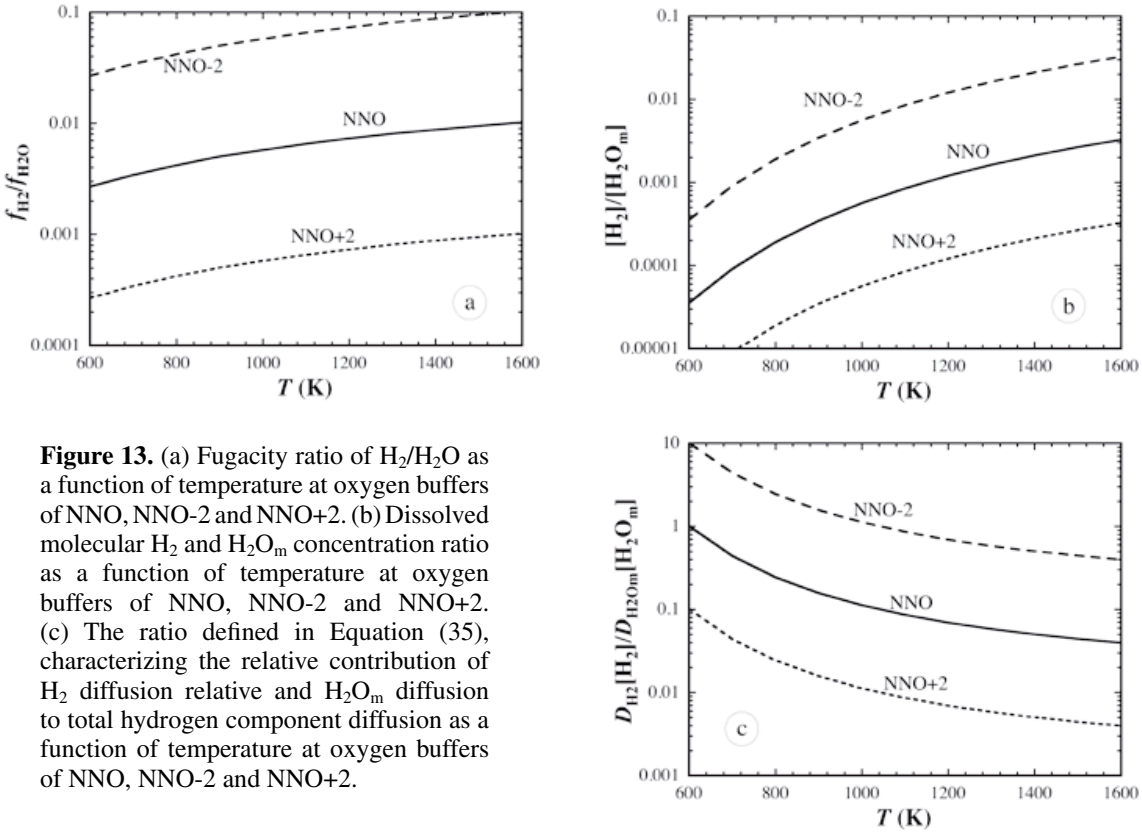

Figure 13. (a) Fugacity ratio of H_2/H_2O as a function of temperature at oxygen buffers of NNO, NNO-2 and NNO+2. (b) Dissolved molecular H_2 and H_2O_m concentration ratio as a function of temperature at oxygen buffers of NNO, NNO-2 and NNO+2. (c) The ratio defined in Equation (35), characterizing the relative contribution of H_2 diffusion relative and H_2O_m diffusion to total hydrogen component diffusion as a function of temperature at oxygen buffers of NNO, NNO-2 and NNO+2.

silica melt and glass (Shackelford et al. 1972; Shelby 1977; Shang et al. 2009) but no H_2O_m solubility and diffusivity data (though there are extensive H_2O_t solubility and diffusivity data, e.g., Moulson and Roberts 1961; Roberts and Roberts 1964; Doremus 1969, 1973; Tomozawa 1985). There are H_2O_m solubility and diffusivity data on rhyolite melt (Zhang et al. 1991a; Zhang 1999b; Ni and Zhang 2008). For a rough estimation, we assume the H_2 solubility and diffusivity in silica melt are similar to those in rhyolite melt. The molecular solubilities of H_2 (Shackelford et al. 1972) and H_2O_m (Zhang 1999b) are as follows:

$$S_{H_2}^{\text{silica melt}} = \exp\left(-13.662 + \frac{1068}{T}\right) \tag{39}$$

$$S_{H_2O_m}^{\text{rhyolite melt}} = \exp\left(-14.193 + \frac{3890}{T}\right) \tag{40}$$

where the solubilities (S_{H_2} and $S_{H_2O_m}$) are in $mol \cdot m^{-3} \cdot Pa^{-1}$. Hence, at a given f_{O_2} buffer, the molar concentration ratio of $[H_2]/[H_2O_m]$ can be estimated from $(f_{H_2}/f_{H_2O}) \cdot (S_{H_2}/S_{H_2O_m})$, as shown in Figure 13b (assuming H_2 solubility in rhyolite is the same as that in silica melt). It can be seen that under typical terrestrial conditions, $[H_2]/[H_2O_m]$ is low. Because the ratio of $[H_2]/[H_2O_m]$ is low in terrestrial melts, the total hydrogen component is largely in the form of H_2O_m and OH. It is hence appropriate to refer to the total hydrogen component as the hydrous component (but molecular hydrogen can still play a role in the diffusion of the hydrous component, see below). However, in lunar melts that are much more reducing, the $[H_2]/[H_2O_m]$ ratio may be greater than 1, and the total hydrogen component is not simply the hydrous component.

Next, again assuming the H_2 diffusivity in rhyolite melt is the same as that in silica melt, using the molecular H_2 diffusivity of Shang et al. (2009) (Eqn. 28) and the molecular H_2O_m diffusivity of Ni and Zhang (2008) (Eqn. 14), the ratio $(D_{H_2}[H_2])/(D_{H_2O_m}[H_2O_m])$ as a function of temperature and oxygen fugacity buffer is plotted in Figure 13c. It can be seen that when oxygen fugacity is at NNO or higher, diffusion of the total hydrogen component is dominantly due to H_2O_m diffusion except for temperatures below 600 K. Under more reducing conditions (that can be encountered in terrestrial melts), at typical magmatic temperatures (≥ 1100 K), H_2O_m diffusion still dominates the total hydrogen component flux, but molecular H_2 diffusion may dominate the diffusive flux of the total hydrogen component at temperatures below typical magmatic temperatures. It is emphasized that this conclusion is tentative because of the many assumptions involved. Previous experimental diffusion studies (e.g., Shaw 1974; Delaney and Karsten 1981; Karsten et al. 1982; Zhang et al. 1991a; Zhang and Stolper 1991; Nowak and Behrens 1997; Zhang and Behrens 2000; Behrens et al. 2004; Liu et al. 2004b; Okumura and Nakashima 2004, 2006; Ni and Zhang 2008; Behrens and Zhang 2009; Ni et al. 2009a,b; Wang et al. 2009) on the H_2O component were conducted without detailed characterization of the oxygen fugacity. Nonetheless, the consistency of these experimental data (e.g., Ni and Zhang 2008) show that H_2 diffusion probably did not play a major role in any of these studies. Furthermore, simultaneous H_2O and ^{18}O diffusion studies in the same experiments (Behrens et al. 2007) show that H_2O_m that carries O, not H_2 that does not carry O, is the diffusing species for the hydrous component. In the future, it will be important to investigate diffusion of the total hydrous component under very reducing conditions with well-characterized oxygen fugacity (e.g., oxygen fugacity that is uniform in the sample and independent of time).

In short, it is possible that molecular H_2 diffusion could play a major role in transporting the hydrous component under reducing conditions that may be encountered in terrestrial melts. However, this inference is uncertain at present because of the many assumptions involved. New experimental studies are necessary to resolve this issue.

DIFFUSION OF THE CO_2 COMPONENT

Zhang et al. (2007) reviewed CO_2 diffusion in silicate melts. Not much new work has been published on natural melts since then. For completeness of this chapter and this review volume, a brief summary is provided here. Dissolved CO_2 is present in silicate melts in either CO_2 molecules or carbonate groups (Fine and Stolper 1985; Blank and Brooker 1994). Hence, CO_2 diffusion is also a multi-species diffusion. However, the presence of multiple species seems to contrive to simplify the diffusion properties of CO_2, contrary to the case of H_2O diffusion (Zhang et al. 2007).

Watson et al. (1982) were the first to investigate tracer diffusion of carbonate (using ^{14}C tracer diffusion) in silicate melts, and made the surprise discovery that CO_2 diffusivity does not depend on the anhydrous melt composition (from a haplobasalt to melt containing 30 wt% Na_2O). More extensive ^{14}C tracer diffusion studies by Watson (1991) confirmed this conclusion but also showed that the diffusivity depends strongly on H_2O_t. Watson et al. (1982) and Watson (1991) determined concentration profiles using β-track maps made by exposing nuclear emulsion plates to the quenched and sectioned diffusion capsules. As discussed in Mungall (2002), the β-particle range is of the order of a hundred μm (International Commission on Radiation Units and Measurements 1984), much more than initially thought. Hence, tracer diffusion data using β-track maps may be compromised by this effect (those diffusivities extracted from concentration profiles longer than 1 mm are less affected). Furthermore, Zhang et al. (2007) showed that the data are inconsistent with effective binary diffusivities of CO_2. Hence, ^{14}C tracer diffusion data of Watson et al. (1982) and Watson (1991) are not discussed further in quantitative treatment.

Blank (1993), Sierralta et al. (2002) and Nowak et al. (2004) (as well as Fogel and Rutherford 1990, Zhang and Stolper 1991, and Liu 2003) investigated effective binary diffusion of CO_2 at CO_2 concentration levels of hundreds to thousands of ppm. For the purpose of modeling natural magmatic processes (e.g., CO_2 bubble growth in a basalt melt), the effective binary diffusivities of total CO_2 are the necessary diffusivities. These studies further confirmed the rough independence of CO_2 diffusivity on anhydrous melt composition. This independence is even more surprising considering that CO_2 is present as CO_2 molecules in rhyolite melt but as CO_3^{2-} ion in basalt melt. Nowak et al. (2004) explained the dependence as follows: Assume molecular CO_2 is the diffusing species whereas CO_3^{2-} is roughly immobile. From rhyolite melt to basalt melts, molecular CO_2 diffusivity increases (similar to Ar diffusivity), which increases total CO_2 diffusivity, but the fraction of dissolved CO_2 present as molecular CO_2 decreases (the rest is CO_3^{2-}), which decreases the total CO_2 diffusivity. The two factors roughly cancel each other, leading to a total CO_2 diffusivity roughly independent of the anhydrous melt composition. Baker et al. (2005) carried out three carbonate dissolution experiments and measured total CO_2 concentration profiles by difference-from-100% method, and two diffusion couple experiments and measured CO_2 concentration profiles by FTIR. The compositions for which CO_2 diffusion has been investigated are listed in Table 2.

Because of its rough independence of the anhydrous melt composition, CO_2 is likely to be the first component for which the diffusivity in various melts can be predicted based on a limited number of studies, which can be compared to the large number of experimental studies on H_2O diffusion reviewed in the previous section. Existing experimental data on the effective binary diffusion of CO_2 cover 723-1623 K and ≤ 1 GPa. However, they are mostly on dry melts, with only 4 data points on hydrous melts containing ≥ 1 wt% H_2O_t, of which two points with 5 wt% H_2O_t by the reconnaissance experiments of Baker et al. (2005) apparently showed that adding 5 wt% H_2O_t does not affect CO_2 diffusivity in a trachyte melt, contrary to results by Sierralta et al. (2002) on albite melt and Watson (1991) on other melts. A possible explanation of the discrepancy is that determination of CO_2 concentration profiles by the difference-from-100% method used by Baker et al. (2005) does not work well for hydrous

Table 2. Chemical composition (wt% on dry basis) for CO_2 diffusion studies.

ID	Comp.	SiO_2	TiO_2	Al_2O_3	FeO	MnO	MgO	CaO	Na_2O	K_2O	P_2O_5	Ref
1	Rhyolite	76.45	0.08	12.56	1.02	.08	.06	.25	4.21	4.78		a
2	Rhyolite	77.5	0.07	13.0	0.56	0.04	0.05	0.52	4.10	4.18		b
3	Basalt	50.6	1.88	13.9	12.5	0.23	6.56	11.4	2.64	0.17	0.21	c
4	Ab	69.03		19.33					11.41			d
5	AbNa1	68.87		19.24					12.45			d
6	AbNa2	68.56		18.58					13.38			d
7	AbNa3	68.43		18.62					13.92			d
8	AbNa4	66.66		18.63					15.24			d
9	AbNa6	67.38		18.18					15.95			d
10	AbNa7	65.73		17.60					17.57			d
11	Rh (CO_2)	75.09	0.22	13.83			1.47	1.40	3.86	4.10		e
12	Da (CO_2)	71.78	0.40	15.31			2.26	3.09	4.52	2.97		e
13	DaAn (CO_2)	66.13	0.68	16.18			4.59	4.79	4.26	1.90		e
14	An (CO_2)	63.37	1.11	16.90			8.08	6.81	4.04	0.88		e
15	AnTh (CO_2)	61.92	1.55	15.22			8.79	6.74	3.73	1.33		e
16	Th (CO_2)	60.48	2.01	14.54			9.95	8.79	3.32	1.61		e
17	Ha (CO_2)	53.55	3.74	16.93			11.32	9.19	4.71	1.44		e
18	Trachyte	59.9	0.39	18.0	0.89	0.12	3.86	2.92	4.05	8.35	0.21	f

The compositions are listed on the anhydrous basis.

References: a. Fogel and Rutherford (1990); b. Blank (1993); c. Zhang and Stolper (1991); d. Sierralta et al. (2002); e. Nowak et al. (2004); f. Baker et al. (2005).

melts and hence CO_2 diffusivities in hydrous trachyte melt are incorrect.

Because total CO_2 diffusivity in all melts are similar to Ar diffusivity in silicic melts (Zhang et al. 2007), and extensive Ar diffusion data in silicic melts are available, covering a wide range of temperature, pressure and H_2O contents (673-1773 K, ≤ 1.5 GPa, and ≤ 5 wt% H_2O_t), Zhang et al. (2007) used such data to derive the following equation, which is proposed to be applicable for total effective binary diffusivity of CO_2 in basalt to rhyolite melts:

$$\ln D^{\text{all melts}}_{CO_{2,\text{total}}} = -13.99 - \frac{17367 + 1944.8P}{T} + \frac{(855.2 + 271.2P)}{T} C_w \qquad (41)$$

where D is in m^2/s, T is in K, P is in GPa, and C_w is wt% of H_2O_t.

Figure 14 compares experimental data and the above equation, especially the data by Baker et al. (2005) because the comparison with Baker et al. (2005) was not made in Zhang et al. (2007). It can be seen that the calculated line and the experimental data of the same color (the online version) are in rough agreement, except for the two data points at 5 wt% H_2O_t by Baker et al. (2005) (purple short-dashed line and purple solid squares in Fig. 14; the color can be seen in the online version). Excluding these two data points, the maximum uncertainty of the above equation in predicting $\ln D_{CO_{2,\text{total}}}$ (Fogel and Rutherford 1990; Zhang and Stolper 1991; Blank 1993; Sierralta et al. 2002; Nowak et al. 2004; Baker et al. 2005) is 1.13. This 2σ uncertainty is larger than typical experimental data uncertainty (with a 2σ of about 0.6 in ln$D$), because $D_{CO_{2,\text{total}}}$ depends weakly on melt compositions, which is ignored in the above treatment. New experimental data on CO_2 diffusion under conditions of high H_2O_t content are necessary to further constrain CO_2 diffusivities.

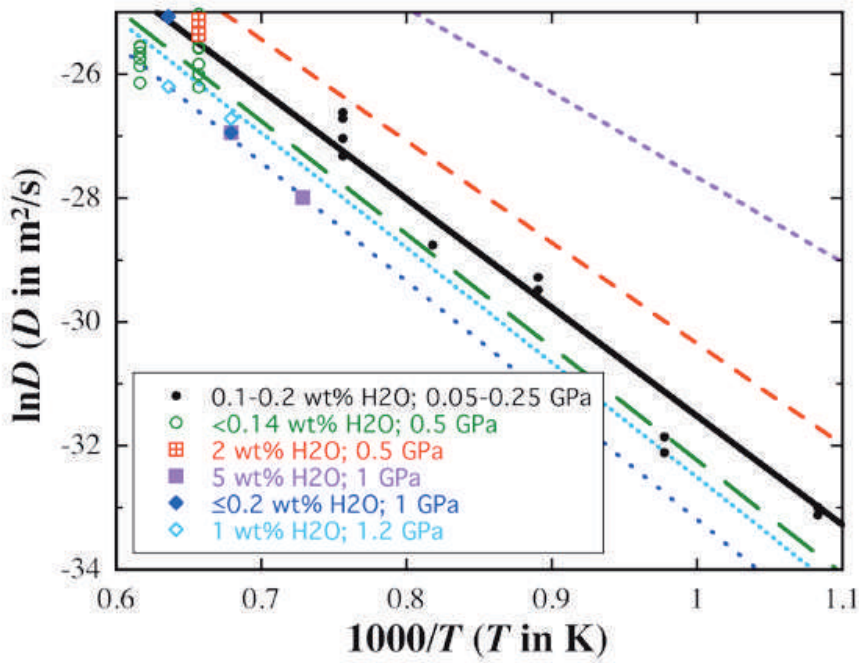

Figure 14. Comparison of experimental data of effective binary diffusivity of bulk CO_2 with Equation (41) under some conditions. The lines in matching color with data points (the colors can be seen in the online version) are calculated from Equation (41); solid line corresponding to solid circles; long dashes to open circles; medium dashes to squares with plus inside; short dashes (the uppermost line) to solid squares; sparse dot line to solid diamonds; and dense dot line to open diamonds. For clarity, low-temperature data are not shown. Data sources: "0.1-0.2 wt% H_2O; 0.05-0.25 GPa": Blank (1993) and Fogel and Rutherford (1990); "< 0.14 wt% H_2O; 0.5 GPa": Sierralta et al. (2002) and Nowak et al. (2004); "2 wt% H_2O and 0.5 GPa": Sierralta et al. (2002); "5 wt% H_2O; 1 GPa": Baker et al. (2005); "≤ 0.2 wt% H_2O; 1 GPa": Zhang and Stolper (1991) and Baker et al. (2005); "1 wt% H_2O; 1.2 GPa": Baker et al. (2005).

Comparison of CO_2 and H_2O diffusivities. Comparison between $D_{CO_{2,total}}$, $D_{H_2O_m}$, and $D_{H_2O_t}$ using data and equations summarized above reveal that $D_{H_2O_m}$ is greater than $D_{CO_{2,total}}$, and $D_{H_2O_t}$ is usually greater than $D_{CO_{2,total}}$ (Fig. 15). This is not unexpected since the effective radius of H_2O molecules (1.37 Å, Shannon 1976; Zhang and Xu 1995) is smaller than the effective radius of CO_2 molecules (1.7 Å, Behrens and Zhang 2001; Zhang et al. 2007) that dominates CO_2 diffusion. However, because $D_{CO_{2,total}}$ approaches a non-zero constant but $D_{H_2O_t}$ approaches essentially zero as H_2O_t approaches zero, $D_{CO_{2,total}}$ can become larger than $D_{H_2O_t}$ at magmatic temperatures at $H_2O_t < 0.2$ wt% with this content depending temperature, pressure and anhydrous melt composition. In natural silicate melts, H_2O_t is usually greater than 0.2 wt% and hence $D_{H_2O_t}$ is greater than $D_{CO_{2,total}}$.

The diffusion of the two most important volatile components, H_2O and CO_2, shows similarities and distinctions (Zhang et al. 2007). In both cases, speciation plays a critical role, the neutral species (molecular H_2O or CO_2) is the dominant diffusing species, and the diffusivity of the neutral species increases with H_2O_t. However, there are also major differences. Most importantly, H_2O speciation results in $D_{H_2O_t}$ that depends strongly on H_2O_t (as well as melt composition); while CO_2 speciation results in CO_2 diffusivity that is independent of CO_2 concentration, and more surprisingly, even independent of the anhydrous melt composition, which is a blessing for quantifying CO_2 diffusion.

OXYGEN DIFFUSION

Oxygen is the major constituent and a framework element in silicate melts. Therefore, oxygen diffusivities are essential for characterizing reactions and transport in silicate melts.

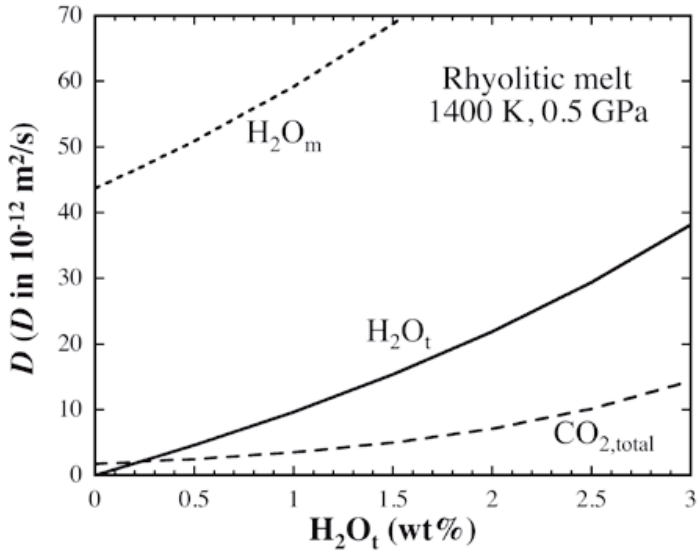

Figure 15. Comparison of H_2O_m, H_2O_t diffusivity and total CO_2 diffusivity at 1400 K and 0.5 GPa. $CO_{2,total}$ diffusivity is from Equation (41), H_2O_m diffusivity in rhyolitic melt is from Equation (14), and H_2O_t diffusivity in rhyolitic melt is calculated from Equations (13), (14), and (7a).

Because oxygen can be present in many different components and species, including molecular H_2O, O_2, CO_2, ionic CO_3^{2-} and OH, as well as oxygen bonded to Si, Ti, Al, Fe, Mg, Ca, Na, K, and P (often simplified as bridging oxygen, non-bridging oxygen and free O^{2-}), oxygen diffusion kinetics can be complicated but may also yield structural information for silicate melts. Hence, oxygen diffusion has been investigated extensively in the geological, materials science, and glass science literature. However, the various reports can be confusing. Some authors investigated chemical (or effective binary) diffusion of various oxygen species and components, and others investigated self-diffusion of oxygen, which is sometimes due to chemical diffusion of H_2O. In earlier studies, bulk exchange and analytical methods often using mass spectrometry are applied; and in more recent studies, profiling methods typically using the ion microprobe are applied. As a general rule, the studies employing profiling techniques provide more reliable data (e.g., Zhang 2008). In addition to studies by geologists, there is also a significant body of glass and materials science literature on oxygen diffusion. Here, we focus on the geological literature.

Geochemists have investigated oxygen diffusion in melts with natural rock compositions as well as mineral or mineral mixture compositions. Dacite, $Di_{58}An_{42}$, $Na_2Si_4O_9$, jadeite and basalt melts have been investigated more systematically. Limited data are available for diopside, CaO-Al_2O_3-SiO_2, nephelinite, andesite, and rhyolite melts. Because diffusion under wet conditions and that under dry conditions have different mechanisms, they are discussed separately. ^{18}O self-diffusion and oxygen chemical diffusion are also discussed separately.

Self-diffusion of oxygen in silicate melts under dry conditions

There is a large literature on oxygen self-diffusion in dry silicate glasses by glass scientists, which is not covered here. Muehlenbachs and Kushiro (1974) were the first in the geological literature to explore self-diffusion of ^{18}O (or ^{18}O-^{16}O exchange diffusion) in various melts at high temperature and room pressure (about 0.1 MPa). Even though the diffusion data turned out to have large errors (see discussion below), the method is introduced below because many other authors used the same or a similar experimental technique. A melt blob suspended from a Pt loop is first equilibrated with a gas (either CO_2 or O_2) of some normal $\delta^{18}O$ in a one-atmosphere furnace. This equilibrated melt is the initial state with known initial $^{18}O/^{16}O$ ratio. Then a gas with a new and constant $\delta^{18}O$ is continuously led into the furnace so that ^{18}O and ^{16}O in the gas exchange with those in the melt blob through diffusion. That is, the experiments investigate

the interdiffusivities between ^{18}O and ^{16}O, which are also oxygen self-diffusivities. After some duration, the sample is quenched and average $\delta^{18}O$ in the whole melt blob is measured by mass spectrometry. The result is compared with the analytical solution for diffusion in a sphere:

$$\frac{M_t}{M_\infty} = 1 - \frac{6}{\pi^2}\sum_{n=1}^{\infty}\frac{1}{n^2}\exp(-\frac{n^2\pi^2 Dt}{r^2}) \tag{42}$$

where M_t and M_∞ are the amount of ^{18}O entering the sphere of radius r at time t and time ∞. The specific equation is often written in the following form:

$$\frac{\delta^{18}O_t - \delta^{18}O_{gas}}{\delta^{18}O_0 - \delta^{18}O_{gas}} = \frac{6}{\pi^2}\sum_{n=1}^{\infty}\frac{1}{n^2}\exp\left(-\frac{n^2\pi^2 Dt}{r^2}\right) \tag{43}$$

where the subscripts 0 and t mean experimental time 0 (i.e., the initial state of equilibration) and time t, and the subscript "gas" means the gas phase. The final $\delta^{18}O$ in the melt is assumed to be the same as that of the gas by treating gas as an infinite reservoir and ignoring isotopic fractionation between the gas and the melt at high experimental temperatures. The above equation is used to fit experimental data of $\delta^{18}O_t$ versus t, from which the diffusivity is extracted.

Muehlenbachs and Kushiro (1974) reported diffusion data in basalt melt (Fig. 16) and the mineral anorthite at room pressure and 1553-1803 K, as well as andesite, rhyolite, and $Di_{40}An_{30}Ab_{30}$ melts (and plagioclase, anorthite, diopside, enstatite, and forsterite minerals) at 1553 K. The diffusivity does not depend on whether the gas phase is O_2 or CO_2. For basalt melt, the activation energy was found to be 377 kJ/mol, which is very high for a melt. Comparison of different melts at 1553 K indicates that ^{18}O diffusivity in basalt melt is highest, followed by andesite melt and $Di_{40}An_{30}Ab_{30}$ melt (about an order of magnitude lower than in basalt), then rhyolite melt (about three orders of magnitude lower than in basalt) (Fig. 16). The mineral data are not of concern here; they will be discussed in another chapter (Farver 2010, this volume).

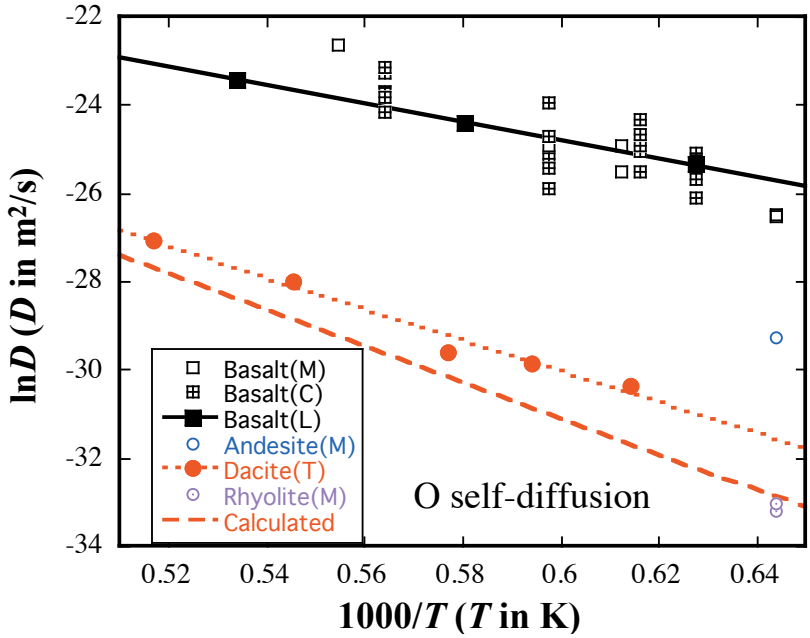

Figure 16. Oxygen self-diffusivity in dry basalt, andesite, dacite and rhyolite melts. Data sources: Basalt(M), Andesite(M) and Rhyolite(M): room pressure data by Muehlenbachs and Kushiro (1974); Basalt(C): room pressure data by Canil and Muehlenbachs (1990); Basalt(L): 1 GPa data by Lesher et al. (1996); Dacite(T): 1 GPa data by Tinker and Lesher (2001). Calculated line is for dacite at room pressure using Equation (44) to compare with the data by Muehlenbachs and Kushiro (1974) and Canil and Muehlenbachs (1990).

Dunn (1982) used the experimental and analytical approach of Muehlenbachs and Kushiro (1974) and investigated ^{18}O diffusion in $Di_{58}An_{42}$, $Di_{40}An_{60}$, and diopside melts at room pressure. Canil and Muehlenbachs (1990) followed with an Fe-rich basalt melt. The activation energy for ^{18}O diffusion in dry basalt was estimated to be about 251 kJ/mol by Canil and Muehlenbachs (1990), much lower than that of Muehlenbachs and Kushiro (1974), but the two data sets are in good agreement (Fig. 16; compare Basalt(M) and Basalt(C)). This comparison shows that activation energy based on limited data is not reliable especially when there is large data scatter. Compared to more recent diffusion data based on the profiling method, these early data based on bulk gain or loss methods show large scatter (2σ error is a factor of 3 in D, or about 1.1 in $\ln D$, Fig. 16) and often do not provide much quantitative constraint in our discussion below on how oxygen diffusivities depend on various parameters.

Major advancements in ^{18}O self-diffusion studies came with the development of the ion microprobe for microscopic measurement of isotopic ratios, although with the requirements of using materials highly enriched in ^{18}O. Coles and Long (1974) and Hofmann et al. (1974) were the first to apply the ion microprobe to study self-diffusion in minerals. Shimizu and Kushiro (1984) were the first to determine ^{18}O self-diffusivities in silicate melts by carrying out diffusion couple experiments and by measuring $^{18}O/^{16}O$ ratios using an ion microprobe. They examined oxygen self-diffusion (^{18}O-^{16}O exchange diffusion) in jadeite and diopside melts. Rubie et al. (1993), Lesher et al. (1996), Liang et al. (1996), Poe et al. (1997), Reid et al. (2001), Tinker and Lesher (2001), and Tinker et al. (2003) followed the approach of Shimizu and Kushiro (1984). Rubie et al. (1993) and Poe et al. (1997) measured oxygen self-diffusivities in dry $Na_2Si_4O_9$ melt at 1898-2800 K and 2.5-15 GPa, as well as in $Na_3AlSi_7O_{17}$ and albite melts. Lesher et al. (1996) determined oxygen (and silicon) self-diffusion in dry basalt melt at 1593-1873 K and 1-2 GPa. Liang et al. (1996) examined oxygen (as well as Ca, Al and Si) self-diffusivities in various CaO-Al_2O_3-SiO_2 melts at 1773 K and 1 GPa. Reid et al. (2001) studied oxygen (and silicon) self-diffusion in dry diopside melt at 2073-2573 K and 3-15 GPa. Tinker and Lesher (2001) investigated oxygen (and silicon) self-diffusion in dry dacite melt at 1628-1935 K and 1-5.7 GPa. Tinker et al. (2003) reported oxygen (and silicon) diffusivities in dry $Di_{58}An_{42}$ melt at 1783-2037 K and 1-4 GPa. These new data generally have higher precision, with the possible exception of Reid et al. (2001) (see below). Studies on wet melts are not summarized here and will be discussed in a later section.

The melt that has been most systematically investigated for oxygen self-diffusion is dry dacite even though the number of data points is not extensive (Tinker and Lesher 2001). Figure 17 shows all available experimental data. The data indicate that oxygen self-diffusivity exhibits Arrhenian behavior within the T-P range investigated, and increases with increasing pressure from 1 to 4 GPa and then decreases at pressures above 5 GPa. The decrease of the diffusivity with pressure at ≥ 5 GPa may have structural implications, such as possible end of the formation of highly coordinated Si or Al species (Tinker and Lesher 2001). For the purpose of predicting oxygen self-diffusion in dacite melt, there are not enough data at ≥ 5 GPa to constrain the relation. Hence, the data at 1628 to 1935 K and 1 to 4 GPa are fit to obtain the following expression for the self-diffusivity of oxygen in dry dacite melt:

$$\ln D_{^{18}O}^{\text{dacite melt}} = -\left(6.57 + 2.148P\right) - \frac{40830 - 5223P}{T} \tag{44}$$

where T is in K and P is in GPa. The activation energy decreases with pressure as $(339 - 43P)$ kJ/mol. The activation volume is $-RT\partial(\ln D)/\partial P = -(43.4 - 0.018T)\times10^{-6}$ m^3/mol, a fairly large negative activation volume, in contrast with the positive activation volumes for H_2O and CO_2 diffusion. The maximum error by Equation (44) to reproduce the experimental data at 1500-1950 K and ≤ 4 GPa is 0.32 in terms of $\ln D$. Equation (44) cannot be extrapolated at all to $P >$ 4 GPa because the linearity between $\ln D$ and P does not hold at higher pressures.

Oxygen self-diffusion in dry $Di_{58}An_{42}$ melt has also been examined systematically (Dunn 1982; Tinker et al. 2003). Figure 18 shows all the available data. It can be seen that the data by Dunn (1982) at room pressure are scattered and do not provide much constraint. The $Di_{58}An_{42}$ melt is often treated as a basalt-like melt or an FeO-free basalt. However, when oxygen self-diffusivities in dry basalt (solid diamonds and a single plus in Fig. 18) are compared with those in dry $Di_{58}An_{42}$, those in basalt are greater by about 1.2 ln$D$ units. The diffusivity data on $Di_{58}An_{42}$ melt by Tinker et al. (2003) at 1738 to 2037 K and 1 to 4 GPa can be expressed as:

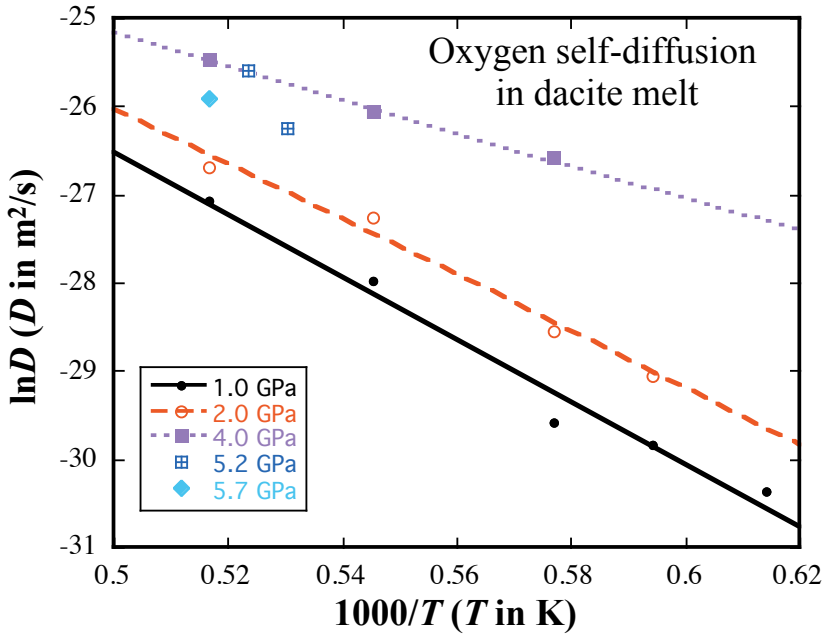

Figure 17. Oxygen self-diffusion data in dacite melt (Tinker and Lesher 2001).

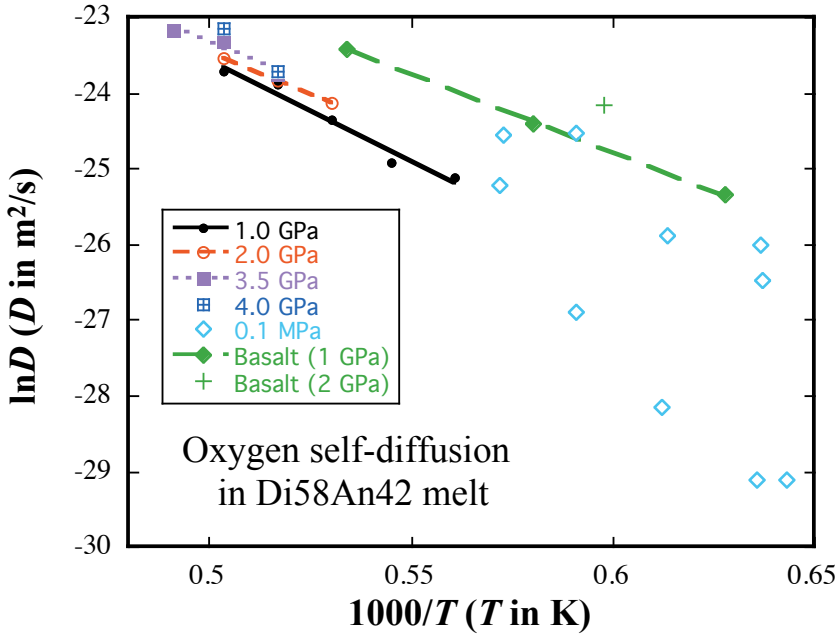

Figure 18. Oxygen self-diffusion data in $Di_{58}An_{42}$ melt compared with those in basalt. Data for $Di_{58}An_{42}$ melt are from Dunn (1982) (0.1 MPa; open diamonds) and Tinker et al. (2003) (1.0, 2.0, 3.5 and 4.0 GPa). Data for basalt are from Lesher et al. (1996).

$$\ln D_{^{18}O}^{Di_{58}An_{42}\ melt} = -10.52 - \frac{26331 - 240P}{T} \quad (45)$$

where T is in K and P is in GPa (adding an additional P term such as that in Equation (44) does not significantly improve the fit). The activation energy is (219 – 2.0P) kJ/mol. The activation volume is $-RT\partial(\ln D)/\partial P = -2.0\times10^{-6}$ m^3/mol, an order of magnitude smaller than that for oxygen diffusion in dacite melt. The maximum error by the above equation to reproduce the data of Tinker et al. (2003) is 0.18 in terms of ln$D$. Extrapolation of the above equation to lower pressures of 0-1 GPa is likely acceptable, but probably not to higher pressures of > 4 GPa.

Rubie et al. (1993) and Poe et al. (1997) studied oxygen self-diffusion in dry $Na_2Si_4O_9$ (or $Na_2O{\cdot}4SiO_2$, NS4) melt. The data (Fig. 19) covering 1893-2800 K and 2.5-15 GPa can be fit by

$$\ln D_{^{18}O}^{Na_2Si_4O_9\ melt} = -17.19 - \frac{12693 - 360P}{T} \quad (46)$$

where D is in m^2/s, T is in K. and P is in GPa. The activation energy is surprisingly low, only about 100 kJ/mol (depending on pressure). The activation volume is negative and small, about -3.0×10^{-6} m^3/mol. The maximum error of the above equation in reproducing the experimental data is 0.22 in terms of ln$D$.

Three papers explored oxygen self-diffusion in dry basalt melt (Muehlenbachs and Kushiro 1974; Canil and Muehlenbachs 1990; Lesher et al. 1996). However, the earlier data by Muehlenbachs and Kushiro (1974) and Canil and Muehlenbachs (1990) are scattered (Fig. 16). Lesher et al. (1996) reported three data points at 1 GPa and one datum at 2 GPa. Oxygen self-diffusivities at 1593-1873 K and 1 GPa (solid squares in Fig. 16) can be represented by the following equation (Lesher et al. 1996):

$$\ln D_{^{18}O}^{basalt\ melt} = -12.5 - \frac{20447}{T} \quad (47)$$

where T is in K and D is in m^2/s. The activation energy is 170 kJ/mol, smaller than those obtained from other ^{18}O diffusion data in basalt melt at room pressure (377 kJ/mol by Muehlenbachs

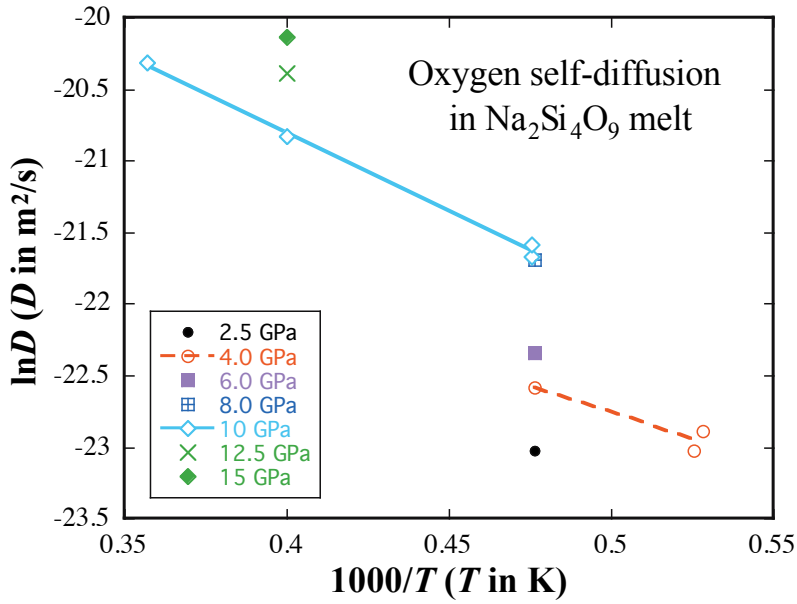

Figure 19. Oxygen self-diffusivity in $Na_2Si_4O_9$ melt with data from Rubie et al. (1993) (with $1000/T > 0.45$) and Poe et al. (1997) (with $1000/T < 0.45$).

and Kushiro 1974, and 251 kJ/mol by Canil and Muehlenbachs 1990). The large difference in activation energy is likely due to data uncertainty rather than being real. Because the activation volume is highly variable from dacite to $Di_{58}An_{42}$ melts (-11×10^{-6} to -2.0×10^{-6} m^3/mol; see also Tinker et al. 2003), it is not possible to use information from other melts to constrain the pressure effect on oxygen diffusivity in basalt.

Three papers investigated oxygen self-diffusion in diopside melt (Dunn 1982; Shimizu and Kushiro 1984; Reid et al. 2001). However, the temperature dependence was not constrained: only at two pressures (0.1 MPa by Dunn 1982 and 3 GPa by Reid et al. 2001) were there diffusion data at different temperatures. The data at 0.1 MPa are scattered and those at 3 GPa are strange in that the diffusivity does not change much from 2073 to 2273 K, with an implied activation energy of only 4 kJ/mol (Fig. 20). An error of a factor of 2.5 on individual D values is needed to allow a more reasonable activation energy of about 250 kJ/mol. Hence, the precision of the oxygen self-diffusion data by Reid et al. (2001) is not high. The reason is not clear.

Shimizu and Kushiro (1984) reported oxygen self-diffusion data in jadeite melt at 1673 to 1883 K at 1.5 GPa, and 0.5 to 2.0 GPa at 1673 K (Fig. 21). The diffusivity at 1.5 GPa can be expressed as:

$$\ln D_{^{18}O}^{\text{jadeite melt}} = -10.84 - \frac{31815}{T} \tag{48}$$

where D is in m^2/s, and T is in K. The activation energy is 265 kJ/mol. At 1673 K, the activation volume is -6.4×10^{-6} m^3/mol. Assuming the activation volume is independent of temperature, the P-T dependence of ^{18}O diffusivity in jadeite melt may be written as:

$$\ln D_{^{18}O}^{\text{jadeite melt}} = -10.84 - \frac{32970 - 770P}{T} \tag{49}$$

where D is in m^2/s, T is in K, and P is in GPa.

Liang et al. (1996) investigated the compositional effect of ^{18}O self-diffusion in various CaO-Al_2O_3-SiO_2 melts at 1773 K and 1 GPa. They found that ^{18}O self-diffusivity increases

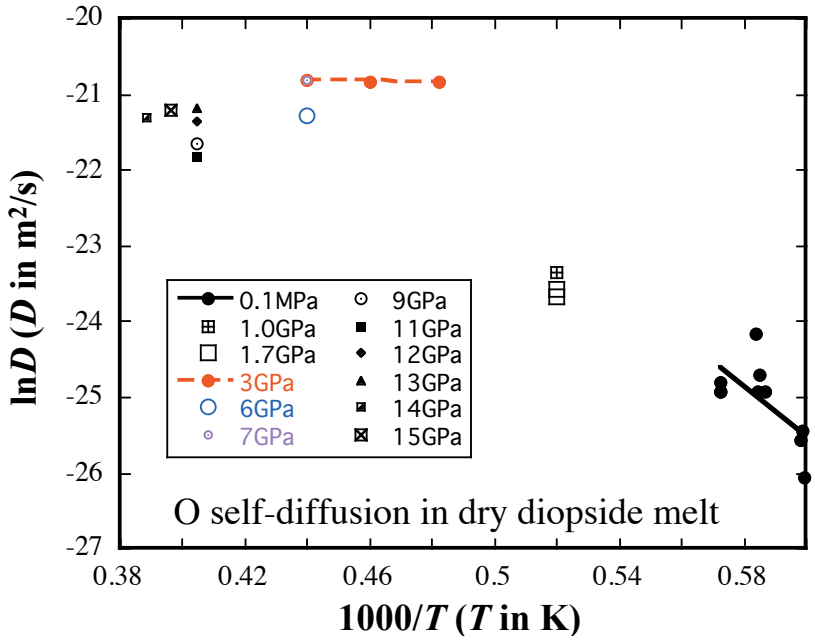

Figure 20. Oxygen self-diffusivities in dry diopside melt. Data sources are: 0.1 MPa from Dunn (1982); 1.0 GPa and 1.7 GPa from Shimizu and Kushiro (1984); and the rest from Reid et al. (2001).

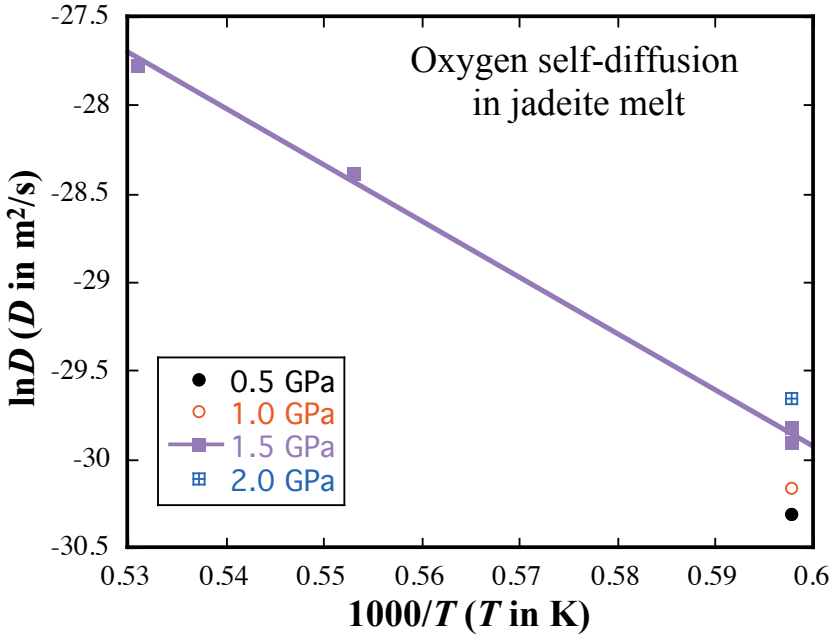

Figure 21. Oxygen self-diffusivities in jadeite melt (Shimizu and Kushiro 1984).

with decreasing silica and alumina content, as expected. As NBO/T increases from 0.3 to about 0.9 in CaO-Al_2O_3-SiO_2 system, ^{18}O self-diffusivity increases by about an order of magnitude.

Figure 22 compares oxygen self-diffusivity in all melts for which the temperature dependence of diffusivity has been determined well at 1 GPa. Oxygen self-diffusivities increase with decreasing SiO_2 and Al_2O_3 contents, or from polymerized to depolymerized melts. From dacite melt (NBO/T ≈ 0.1) to basalt melt (NBO/T ≈ 1), oxygen self-diffusivity increases by two orders of magnitude. It may be inferred that oxygen self-diffusivities depend on oxygen speciation, increasing from bridging oxygen (BO) to non-bridging oxygen (NBO) and then to free oxygen (O^{2-}). The diffusivity of each oxygen species may depend on the overall melt composition.

In terms of oxygen self-diffusion, basalt melt (NBO/T ≈ 1) is similar to diopside melt (NBO/T = 2) and $Na_2Si_4O_9$ melt (NS4 melt, NBO/T = 0.5), whereas dacite melt (NBO/T ≈ 0.1) is similar to jadeite melt (NBO/T = 0) (Fig. 22). But the similarity in each group is not close enough for diffusivities to be merged for a combined fitting. For different melts, there does not seem to be a single compensation temperature where ^{18}O diffusivities in all melts are the same.

There are not enough data yet to contemplate a general relation between oxygen self-diffusivity and natural melt composition under dry conditions. To achieve such a goal, it is necessary to investigate ^{18}O diffusion in dry basalt, dry andesite, and dry rhyolite as a function of temperature and pressure systematically (on par with the investigation of dacite melt), and to examine the compositional dependence. In highly polymerized melts (rhyolite and pure silica), it will be important to make the dry system very dry, e.g., less than 50 ppm H_2O_t (depending on temperature), so that the diffusive flux is due to true ^{18}O self-diffusion, not H_2O chemical diffusion (see later sections). One may try to use self-diffusivities of other elements such as Si to constrain those of oxygen. However, even though self-diffusivities of oxygen and silicon (both are structural elements) in dry melts are often similar (e.g., Lesher et al. 1996; Poe et al. 1997; Tinker et al. 2003), they may also be significantly different (e.g., Tinker and Lesher 2001; see review by Lesher 2010 and Zhang et al. 2010).

It has been shown that oxygen self-diffusivity in dry melts is similar to the Eyring diffusivity defined as $D = kT/(\lambda\eta)$ where λ is the jump distance and η is the melt viscosity (e.g., Shimizu

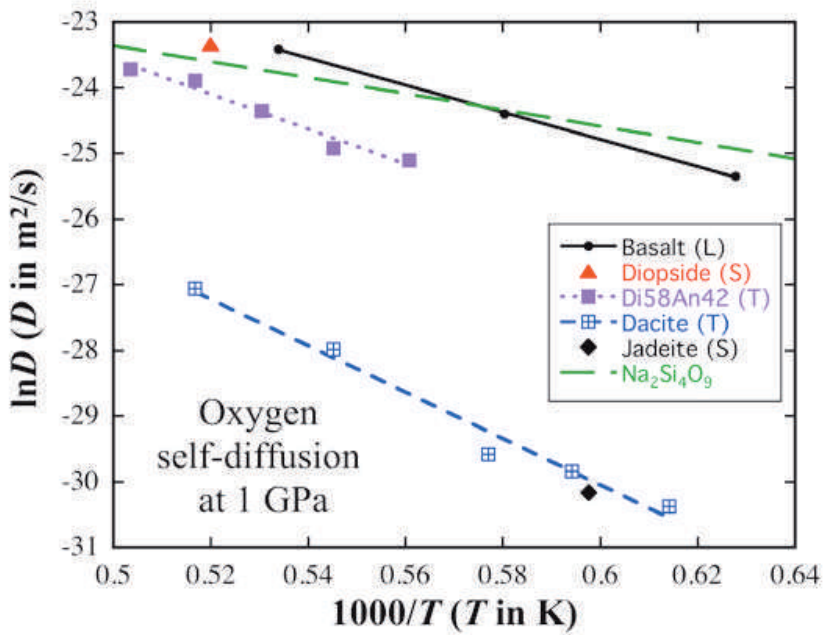

Figure 22. Oxygen self-diffusion data in different melts at 1 GPa. Data sources are: Basalt: Lesher et al. (1996); Diopside and Jadeite: Shimizu and Kushiro (1984); $Di_{58}An_{42}$: Tinker et al. (2003); and Dacite: Tinker and Lesher (2001). The long dashed line is for $Na_2Si_4O_9$ extrapolated using Equation (46).

and Kushiro 1984; Tinker et al. 1994; Fig. 27a in this chapter). Therefore, even though ^{18}O self-diffusion in dry basalt, andesite and rhyolite melts has not been investigated extensively, ^{18}O self-diffusivity in these dry melts may be estimated using the Eyring equation with a jump distance of 2.8×10^{-10} m as long as the melt viscosity can be estimated. In the last 10 years, viscosity models for specific melts have been advanced to high precision (e.g., Zhang et al. 2003 and Hui et al. 2009 for rhyolite melt; Whittington et al. 2009 for dacite melt; Vetere et al. 2006 for andesite melt) and general viscosity models are also available (Hui and Zhang 2007; Giordano et al. 2008) although with larger uncertainties (see Wang et al. 2009 for a comparison of the models of Hui and Zhang 2007 and Giordano et al. 2008). Hence, ^{18}O self-diffusivities in dry melts can now be estimated with a precision similar to the precision of the viscosity models. For hydrous melts, ^{18}O "self" diffusivity is much greater than the Eyring diffusivity, and must be understood and predicted in the context of H_2O diffusion and the role of H_2O in oxygen diffusion (see discussion in a later section).

Chemical diffusion of oxygen under dry conditions

Chemical diffusion of oxygen under dry conditions is not well understood. Dunn (1983) reported oxygen chemical diffusion data in nephelinite, alkali basalt and tholeiite melts at 1553 to 1723 K and 0.4 to 2 GPa. Oxidized spheres of glass with Fe^{3+}/Fe^{2+} ratio of 3.7 to 5.8 were packed with graphite powder in a graphite capsule in piston-cylinder experiments. After an experiment, the spheres were retrieved and average FeO concentration in the bulk sample was determined by wet chemical analyses (the Fe_2O_3 concentration is obtained by difference). Then the diffusivity is estimated using an equation similar to Equation (42). The experimental data of Dunn (1983) on basalt melt are shown in Figure 23. Dunn and Scarfe (1986) used the same approach to obtain diffusivities in an andesite melt at 1623 K and 0.35 to 2 GPa. One possible mechanism for the process in the two reports is as follows: Fe_2O_3 on the surface of the melt sphere reacts with graphite as:

$$2Fe_2O_3(\text{melt}) + C(\text{graphite}) \rightleftharpoons 4FeO(\text{melt}) + CO_2(\text{melt}) \qquad (50)$$

Reduction of 1.1 wt% Fe_2O_3 to produce 1 wt% FeO is accompanied by the production of

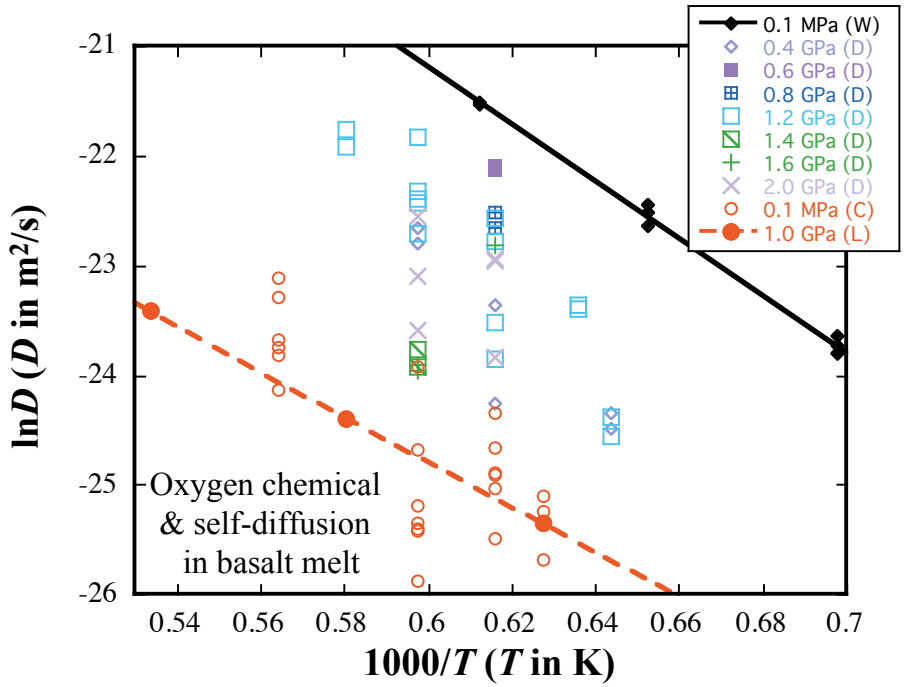

Figure 23. Chemical diffusion and oxygen self-diffusion in basalt melt. Oxygen self-diffusion data (open and solid circles) are: 0.1 MPa (C) from Canil and Muehlenbachs (1990); 1.0 GPa (L) from Lesher et al. (1996). The chemical diffusivities are related to O_2 molecular diffusion or FeO effective binary diffusion (see text for discussion): 0.1 MPa (W) from Wendlandt (1991) based on weight gain (filled diamonds; likely reflecting molecular O_2 diffusion and dehydration), which is about a factor of 30 greater than the self-diffusivities; other data are from Dunn (1983), likely reflecting FeO diffusion.

0.153 wt% CO_2. Then CO_2 and FeO diffuse into the melt, and Fe_2O_3 in the interior of the melt diffuses to the surface of the melt. In this scenario, the chemical diffusivity determined by Dunn (1983) and Dunn and Scarfe (1986) is related to interdiffusion between CO_2+FeO and Fe_2O_3. Data scatter is considerable in these studies.

Wendlandt (1991) reported oxygen chemical diffusion data in basalt and andesite melts at 1433 to 1633 K and 1 atmosphere with controlled oxygen fugacity (Fig. 23). Mass gain or loss of the spherical sample at an imposed oxygen fugacity was monitored by a high precision electrobalance. Diffusivities were obtained by fitting the variation of the total mass with time using Equation (42). The reaction at the surface is likely $2FeO(melt) + (1/2)O_2 \rightleftharpoons Fe_2O_3(melt)$, then FeO and Fe_2O_3 would interdiffuse in the melt. The diffusivity is hence oxygen chemical diffusivity related to FeO and Fe_2O_3. The data precision is high because weight determination is highly reproducible. However, the initial basalt sample contains 1.03 wt% H_2O_t (the initial andesite sample contains 0.44 wt% H_2O). The presence of H_2O in the initial sample may cause two effects:

(1) Oxygen diffusivities may be enhanced due to H_2O diffusion, which can carry oxygen (see next section). Based on H_2O_t diffusivity in basalt (Eqn. 22) and the effect of H_2O diffusion on oxygen diffusion, with 1.0 wt% H_2O_t, the contribution of H_2O diffusion to oxygen self-diffusion would yield a $\ln D_{oxygen}$ of −24.9 at 1633 K, and −25.6 at 1533 K, and −26.5 at 1433 K, which is not enough to account for the high oxygen diffusivities by Wendlandt (1991) (Fig. 23).

(2) Because of the presence of H_2O in the initial sample, there would be simultaneous dehydration as O_2 diffuses in or out of the sample. The effect of dehydration on the weight data was not assessed by Wendlandt (1991). Hence, the accuracy of results in this study is uncertain even though the precision is high.

In summary, the much higher apparent oxygen chemical diffusivity by Wendlandt (1991) might be due to complications that are unaccounted for. Furthermore, even if only the data by Dunn (1983) are considered, the scatter is still considerable, which makes it impossible to infer how chemical oxygen diffusivity depends on pressure, or to infer the activation energy. The large scatter in the data of Dunn (1983), Dunn and Scarfe (1986) and Wendlandt (1991) may be partially related to the use of the bulk mass gain or mass loss method, which is prone to complications. Furthermore, part of the difficulty is likely related to the different meanings of oxygen chemical diffusion (such as molecular O_2 diffusion, or FeO and Fe_2O_3 diffusion, or CO_2 or H_2O diffusion, etc).

"Self" diffusion of oxygen in the presence of H_2O

In experimental studies or natural systems, H_2O is often present: ^{18}O-enriched H_2O may enter the sample of interest from a fluid phase, or H_2O may be initially in the sample. Because H_2O contains oxygen, the transport of H_2O as molecular H_2O (or as OH groups) would result in an oxygen flux. Hence, oxygen diffusivity can be affected or controlled by H_2O diffusion.

The relation between apparent ^{18}O diffusivity in silicate melts and the presence of H_2O vapor (as well as H_2O in the melt) has been explored. DeBerg and Lauder (1980) conducted ^{18}O-^{16}O exchange experiments between melt spheres (composition: 62.2 wt% SiO_2 and 37.2 wt% K_2O prepared under a vacuum of 0.013 Pa) and an ^{18}O-enriched O_2 or H_2O gas, and then extracted ^{18}O diffusivity. At 1175 K, ^{18}O diffusivity does not depend on pressure of O_2 from 7.5 to 56.3 kPa. On the other hand, the presence of 1.3 kPa of H_2O vapor (in addition to 7.5 kPa of O_2) yielded an ^{18}O diffusivity about 2 times the dry ^{18}O diffusivity at 1093 to 1143 K. The solubility of H_2O in this melt is not known. If we assume that the solubility in the potassic silicate melt is roughly the same as that in rhyolite melt (Liu et al. 2005), the solubility at 1.3 kPa of H_2O vapor pressure would be about 0.011 wt% (110 ppm). Hence, the observation by DeBerg and Lauder (1980) would imply that when H_2O_t concentration is of the order 100 ppm, the contribution to ^{18}O flux by H_2O chemical diffusion is about the same as that of dry oxygen diffusion for this potassic silicate melt at about 1100 K. As H_2O partial pressure increases, dissolved H_2O_t in the melt increases, and ^{18}O diffusivity increases. DeBerg and Lauder (1980) concluded that the dissolution and diffusion of O_2 in the melt do not play an important role (due to the small solubility and small diffusivity of O_2 molecules in the melt), but the dissolution and diffusion of H_2O in the melt play a critical role in ^{18}O diffusion in addition to dry ^{18}O diffusion. Pfeffer and Ohring (1981) investigated ^{18}O diffusion in silica in controlled water steam pressure and reached a similar conclusion.

Zhang et al. (1991b) developed the general theory of diffusion of a multi-species component, using the diffusion of H_2O and ^{18}O as specific examples. For ^{18}O diffusion in the presence of H_2O in the sample (either high or low H_2O_t), because both H_2O_m and OH carry an oxygen atom, H_2O diffusion also carries an ^{18}O diffusion flux. Because it has been shown from H_2O diffusion studies that in silicate melts OH diffusion is negligible compared to H_2O_m diffusion under almost all conditions, ^{18}O diffusivity may be viewed as being enhanced by H_2O_m diffusion alone. In such a case, the general equation for ^{18}O diffusion can be written as (Eqn. 6 in Behrens et al. 2007 plus the anhydrous diffusion term):

$$\frac{\partial R_i}{\partial t} = \frac{\partial}{\partial x}\left(D_{^{18}O,\text{anhydrous}} \frac{\partial R_i}{\partial x} \right) + \frac{\partial}{\partial x}\left(D_{H_2O_m} \frac{\partial (R_i \cdot X_m)}{\partial x} \right) - R_i \frac{\partial}{\partial x}\left(D_{H_2O_m} \frac{\partial X_m}{\partial x} \right) \qquad (51)$$

where R_i is the isotopic fraction of ^{18}O, $^{18}O/(^{16}O+^{17}O+^{18}O)$, X_m is the mole fraction of H_2O_m on a single oxygen basis, and $D_{^{18}O,\text{anhydrous}}$ is ^{18}O diffusivity of oxygen species not associated with H in the presence or absence of H_2O. The first term on the right hand side accounts for ^{18}O diffusive flux due to network oxygen diffusion (not associated with H); the second term accounts for ^{18}O diffusive flux due to H_2O_m diffusion; and the third term accounts for mass

balance (so that at constant R_i there is no ^{18}O flux, meaning that the sum of the second and third terms is zero). $D_{^{18}O,anhydrous}$ is expected to depend on H_2O_t concentration because addition of H_2O would loosen the melt structure, which would likely cause a higher diffusivity of even anhydrous oxygen species, such as those bonded to Si and Mg. Based on the above equation, ^{18}O diffusivity can often be estimated as (from Eqn. 15 in Zhang et al. 1991b by removing the OH term):

$$D_{^{18}O} \approx D_{^{18}O,anhydrous} + D_{H_2O_m} X_m \tag{52}$$

The $D_{H_2O_m}X_m$ term in the above equation is the apparent ^{18}O "self" diffusivity contributed by H_2O diffusion. Using the relation between $D_{H_2O_m}$ and $D_{H_2O_t}$ (Eqn. 13), the above can be written as:

$$D_{^{18}O} \approx D_{^{18}O,anhydrous} + D_{H_2O_t} X_m \frac{dX}{dX_m} \tag{53}$$

where X is the mole fraction of H_2O_t on a single oxygen basis. The expression $X_m dX/dX_m$ is shown in Figure 3 for $K = 0.5$. At low H_2O_t (e.g., when $X \le 0.01$), the above can be simplified as (Eqn. 16 in Zhang et al. 1991b):

$$D_{^{18}O} \approx D_{^{18}O,anhydrous} + \frac{X}{2} D_{H_2O_t} \tag{54}$$

Zhang et al. (1991b) summarized literature data to evaluate the role of H_2O diffusion in ^{18}O "self" diffusion. Behrens et al. (2007) experimentally investigated $H_2{}^{18}O$ sorption into a rhyolite melt, from which both H_2O_t and ^{18}O diffusion profiles were measured. Their results show that both H_2O_t and ^{18}O profiles indicate the same H_2O_m diffusivity (Fig. 24) under the assumption that H_2O_m is the diffusing species and there is chemical and isotopic equilibrium. Thus, their experimental data confirm that H_2O_m is the diffusing species in both H_2O_t diffusion and ^{18}O "self" diffusion, as well as the quantitative theory of Zhang et al. (1991b) presented above.

In summary, H_2O chemical diffusion (or effective binary diffusion) carries an ^{18}O flux, which contributes to an apparent ^{18}O diffusivity. If the H_2O content is uniform in the sample and there is no chemical diffusion of H_2O (e.g., diffusion couple with similar starting H_2O_t but different $^{18}O/^{16}O$ in the two halves, or sorption of ^{18}O-enriched H_2O into a sample already containing the equilibrium concentration of H_2O), ^{18}O-^{16}O exchange can still be due to the

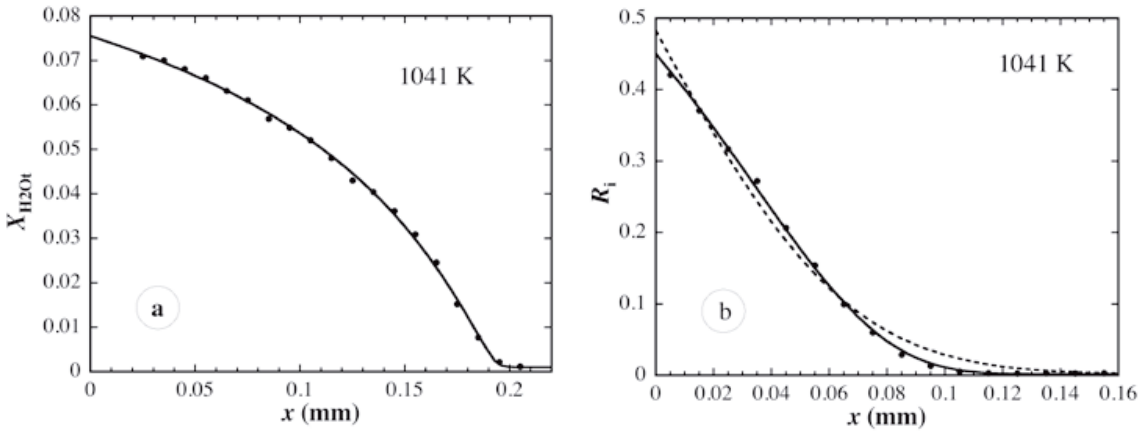

Figure 24. Experimental data on H_2O_t and $R_i = {}^{18}O/({}^{16}O+{}^{17}O+{}^{18}O)$ profiles (data points) during hydration using ^{18}O-enriched H_2O. The solid lines are fit by Equation (11) (for the H_2O_t profile) and Equation (51) (for the R_i profile) assuming H_2O_m is the diffusing species and $D_{H_2O_m} = D_0 e^{aX}$ with the same a and D_0 values for both profiles. From Behrens et al. (2007).

mobility (self-diffusion) of H_2O, and the diffusion may be said to be self-diffusion. In both cases, the diffusing species is H_2O_m. The resulting ^{18}O diffusivities from H_2O chemical diffusion and from H_2O self-diffusion are not much different. In the next section, we examine the conditions for ^{18}O diffusion in natural silicate melts to be true oxygen "self" diffusion or through H_2O diffusion, and quantify apparent ^{18}O diffusivity in hydrous rhyolite and dacite melts.

"Self" diffusion of oxygen in natural silicate melts in natural environments

Using the theory presented above, if we know both the true ^{18}O self-diffusivity under dry conditions and the H_2O diffusivity, we can compare $D_{^{18}O,anhydrous}$ with $D_{H_2O_m}X_m$, or $D_{^{18}O,anhydrous}$ with $D_{H_2O_t}X_m dX/dX_m$, to determine whether the true ^{18}O self-diffusion or the apparent ^{18}O flux due to H_2O diffusion dominates the ^{18}O flux. Below, we employ data on H_2O diffusion and dry ^{18}O self-diffusion to evaluate quantitatively the conditions when H_2O diffusion dominates ^{18}O "self" diffusion.

(1) Dacite melt. This melt is considered first because extensive data are available. Figure 25 compares dry ^{18}O self-diffusivity (Tinker and Lesher 2001) and apparent ^{18}O diffusivity contributed by H_2O diffusion. First consider a numerical case at 1600 K and 1 GPa (which are close to the covered experimental conditions of both ^{18}O self-diffusion and H_2O diffusion). From Equation (44), dry ^{18}O self-diffusivity is 3.5×10^{-14} m^2/s. Based on Equations 18 and 53, about 0.32 wt% H_2O_t is required to contribute 3.5×10^{-14} m^2/s to the oxygen diffusivity. Because synthesized experimental dry melts typically contains only ≤ 0.1 wt% H_2O_t, the experimental dry ^{18}O self-diffusivities at such high temperatures by Tinker and Lesher (2001) are true $D_{^{18}O,anhydrous}$. Now consider 1200 K (a more reasonable magmatic temperature for natural dacite) and 1 GPa. Data by Tinker and Lesher (2001) do not cover such a low temperature (metastable melt). Dry ^{18}O self-diffusivity extrapolated using Equation (44) is 2.1×10^{-17} m^2/s. Based on Equation (18), about 0.05 wt% (500 ppm) H_2O_t is required to contribute 2.1×10^{-17}

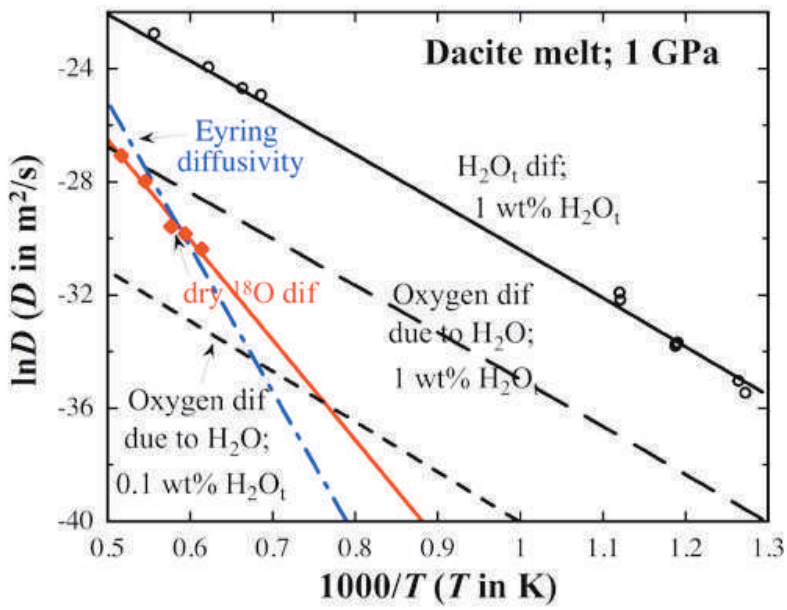

Figure 25. Oxygen and H_2O_t diffusion at 1 GPa in dacite melt. The open circles and the solid line are H_2O_t diffusivity at 0.95 to 1 GPa from Behrens et al. (2004) and Ni et al. (2009b). The two dashed lines are calculated oxygen diffusivities due to H_2O diffusion based on the H_2O diffusivity of Ni et al. (2009b). The filled diamonds (in red in the online version) with a best-fit line (in red in the online version) are experimental ^{18}O self-diffusion data at 1 GPa from Tinker and Lesher (2001). The dotted line is Eyring diffusivity calculated using the viscosity model of Hui and Zhang (2007) at 0.1 MPa to 1 GPa assuming a jumping distance of 2.8×10^{-10} m.

m^2/s to the oxygen diffusivity. The difference at the two temperatures is due to lower activation energy for H_2O diffusion and higher activation energy for dry ^{18}O diffusion. As the temperature is lowered further, H_2O diffusion would dominate the apparent ^{18}O "self" diffusion (Fig. 25) at even lower H_2O_t. Because most natural dacite melts are expected to contain more than 0.2 wt% H_2O_t, we conclude that apparent ^{18}O diffusion in natural dacite melts is almost always dominated by H_2O diffusion.

(2) Basalt melt. Both ^{18}O and H_2O diffusion data are limited on basalt melt. Consider 1600 K and 1 GPa. From Equation (47), dry ^{18}O self-diffusivity is about 1.1×10^{-11} m^2/s. Based on Equation (22), about 1 wt% H_2O_t is necessary to contribute 1.1×10^{-11} m^2/s to apparent ^{18}O diffusivity. That is, for basalt melt, due to high dry ^{18}O self-diffusivity and magmatic temperatures, about 1 wt% H_2O_t is needed for H_2O diffusion to dominate ^{18}O "self" diffusion. Therefore, in almost all mid-ocean ridge basalt melts (typically containing 0.2 to 0.7 wt% H_2O_t, but can be up to 1.2 wt%; Dixon et al. 1988; Michael 1988; Workman et al. 2006) and most ocean island basalt melts (often more volatiles than MORB; Dixon et al. 1997; Hauri 2002; Workman et al. 2006), ^{18}O diffusivity is most likely dominated by true ^{18}O self-diffusion. However, in pre-eruptive island arc basalt (IAB) melts, and even in melt inclusions in mantle megacrysts likely influenced by subduction, H_2O_t concentration are 2-6 wt% (Stolper and Newman 1994; Wang et al. 1999; Newman et al. 2000; Gurenko et al. 2005; Wallace 2005), meaning apparent ^{18}O self-diffusion in these melts is dominated by H_2O diffusion.

(3) Rhyolite melt. There are only limited ^{18}O diffusivity data in dry rhyolite melt at 1553 K and 0.1 MPa (Muehlenbachs and Kushiro 1974) and the quality of the data is not high (see discussion in an earlier section). On the other hand, H_2O diffusion in rhyolite melt has been investigated extensively (e.g., comprehensive model by Ni and Zhang 2008). Figure 26 compares the contribution to ^{18}O diffusion by the H_2O flux with that by true network ^{18}O self-diffusion. Oxygen self-diffusivities by Muehlenbachs and Kushiro (1974) are higher by a factor of about 24 than the Eyring diffusivity for dry melt calculated from the viscosity model of Zhang et al. (2003). If the data by Muehlenbachs and Kushiro (1974) are accurate and the melt was indeed dry (much less than 0.1 wt% H_2O_t), oxygen flux due to chemical diffusion of H_2O when H_2O_t content is about 0.1 wt% would be roughly the same as the oxygen flux due to true oxygen self-diffusion. On one hand, oxygen self-diffusivities obtained by Muehlenbachs and Kushiro (1974) are close to effective binary diffusivity of P, which seems to imply the Eyring diffusivity limit. On the other hand, typical "dry" rhyolite glasses (either natural or synthesized) contain ≥ 0.1 wt% H_2O_t. If the rhyolite used by Muehlenbachs and Kushiro (1974) also contained about 0.1 wt% H_2O_t, their measurements would actually mean apparent ^{18}O "self" diffusivity due to H_2O diffusion, implying true dry ^{18}O self-diffusivities are yet to be determined. Regardless how this issue is resolved, at typical rhyolite melt temperatures (such as 1200 K), H_2O diffusion would dominate oxygen transport at much lower H_2O_t, such as 10 to 100 ppm level. That means, in natural rhyolite melt in which H_2O content if often 4-6 wt% (e.g, Wallace et al. 2003), diffusive transport of oxygen isotopes is through H_2O diffusion.

There are no ^{18}O diffusivity data in dry andesite melts, and hence similar quantitative comparisons cannot be carried out. Nonetheless, it is expected that H_2O diffusion plays a more important role in transporting ^{18}O flux as temperature is lowered and as the melt becomes more silicic. Hence, the behavior of andesite melt is expected to be between that of basalt melt and dacite melt. When H_2O_t is high enough (e.g., ≥ 0.5 wt%), the apparent ^{18}O diffusivity in andesite melt is likely dominated by H_2O diffusion. Because pre-eruptive natural andesite melt often contains ≥ 0.5 wt% H_2O_t, we expect the ^{18}O flux in natural andesite melt to be often dominated by H_2O chemical diffusion. In summary, in nature, true ^{18}O self-diffusion is the diffusion mechanism only for relatively dry basalt melt (such as MORB and OIB).

The realization that diffusive transport of ^{18}O in natural rhyolite and dacite melts is almost always due to H_2O diffusion means it is possible to predict ^{18}O diffusive transport using Equation

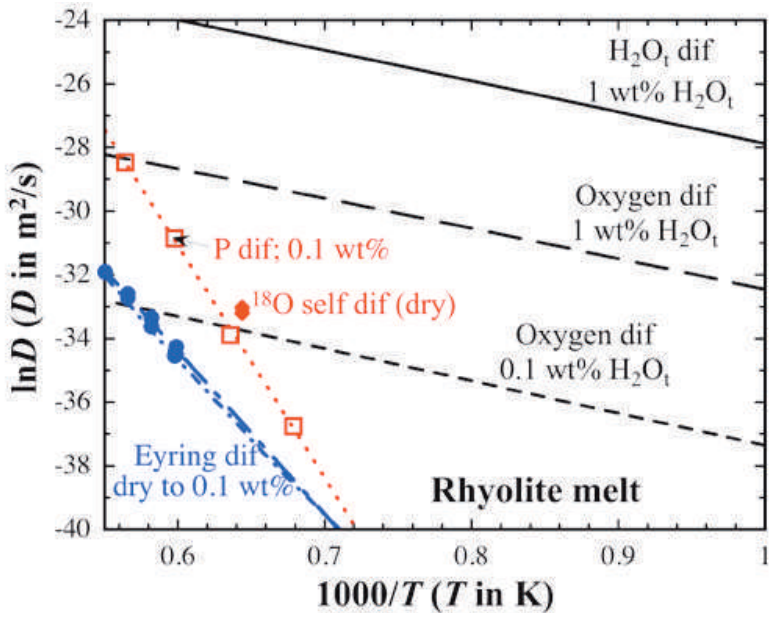

Figure 26. Oxygen and H_2O_t diffusion at 0.1-100 MPa in rhyolite melt. The pressure effect in this small pressure range is smaller than 0.2 ln*D* units. The solid line is the calculated H_2O_t diffusivity. The two dashed lines (roughly parallel to the solid line) are oxygen diffusivities due to H_2O diffusion calculated at 0.1 GPa based on Ni and Zhang (2008). The Eyring diffusivity at 0-0.1 wt% H_2O_t is calculated from viscosity data (solid circles; Neuville et al. 1993; Schulze et al. 1996) and the viscosity model (lines; Zhang et al. 2003) assuming a jumping distance of 2.8×10^{-10} m. The two filled diamonds are experimental ^{18}O self-diffusion data at 0.1 MPa from Muehlenbachs and Kushiro (1974). The open squares and short dashed line are effective binary diffusion data of *P* and fit at 0.8 GPa and 0.1 wt% H_2O_t (Harrison and Watson 1984), which are somewhat higher than the Eyring diffusivity.

(52) or (53) because H_2O diffusion in these melts has already been investigated well (e.g., Behrens et al. 2004; Liu et al. 2004b; Ni and Zhang 2008; Ni et al. 2009b). For the convenience of the readers, calculated apparent ^{18}O diffusivities in hydrous rhyolite and dacite melts as a function of *T*, *P* and H_2O_t are listed in Tables 3 and 4. In the calculation, the diffusivity of oxygen not associated with H is approximated by Eyring diffusivity. The calculated diffusivities have a 2σ uncertainty of about 0.6 in ln*D* and may be applied in rough estimation of diffusion rates. For calculation of the ^{18}O diffusion profile, it is more accurate to use Equation (51). Prediction of ^{18}O diffusion in basalt and andesite melts require more experimental work in terms of both H_2O diffusion and dry ^{18}O diffusion.

Contribution of CO_2 diffusion to ^{18}O transport in CO_2-bearing melts

Because carbon species (CO_2 molecule and CO_3^{2-}) also carry oxygen, oxygen transfer in natural systems may also be realized through the diffusion of these species, especially molecular CO_2. One-atmosphere experiments on ^{18}O diffusion often use ^{18}O-enriched CO_2 gas as the source for ^{18}O (Muehlenbachs and Kushiro 1974; Canil and Muehlenbachs 1990). Not withstanding the quality of such data, one may wonder whether the extracted diffusivity is true ^{18}O self-diffusivity, or just a reflection of CO_2 diffusion carrying ^{18}O into the sample. No simultaneous investigation of ^{18}O and CO_2 diffusion has been carried out yet.

Although experimental data are lacking, the role of CO_2 diffusion in transporting ^{18}O can be treated similarly as the role of H_2O diffusion in transporting ^{18}O. However, it is more convenient to consider total CO_2 diffusion rather than the diffusion of CO_2 molecules because $D_{CO_2,total}$ is roughly independent of melt composition. The diffusion equation for the isotopic fraction of ^{18}O can be written as follows (comparing with Eqn. 51):

Table 3. Calculated $\ln D^{18}_{O}$ (D in m^2/s) in hydrous rhyolite melt.

H_2O_t (wt%)	0.1 GPa			0.5 GPa			1 GPa		
	1000 K	1300 K	1600 K	1000 K	1300 K	1600 K	1000 K	1300 K	1600 K
0.1	−37.36	−35.02	−33.43	−38.06	−35.38	−33.56	−38.93	−35.83	−33.72
0.3	−35.11	−32.78	−31.31	−35.80	−33.14	−31.46	−36.67	−33.59	−31.64
0.5	−34.02	−31.73	−30.28	−34.72	−32.08	−30.43	−35.59	−32.53	−30.61
1.0	−32.45	−30.24	−28.86	−33.15	−30.60	−29.01	−34.02	−31.05	−29.19
1.5	−31.43	−29.32	−28.02	−32.13	−29.68	−28.16	−33.00	−30.13	−28.34
2.0	−30.63	−28.63	−27.40	−31.33	−28.99	−27.55	−32.19	−29.44	−27.73
3.0	−29.34	−27.58	−26.51	−30.03	−27.94	−26.66	−30.90	−28.39	−26.84
4.0	−28.26	−26.76	−25.85	−28.95	−27.12	−25.99	−29.82	−27.56	−26.17
5.0				−27.99	−26.42	−25.46	−28.86	−26.86	−25.64
6.0				−27.1	−25.79	−25.00	−27.97	−26.24	−25.18
7.0				−26.26	−25.22	−24.59	−27.13	−25.67	−24.77
8.0				−25.47	−24.69	−24.22	−26.34	−25.14	−24.41

Each cell lists $\ln D^{18}_{O}$ values where D^{18}_{O} is calculated total ^{18}O diffusivity in m^2/s using Equation (52), with $D_{H_2O_m}$ from Equation (14), K from Equation (7a), and $D^{18}_{O,anhydrous}$ approximated by D_{Eyring} calculated using the viscosity model of Zhang et al. (2003). Values of $\ln D$ at other temperatures can be obtained using the Arrhenius relation.

Table 4. Calculated $\ln D^{18}_{O}$ (D in m^2/s) in hydrous dacite melt.

H_2O_t (wt%)	0.1 GPa			0.5 GPa			1 GPa		
	1000 K	1300 K	1600 K	1000 K	1300 K	1600 K	1000 K	1300 K	1600 K
0.1	−38.62	−34.60	−29.51	−39.21	−34.95	−29.53	−39.95	−35.33	−29.54
0.3	−36.33	−32.47	−28.54	−36.92	−32.86	−28.60	−37.65	−33.31	−28.65
0.5	−35.20	−31.42	−27.91	−35.79	−31.82	−27.99	−36.53	−32.28	−28.07
1.0	−33.54	−29.94	−26.93	−34.13	−30.34	−27.06	−34.87	−30.80	−27.18
1.5	−32.43	−29.02	−26.32	−33.02	−29.43	−26.47	−33.76	−29.90	−26.63
2.0	−31.54	−28.34	−25.87	−32.13	−28.75	−26.05	−32.87	−29.23	−26.22
3.0	−30.08	−27.30	−25.21	−30.67	−27.72	−25.42	−31.40	−28.22	−25.64
4.0	−28.83	−26.48	−24.72	−29.42	−26.91	−24.96	−30.16	−27.42	−25.21
5.0				−28.30	−26.21	−24.59	−29.04	−26.74	−24.86
6.0				−27.25	−25.58	−24.27	−27.99	−26.13	−24.57
7.0				−26.27	−25.01	−23.99	−27.00	−25.56	−24.31
8.0				−25.32	−24.47	−23.74	−26.06	−25.03	−24.07

Each cell lists $\ln D^{18}_{O}$ values where D^{18}_{O} is calculated total ^{18}O diffusivity in m^2/s using Equation (52), with $D_{H_2O_m}$ from Equation (18), K from Equation (7b), and $D^{18}_{O,anhydrous}$ approximated by D_{Eyring} calculated using the viscosity model of Whittington et al. (2009).

$$\frac{\partial R}{\partial t} = D_{^{18}O,noncarbonated}\frac{\partial^2 R}{\partial x^2} + D_{CO_{2,total}}\frac{\partial^2 (R \cdot X_{C_{0.5}O_{total}})}{\partial x^2} - D_{CO_{2,total}} R \frac{\partial^2 X_{C_{0.5}O_{total}}}{\partial x^2} \quad (55)$$

where $X_{C_{0.5}O_{total}}$ is mole fraction of total $C_{0.5}O_{total}$ (each $C_{0.5}O_{total}$ contains a single oxygen and two $C_{0.5}O_{total}$ makes one $CO_{2,total}$) on a single oxygen basis, and $D^{18}_{O,anhydrous}$ is diffusivity of ^{18}O unassociated with carbon. $X_{C_{0.5}O_{total}}$, is calculated as $(C_{cd}/22.005)/[C_{cd}/22.005+(100-C_{cd})/W]$ where C_{cd} is wt% of $CO_{2,total}$ and W is the molar mass of the dry melt on a single oxygen basis (Table 1). $X_{CO_{2,total}}$ may be used instead of $X_{C_{0.5}O_{total}}$, but a factor of 2 would have to be incorporated because each CO_2 molecule carries two oxygen atoms. $D_{CO_{2,total}}$ does not depend on CO_2 concentration or anhydrous melt composition and hence can be taken out of

the differentials. Based on the above equation, the ^{18}O diffusivity can often be estimated as (comparing with Eqn. 52):

$$D_{^{18}O} \approx D_{^{18}O,\text{noncarbonated}} + D_{CO_{2,\text{total}}} X_{C_{0.5}O_{\text{total}}} \quad (56)$$

The $D_{CO_{2,\text{total}}} X_{C_{0.5}O_{\text{total}}}$ term in the above equation is apparent ^{18}O "self" diffusivity contributed by CO_2 diffusion. Because $D_{CO_{2,\text{total}}}$ can be estimated from Equation (41), we examine quantitatively possible contributions by CO_2 to ^{18}O diffusion below.

For rhyolite melt at 1553 K and 0.1 MPa (the condition at which ^{18}O diffusivity was determined in a CO_2 gas by Muehlenbachs and Kushiro 1974), $D_{CO_{2,\text{total}}}$ is 1.2×10^{-11} m^2/s from Equation (41). The measured ^{18}O diffusivity is 4.5×10^{-15} m^2/s. For CO_2 diffusion to contribute to such an ^{18}O diffusivity, a CO_2 concentration of 260 ppm is needed (equivalent to a CO_2 partial pressure of 52 MPa). Typical natural rhyolite does not contain this much CO_2. We hence conclude that in this case, ^{18}O diffusivity is not due to chemical CO_2 diffusion. This is consistent with the similarity of ^{18}O diffusivities in CO_2 gas and in O_2 gas.

For the convenience of readers, contribution to apparent $D_{^{18}O}$ by CO_2 chemical diffusion are calculated and listed in Table 5. Note that this table does not give the apparent $D_{^{18}O}$ values as in Tables 3 and 4 where the dry ^{18}O self-diffusivity has been added or is assessed to be negligible. Table 5 only lists the part of apparent $D_{^{18}O}$ contributed by CO_2 chemical diffusion when the CO_2 concentration is 100 ppm. The 2σ uncertainty in the calculated values is about 1.1 ln$D$ units. For the full apparent ^{18}O diffusivity, the anhydrous and non-carbonated true ^{18}O self-diffusivity and that contributed by CO_2 diffusion must be added. Because $D_{CO_{2,\text{total}}}$ (Equation 41) does not depend on the anhydrous melt composition, Table 5 is roughly applicable to all silicate melts. The contribution to the apparent ^{18}O diffusivity is proportional to $CO_{2,\text{total}}$ concentration (Eqn. 56), which can be used to estimate the contribution to $D_{^{18}O}$ by CO_2 chemical diffusion at other $CO_{2,\text{total}}$ concentrations. Comparing Table 5 with Tables 3 and 4, the contribution by CO_2 chemical diffusion to ^{18}O diffusion at the 100 ppm CO_2 level is not important to dacite melt or rhyolite, with the possible exception of very dry rhyolite melt (≤ 0.2 wt% H_2O_t) at very high temperatures (≥ 1500 K).

Table 5. Calculated ln$D_{^{18}O}$ (D in m^2/s) contributed by CO_2 diffusion at 100 ppm CO_2,total.

H_2O_t (wt%)	0.1 GPa			0.5 GPa			1 GPa		
	1000 K	1300 K	1600 K	1000 K	1300 K	1600 K	1000 K	1300 K	1600 K
0	−39.27	−35.22	−32.69	−40.05	−35.82	−33.17	−41.02	−36.57	−33.78
0.1	−39.19	−35.15	−32.63	−39.95	−35.74	−33.11	−40.91	−36.48	−33.71
0.3	−39.01	−35.02	−32.52	−39.75	−35.59	−32.99	−40.69	−36.31	−33.57
0.5	−38.83	−34.88	−32.41	−39.56	−35.44	−32.86	−40.46	−36.13	−33.43
1.0	−38.39	−34.54	−32.14	−39.06	−35.06	−32.56	−39.9	−35.7	−33.08
1.5	−37.95	−34.2	−31.86	−38.57	−34.68	−32.25	−39.33	−35.27	−32.73
2.0	−37.51	−33.86	−31.59	−38.07	−34.3	−31.94	−38.77	−34.83	−32.37
3.0	−36.63	−33.18	−31.03	−37.08	−33.53	−31.32	−37.64	−33.97	−31.67
4.0	−35.74	−32.51	−30.48	−36.09	−32.77	−30.7	−36.52	−33.1	−30.97
5.0				−35.1	−32.01	−30.08	−35.39	−32.24	−30.26

Each cell lists ln$D_{^{18}O}$ values contributed by CO_2 chemical diffusion with D calculated as $D_{CO_{2,\text{total}}} X_{C_{0.5}O_{\text{total}}}$ at 100 ppm $CO_{2,\text{total}}$ and $D_{CO_{2,\text{total}}}$ from Equation (41). To estimate $D_{^{18}O}$ at other CO_2 concentrations, multiply $D_{^{18}O}$ (not ln$D_{^{18}O}$) by the concentration ratio. For example, for 500 ppm CO_2, multiply $D_{^{18}O}$ values in this table by 5. Add $D_{^{18}O}$ here to $D_{^{18}O}$ in Tables 3 or 4 (do not add ln$D_{^{18}O}$) would give the full $D_{^{18}O}$ in hydrous and carbonated rhyolite and dacite melts.

Oxygen diffusion and viscosity: applicability of the Eyring equation

Oishi et al. (1975) showed that the ^{18}O diffusivity in $4Na_2O{\cdot}3CaO{\cdot}18SiO_2$, $2CaO{\cdot}Al_2O_3{\cdot}2SiO_2$, and $Na_2O{\cdot}4SiO_2$ melts is inversely proportional to melt viscosity. Shimizu and Kushiro (1984) showed that the Eyring equation relates ^{18}O diffusivity well with viscosity for dry diopside and jadeite melts (Fig. 27a). ^{18}O diffusion data in other dry melts (e.g., Liang et al. 1996; Tinker and Lesher 2001; Tinker et al. 2004) also roughly follow the Eyring relation (Fig. 27a) even though in detail there are differences (e.g., Liang et al. 1996; Tinker et al. 2004). Figure 25 shows that the Eyring relation roughly applies to dry dacite melt at 1 GPa (rough agreement between solid diamonds and dotted line). However, Figure 26 indicates either limited experimental ^{18}O diffusion data in dry rhyolite melt do not represent true $D_{^{18}O,anhydrous}$, or the Eyring relation does not apply to dry rhyolite (comparing solid diamonds and solid circles). Overall, available data largely indicate that the Eyring equation is applicable to ^{18}O diffusion in dry silicate melts.

For hydrous silicate melts, the available data indicate that the apparent ^{18}O diffusivity is often orders of magnitude greater than the Eyring diffusivity (or Stokes-Einstein diffusivity or any of the other models of inverse proportionality between diffusivity and viscosity) (Behrens

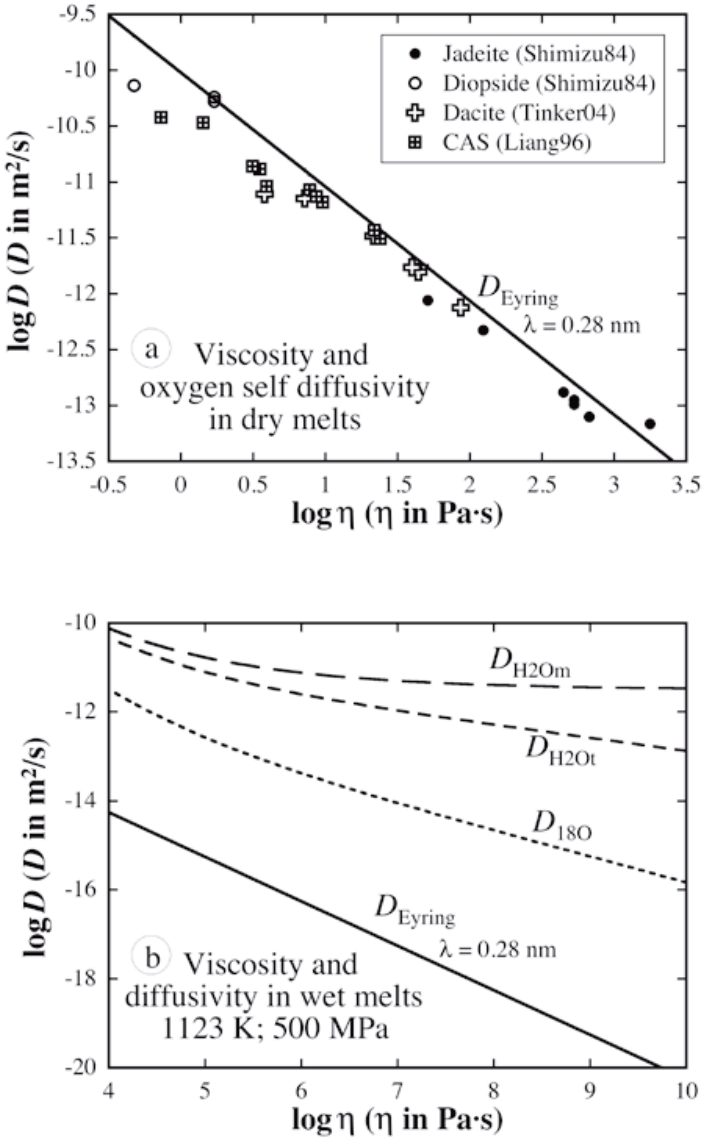

Figure 27. Comparison of the Eyring diffusivity with ^{18}O diffusivity in (a) dry melts, and (b) hydrous rhyolite melts. Note that the scale is base-10 logarithm, not base-e logarithm. Data sources for (a): Shimuzu84 = Shimizu and Kushiro (1984); Tinker04 = Tinker et al. (2004); Liang96 = Liang et al. (1996). Data sources for (b): Viscosity model used for the calculation of rhyolite melt viscosity is from Zhang et al. (2003). H_2O_m, H_2O_t and ^{18}O diffusivities are from Behrens et al. (2007) and Ni and Zhang (2008).

et al. 2007; Fig. 27b). Because natural silicate melts often contain a significant amount of H_2O, the results indicate that the application of the Eyring relation in geological melts is very limited. ^{18}O diffusion in terrestrial silicate melts in natural environments is often dominated by H_2O flux and cannot be predicted by the Eyring equation (but can be predicted from H_2O diffusivities).

The inapplicability of the Eyring equation to ^{18}O diffusion in hydrous silicate melts may be explained as follows. In deriving the Eyring equation, one assumption is that the diffusion and viscous flow are controlled by the same mechanism (motion). For the case of dry silicate melts, viscous flow and diffusion of oxygen (the dominant ion in the melt) are both related to structural mobility, and are hence controlled by the same mechanism. However, for the case of wet silicate melts, viscous flow requires network oxygen mobility, but ^{18}O diffusive flux is carried by the mobility of neutral H_2O_m molecules, whose motion is not necessarily related to network oxygen relaxation. In the context of this explanation, the Eyring equation cannot be applied as a universal relation; it is necessary to know the diffusion mechanism and diffusing species before assessing whether the equation can be applied. Because most natural melts are hydrous, the applicability of the Eyring relation to natural melts is limited.

O_2 DIFFUSION IN PURE SILICA MELT

Dissolved molecular O_2 in silicate melts may also be referred to as physically dissolved oxygen (meaning no reaction between O_2 molecule and other components in the melt or glass because essentially all melts are based on oxygen anions). In natural melts, the oxygen fugacity is low. For example, oxygen fugacity at NNO buffer (about the average oxygen fugacity in typical mantle derived silicate melts), f_{O_2} is only about 3×10^{-7} Pa at 1200 K (calculation based on thermodynamic data of Robie and Hemingway, 1995), lower than that in air by almost 11 orders of magnitude. Therefore, the dissolved O_2 concentration in natural silicate melts is expected to be extremely low. However, in industry and in high-temperature experiments carried out in air or in pure oxygen gas, dissolved O_2 concentration may be noticeable. Under such conditions, pure molecular O_2 diffusion may be studied, and molecular O_2 diffusion may contribute significantly to network oxygen diffusion.

We have shown that oxygen diffusion data in natural or nearly natural silicate melts are complicated, but it is still possible to make sense out of most data in terms of contributions by various oxygen species. Oxygen diffusion data in the glass and materials science literature are even messier (e.g., Fig. 9 in the review by Lamkin et al. 1992), likely due to the contributions by the various oxygen species discussed earlier (especially the hydrous component), plus the additional complexity due to molecular O_2. Because such data are on melts very different from geological silicate melts, they are not the focus in this volume. Hence, we make no attempt to quantitatively explain the complicated behavior of oxygen diffusivity in various silica and silicate melts in the glass and materials science literature. Below, we briefly discuss molecular O_2 diffusion in silica melt for two purposes. First, such data allow us to roughly know the molecular O_2 diffusivity (for the completeness of this volume). Secondly, we may use the O_2 diffusivity to assess the role of molecular O_2 diffusion in oxygen diffusion in natural melts (under oxygen fugacity of terrestrial igneous processes), which turns out to be unimportant due to extremely low oxygen fugacity in natural silicate melts (see below). Molecular diffusion of O_2 in silica melt is best understood compared to other silicate melts due to the simple composition of silica.

Even though there have been numerous studies on oxygen diffusion in silica melt/glass, only a limited number of authors reported genuine molecular O_2 diffusivities. Norton (1961) carried out molecular O_2 permeation experiments in silica glass and obtained molecular O_2 diffusivities at 1223 and 1351 K. Hetherington and Jack (1964) made an order of magnitude estimate of molecular O_2 diffusivities in silica glass, and the values are consistent with the

results of Norton (1961). Susa et al. (1990) reported diffusivities of molecular O_2 in variously prepared silica films at 1073-1273 K. Lamkin et al. (1992) reviewed oxygen diffusion data in silica and silicate glasses. Kajihara et al. (2004, 2005) systematically investigated molecular O_2 diffusion in silica glass with different OH contents. Kajihara et al. (2008) reviewed diffusion and reaction of interstitial oxygen species in silica glass. Molecular O_2 diffusion data in silica glass are shown in Figure 28. Molecular O_2 diffusivity in low-OH silica glass (Kajihara et al. 2004) can be expressed as follows:

$$D_{O_2}^{\text{silica melt}} = \exp\left(-(19.22 \pm 0.39) - \left(\frac{10727 \pm 482}{T}\right)\right) \quad (57)$$

where D is in m^2/s, T is in K and errors are given at the 2σ level. The activation energy for molecular O_2 diffusion is 89±4 kJ/mol, greater than that for Ne diffusion but slightly smaller than that for H_2O_m diffusion. Network oxygen diffusivities (such as ^{18}O diffusivities) in silica melts are 5 to 9 orders of magnitude lower than molecular O_2 diffusivity at 900-1700 K (Fig. 1A in Lamkin et al. 1992) and the activation energy is much higher.

To evaluate the role of molecular O_2 in transporting oxygen in natural silicate melts, we compare $2D_{O_2}[O_2]$ and $D_O[O]$ where O_2 means molecular oxygen and O means network oxygen, and the factor 2 is because each molecular O_2 carries two oxygen atoms. Because molecular O_2 solubility in silica melt is about 10^{-6} mol/m^3 at 1 Pa of O_2 pressure (Norton 1961), the solubility at a typical oxygen fugacity of 10^{-7} Pa in natural silicate melt would be of the order 10^{-13} mol/m^3. The network oxygen concentration in silica melt is about 76560 mol/m^3. Hence the concentration ratio of $2[O_2]/[O]$ is about 3×10^{-18}. Because molecular O_2 diffusivity is no more than 9 orders of magnitude greater than network oxygen diffusivity, at typical oxygen fugacities of natural silicate melts, the ratio of $2D_{O_2}[O_2]$ to $D_O[O]$ is smaller than 3×10^{-9}. Hence, the contribution from molecular oxygen diffusion to oxygen transport is negligible in natural silicate melts. For molecular O_2 to play a significant role in transporting network oxygen, an oxygen fugacity of about 100 Pa or greater is needed.

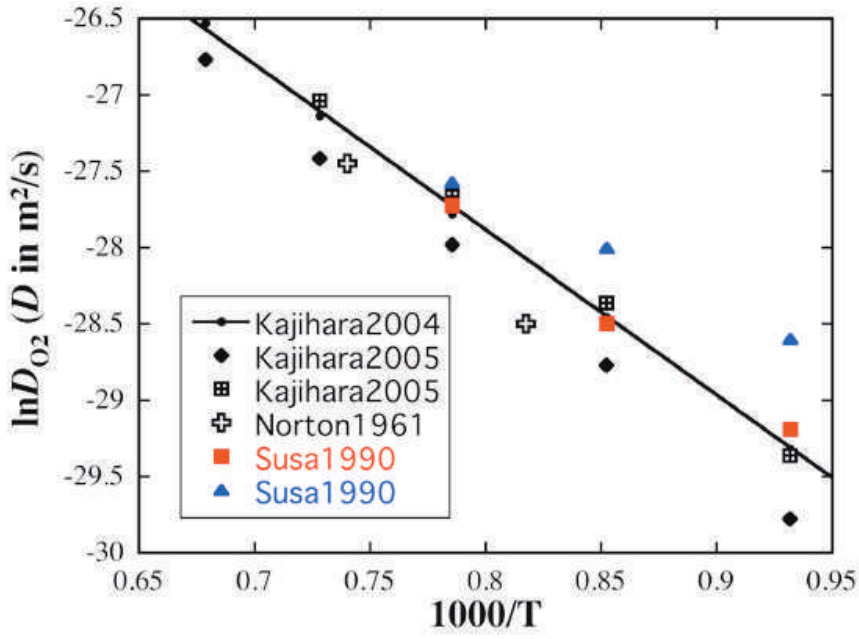

Figure 28. Molecular O_2 diffusivities in silica melts. Susa et al. (1990) and Kajihara et al. (2005) each contain two data sets for slightly different silica melts; these are plotted separately.

SUMMARY AND CONCLUSIONS

Through decades of research, fairly extensive experimental data have been obtained on H_2O, CO_2, and oxygen diffusion in silicate melts. The variation of diffusivities with temperature, pressure, and melt composition (including water content) has led us to fundamental understanding of diffusion mechanisms and melt structure. H_2O diffusion and CO_2 diffusion are both dominated by the diffusion of the respective molecular species. The diffusivity of these two major volatile components increases with temperature and water content, but decreases with pressure. Total CO_2 diffusivity increases exponentially with H_2O_t, whereas H_2O_t diffusivity first increases with H_2O_t proportionally, and then exponentially. While CO_2 diffusivity does not depend much on melt composition except for the H_2O_t concentration, H_2O diffusivity increases with decreasing silica content at superliquidus temperatures, but the trend at intermediate temperatures is less well defined. H_2O diffusivity also increases slightly with increasing alkalinity. H_2O speciation causes proportionality between H_2O_t diffusivity and H_2O_t concentration at low H_2O_t, whereas CO_2 speciation leads to independence of total CO_2 diffusivity on CO_2 concentration, and also causes total CO_2 diffusivity to be independent of the anhydrous melt composition. One complexity that needs to be examined in detail in the future is the possible role of molecular H_2 diffusion in transporting the hydrous component under reducing conditions.

Oxygen chemical diffusivity depends on the specific diffusion mechanisms and more systematic studies are necessary to understand the various chemical oxygen diffusivities. In the presence of H_2O, oxygen "self" diffusion is often controlled by H_2O diffusion. In typical natural silicate melts, especially rhyolite, dacite and andesite melts, ^{18}O diffusion is often carried by H_2O diffusion, and hence can be predicted from experimental H_2O diffusivities that have been well characterized in rhyolite and dacite melts. Predicted ^{18}O diffusivities in hydrous rhyolite and dacite melts are listed in tables and can be many orders of magnitude greater than the Eyring diffusivity. Only in fairly dry basalt melts (such as MORB and OIB), would ^{18}O diffusion occur through true oxygen self-diffusion, in which case the ^{18}O self-diffusivity is not much different from the Eyring diffusivity. ^{18}O flux carried by CO_2 chemical diffusion is also quantitatively evaluated, and the conclusion is that CO_2 diffusion does not significantly enhance ^{18}O diffusion except under very special conditions. The contribution from molecular O_2 diffusion is negligible to network oxygen diffusion under oxygen fugacity encountered in natural silicate melts.

ACKNOWLEDGMENTS

This research is supported by NSF grants EAR-0711050 and EAR-0838127 and NASA grant NNX10AH74G. Huaiwei Ni acknowledges financial support by the visitors program of Bayerisches Geoinstitut. We thank Don Baker and an anonymous reviewer for careful and constructive reviews, and Harald Behrens and Daniele Cherniak for comments.

REFERENCES

Acocella J, Tomozawa M, Watson EB (1984) The nature of dissolved water in sodium silicate glasses and its effect on various properties. J Non-Cryst Solids 65:355-372

Anovitz LM, Elam JM, Riciputi LR, and Cole DR (2004) Isothermal time-series determination of the rate of diffusion of water in Pachuca obsidian. Archaemetry 46:301-326

Anovitz LM, Ricuputi LR, Cole DR, Fayek M, Elam JM (2006) Obsidian hydration: a new paleothermometer. Geology 34:517-520

Anovitz LM, Cole DR, Fayek M (2008) Mechanisms of rhyolitic glass hydration below the glass transition. Am Mineral 93:1166-1178

Baker DR, Freda C, Brooker RA, Scarlato P (2005) Volatile diffusion in silicate melts and its effects on melt inclusions. Ann Geophys 48:699-717

Barrer RM (1941) Diffusion in and through solids. Cambridge Univ Press Cambridge.

Behrens H (2006) Water diffusion in silicate glasses and melts. Adv Sci Tech 46:79-88

Behrens H (2010) Noble gas diffusion in silicate glasses and melts. Rev Mineral Geochem 72:227-267
Behrens H, Nowak M (2003) Quantification of H_2O speciation in silicate glasses and melts by IR spectroscopy – *in situ* versus quench techniques. Phase Transit 76:45-61
Behrens H, Yamashita S (2008) Water speciation in hydrous sodium tetrasilicate and hexasilicate melts: constraints from high temperature NIR spectroscopy. Chem Geol 256:306-315
Behrens H, Zhang Y (2001) Ar diffusion in hydrous silicic melts: implications for volatile diffusion mechanisms and fractionation. Earth Planet Sci Lett 192:363-376
Behrens H, Zhang Y (2009) H_2O diffusion in peralkaline to peraluminous rhyolitic melts. Contrib Mineral Pertrol 157:765-780
Behrens H, Zhang Y, Leschik M, Miedenbeck M, Heide G, Frischat GH (2007) Molecular H_2O as carrier for oxygen diffusion in hydrous silicate melts. Earth Planet Sci Lett 254:69-76
Behrens H, Zhang Y, Xu Z (2004) H_2O diffusion in dacitic and andesitic melts. Geochim Cosmochim Acta 68:5139-5150
Blank JG (1993) An experimental investigation of the behavior of carbon dioxide in rhyolitic melt. PhD Dissertation. California Institute of Technology, Pasadena
Blank JG, Brooker RA (1994) Experimental studies of carbon dioxide in silicate melts: solubility, speciation, and stable carbon isotope behavior. Rev Mineral 30:157-186
Botcharnikov RE, Behrens H, Holtz F (2006) Solubility and speciation of C-O-H fluids in andesitic melt at T=1100-1300°C and P=200 and 500 MPa. Chem Geol 229:125-143
Bottinga Y, Javoy M (1990) MORB degassing: Bubble growth and ascent. Chem Geol 81:255-270
Burn I, Roberts JP (1970) Influence of hydroxyl content on the diffusion of water in silica glass. Phys Chem Glasses 11:106-114
Canil D, Muehlenbachs K (1990) Oxygen diffusion in an Fe-rich basalt melt. Geochim Cosmochim Acta 54:2947-2951
Carmichael ISE, Ghiorso MS (1990) The effect of oxygen fugacity on the redox state of natural liquids and their crystallizing phases. Rev Mineral 24:191-212
Chekhmir AS, Persikov ES, Epel'baum MB, Bukhtiyarov PG (1985) Hydrogen transport through a model magma. Geochem Int 22(8):61-65
Chen Y, Zhang Y (2008) Olivine dissolution in basaltic melt. Geochim Cosmochim Acta 72:4756-4777
Chen Y, Zhang Y (2009) Clinopyroxene dissolution in basaltic melt. Geochim Cosmochim Acta 73:5730-5747
Cherniak DJ, Hervig R, Koepke J, Zhang Y, Zhao D (2010) Analytical methods in diffusion studies. Rev Mineral Geochem 72:107-169
Cockram DR, Haider Z, Roberts GJ (1969) The diffusion of "water" in soda-lime glass within and near the transformation range. Phys Chem Glasses 10:18-22
Cole DR, Chakraborty S (2001) Rates and mechanisms of isotopic exchange. Rev Mineral Geochem 43:83-223
Coles JN, Long JVP (1974) Ion-microprobe study of self-diffusion of Li^+ in lithium-fluoride. Philos Mag 29:457-471
Crank J (1975) The Mathematics of Diffusion. 414 p. Clarendon Press Oxford
De Berg KC, Lauder I (1980) Oxygen tracer diffusion in a potassium silicate glass above the transformation temperature. Phys Chem Glasses 21:106-109
Delaney JR, Karsten JL (1981) Ion microprobe studies of water in silicate melts: concentration-dependent water diffusion in obsidian. Earth Planet Sci Lett 52:191-202
Dingwell DB, Webb SL (1990) Relaxation in silicate melts. Eur J Mineral 2:427-449
Dixon JE, Stolper EM, Delaney JR (1988) Infrared spectroscopic measurements of CO_2 and H_2O in Juan de Fuca Ridge basaltic glasses. Earth Planet Sci Lett 90:87-104
Dixon JE, Clague DA, Wallace PJ, Poreda RJ (1997) Volatiles in alkalic basalts from the North Arch volcanic field, Hawaii: extensive degassing of deep submarine-erupted alkalic series lavas. J Petrol 38:911-939
Doremus RH (1969) The diffusion of water in fused silica. *In:* Reactivity of Solids. Mitchell JW, Devries RC, Roberts RW, Cannon P (eds) Wiley New York, p 667-673
Doremus RH (1973) Glass Science. Wiley New York
Doremus RH (1975) Interdiffusion of hydrogen and alkali ions in a glass surface. J Non-Cryst Solids 19:137-144
Drury T, Roberts JP (1963) Diffusion in silica glass following reaction with tritiated water vapor. Phys Chem Glasses 4:79-90
Dunn T (1982) Oxygen diffusion in three silicate melts along the join diopside-anorthite. Geochim Cosmochim Acta 46:2293-2299
Dunn T (1983) Oxygen chemical diffusion in three basaltic liquids at elevated temperatures and pressures. Geochim Cosmochim Acta 47:1923-1930
Dunn T, Scarfe CM (1986) Variation of the chemical diffusivity of oxygen and viscosity of an andesite melt with pressure at constant temperature. Chem Geol 54:203-215
Ernsberger FM (1980) The role of molecular water in the diffusive transport of protons in glasses. Phys Chem Glasses 21:146-149

Farver JR (2010) Oxygen and hydrogen diffusion in minerals. Rev Mineral Geochem 72:447-507
Fine F, Stolper EM (1985) The speciation of carbon dioxide in sodium aluminosilicate glasses. Contrib Mineral Petrol 91:105-121
Fogel RA, Rutherford MJ (1990) The solubility of carbon dioxide in rhyolitic melts: a quantitative FTIR study. Am Mineral 75:1311-1326
Frank RC, Swets D.E, Lee RW (1961) Diffusion of Ne isotopes in fused quartz. J Chem Phys 35:1451-1459
Freda C, Baker DR, Romano C, Scarlato P (2003) Water diffusion in natural potassic melts. Geol Soc Spec Publ 213:53-62
Friedman I, Long W (1976) Hydration rate of obsidian. Science 191:347-352
Gaillard F, Scaillet B, Pichavant M (2002) Kinetics of iron oxidation-reduction in hydrous silicic melts. Am Mineral 87:829-837
Gaillard F, Schmidt BC, Mackwell S, McCammon C (2003a) Rate of hydrogen-iron redox exchange in silicate melts and glasses. Geochim Cosmochim Acta 67:2427-2441
Gaillard F, Pichavant M, Mackwell S, Champallier R, Scaillet B, McCammon CA (2003b) Chemical transfer during redox exchanges between H_2 and Fe-bearing silicate melts. Am Mineral 88:308-315
Gardner JE, Hilton M, Carroll MR (2000) Bubble growth in highly viscous silicate melts during continuous decompression from high pressure. Geochim Cosmochim Acta 64:1473-1483
Giordano D, Russel JK, Dingwell D (2008) Viscosity of magmatic liquids: a model. Earth Planet Sci Lett 271:123-134
Gurenko AA, Belousov AB, Trumbull RB, Sobolev AV (2005) Explosive basaltic volcanism of the Chikurachki Volcano (Kurile arc, Russia): insight on pre-eruptive magmatic conditions and volatile budget revealed from phenocryst-hosted melt inclusions and groundmass glasses. J Volcanol Geotherm Res 147:203-232
Haller W (1963) Concentration-dependent diffusion coefficient of water in glass. Phys Chem Glasses 4:217-220
Harrison TM, Watson EB (1984) The behavior of apatite during crustal anatexis: equilibrium and kinetic considerations. Geochim Cosmochim Acta 48:1467-1477
Hauri EH (2002) SIMS analysis of volatiles in silicate glasses, 2. isotopes and abundances in Hawaiian melt inclusions. Chem Geol 183:115-141
Hetherington G, Jack KH (1964) The oxidation of vitreous silica. Phys Chem Glasses 5:147-149
Hofmann AW (1974) Strontium diffusion in a basalt melt and implications for Sr isotope geochemistry and geochronology. Carnegie Inst Wash Yearbook 73:935-941
Houser CA, Herman JS, Tsong IST, White WB, Lanford WA (1980) Sodium-hydrogen interdiffusion in sodium silicate glasses. J Non-Cryst Solids 41:89-98
Hui H, Zhang Y (2007) Toward a general viscosity equation for natural anhydrous and hydrous silicate melts. Geochim Cosmochim Acta 71:403-416
Hui H, Zhang Y, Xu Z, Del Gaudio P, Behrens H (2009) Pressure dependnce of viscosity of rhyolitic melts. Geochim Cosmochim Acta 73:3680-3693
Hui H, Zhang Y, Xu Z, Behrens H (2008) Pressure dependence of the speciation of dissolved water in rhyolitic melts. Geochim Cosmochim Acta 72:3229-3240
Ihinger PD, Zhang Y, Stolper EM (1999) The speciation of dissolved water in rhyolitic melt. Geochim Cosmochim Acta 63:3567-3578
International Commission on Radiation Units and Measurements (1984) International Commission on Radiation Units and Measurements (ICRU) Report 37: Stopping Powers for Electrons and Positrons. ICRU, Bethesda, MD
Jambon A (1979) Diffusion of water in a granitic melt: an experimental study. Carnegie Inst Wash Yearbook 78:352-355
Jambon A, Zhang Y, Stolper EM (1992) Experimental dehydration of natural obsidian and estimation of D_{H_2O} at low water contents. Geochim Cosmochim Acta 56:2931-2935
Kajihara K, Kamioka H, Hirano M, Miura T, Skuja L, Hosono H (2005) Interstitial oxygen molecules in amorphous SiO_2. III. measurements of dissolution kinetics, diffusion coefficient, and solubility by infrared photoluminescence. J Appl Phys 98:013529
Kajihara K, Miura T, Kamioka H, Aiba A, Uramoto M, Morimoto Y, Hirano M, Skuja L, Hosono H (2008) Diffusion and relations of interstitial oxygen species in amorphous SiO_2: a review. J Non-Cryst Solids 354:224-232
Kajihara K, Miura T, Kamioka H, Hirano M, Skuja L, Hosono H (2004) Surface dissolution and diffusion of oxygen molecules in SiO_2 glass. J Ceram Soc Japan 112:559-562
Karsten JL, Holloway JR, Delaney JR (1982) Ion microprobe studies of water in silicate melts: temperature-dependent water diffusion in obsidian. Earth Planet Sci Lett 59:420-428
Keppler H, Bagdassarov NS (1993) High-temperature FTIR spectra of H_2O in rhyolite melt to 1300°C. Am Mineral 78:1324-1327
Kohn SC, Dupree R, Smith ME (1989) A multinuclear magnetic resonance study of the structure of hydrous albite glasses. Geochim Cosmochim Acta 53:2925-2935

Lamkin MA, Riley FL, Fordham RJ (1992) Oxygen mobility in silicon dioxide and silicate glasses: a review. J Eur Ceram Soc 10:347-367
Lanford WA, Davis K, Lamarche P, Laursen T, Groleau R, Doremus RH (1979) Hydration of soda-lime glass. J Non-Cryst Solids 33:249-265
Lapham KE, Holloway JR, Delaney JR (1984) Diffusion of H_2O and D_2O in obsidian at elevated temperatures and pressures. J Non-Cryst Solids 67:179-191
Lee RW, Frank RC, Swets DE (1962) Diffusion of hydrogen and deuterium in fused quartz. J Chem Phys 36:1062-1071
Lee RW (1963) Diffusion of hydrogen in natural and synthetic fused quartz. J Chem Phys 38:448-455
Lesher CE (1990) Decoupling of chemical and isotopic exchange during magma mixing. Nature 344:235-237
Lesher CE (1994) Kinetics of Sr and Nd exchange in silicate liquids: theory, experiments, and applications to uphill diffusion, isotopic equilibrium and irreversible mixing of magmas. J Geophys Res 99:9585-9604
Lesher CE, Hervig RL, Tinker D (1996) Self diffusion of network formers (silicon and oxygen) in naturally occurring basaltic liquid. Geochim Cosmochim Acta 60:405-413
Lesher CE (2010) Self-diffusion in silicate melts: theory, observations and applications to magmatic systems. Rev Mineral Geochem 72:269-309
Liang Y, Richter FM, Davis AM, Watson EB (1996) Diffusion in silicate melts: I. Self diffusion in CaO-Al_2O_3-SiO_2 at 1500°C and 1 GPa. Geochim Cosmochim Acta 60:4353-4367
Liu Y (2003) Water in rhyolitic and dacitic melts. Ph.D. dissertation, University of Michigan
Liu Y, Behrens H, Zhang Y (2004a) The speciation of dissolved H_2O in dacitic melt. Am Mineral 89:277-284
Liu Y, Zhang Y (2000) Bubble growth in rhyolitic melt. Earth Planet Sci Lett 181:251-264
Liu Y, Zhang Y, Behrens H (2004b) H_2O diffusion in dacitic melt. Chem Geol 209:327-340
Liu Y, Zhang Y, Behrens H (2005) Solubility of H_2O in rhyolitic melts at low pressures and a new empirical model for mixed H_2O-CO_2 solubility in rhyolitic melts. J Volcanol Geotherm Res 143:219-235
Michael PJ (1988) The concentration, behavior and storage of H_2O in the suboceanic upper mantle: implications for mantle metasomatism. Geochim Cosmochim Acta 52:555-566
Moulson AJ, Roberts JP (1961) Water in silica glass. Trans Faraday Soc 57:1208-1216
Muehlenbachs K, Kushiro I (1974) Oxygen isotope exchange and equilibrium of silicates with CO_2 or O_2. Carnegie Inst Wash Yearbook 73:232-236
Mungall JE (2002) Empirical models relating viscosity and tracer diffusion in magmatic silicate melts. Geochim Cosmochim Acta 66:125-143
Navon O, Lyakhovsky V (1998) Vesiculation processes in silicate magmas. *In:* The Physics of Explosive Volcanic Eruptions, Gilbert JS, Sparks RSJ (eds) Geological Society London, p 27-50
Neuville DR, Courtial P, Dingwell DB, Richet P (1993) Thermodynamic and rheological properties of rhyolite and andesite melts. Contrib Mineral Petrol 113:572-581
Newman S, Stolper EM, Epstein S (1986) Measurement of water in rhyolitic glasses: calibration of an infrared spectroscopic technique. Am Mineral 71:1527-1541
Newman S, Stolper EM, Stern R (2000) H_2O and CO_2 in magmas from the Mariana arc and back arc systems. Geochem Geophys Geosys 1:1999GC000027
Ni H, Behrens H, Zhang Y (2009b) Water diffusion in dacitic melt. Geochim Cosmochim Acta 73:3642-3655
Ni H, Liu Y, Wang L, Zhang Y (2009a) Water speciation and diffusion in haploandesitic melts at 743-873 K and 100 MPa. Geochim Cosmochim Acta 73:3630-3641
Ni H, Zhang Y (2008) H_2O diffusion models in rhyolitic melt with new high pressure data. Chem Geol 250:68-78
Nogami M, Tomozawa M (1984a) Effect of stress on water diffusion in silica glass. J Am Ceram Soc 67:151-154
Nogami M, Tomozawa M (1984b) Diffusion of water in high silica glasses at low temperature. Phys Chem Glasses 25:82-85
Norton FJ (1961) Permeation of gaseous oxygen through vitreous silica. Nature 191:701-701
Nowak M, Behrens H (1995) The speciation of water in haplogranitic glasses and melts determined by *in situ* near infrared spectroscopy. Geochim Cosmochim Acta 59:3445-3450
Nowak M, Behrens H (1997) An experimental investigation on diffusion of water in haplogranitic melts. Contrib Mineral Petrol 126:365-376
Nowak M, Behrens H (2001) Water in rhyolitic magmas: getting a grip on a slippery problem. Earth Planet Sci Lett 184:515-522
Nowak M, Schreen D, Spickenbom K (2004) Argon and CO_2 on the race track in silicate melts: a tool for the development of a CO_2 speciation and diffusion model. Geochim Cosmochim Acta 68:5127-5138
Ohlhorst S, Behrens H, Holtz F, Schmidt BC (2000) Water speciation in aluminosilicate glasses and melts. *In:* Applied Mineralogy in Research, Economy, Technology and Culture. Proc 6th Int Conf Appl Mineral. Rammlmair D, Mederer J, Oberthur TH, Heimannund RB, Pentinghaus H (eds) Balkema, Rotterdam 1:193–196
Oishi Y, Terai R, Ueda H (1975) Oxygen diffusion in liquid silicates and relation to their viscosity. *In:* Mass Transport Phenomena in Ceramics. Cooper A, Heuer A (eds) Plenum, p 297-310

Okumura S, Nakashima S (2004) Water diffusivity in rhyolitic glasses as determined by *in situ* IR spectroscopy. Phys Chem Miner 31:183-189
Okumura S, Nakashima S (2006) Water diffusion in basaltic to dacitic glasses. Chem Geol 227:70-82
Perkins WG, Begeal DR (1971) Diffusion and permeation of He, Ne, Ar, Kr, and D_2 through silicon oxide thin films. J Chem Phys 54:1683-1694
Persikov ES, Newman S, Bukhtiyarov PG, Nekrasov AN, Stolper EM (2010) Experimental study of water diffusion in haplobasaltic and haploandesitic melts. Chem Geol 276:241-256
Pfeffer R, Ohring M (1981) Network oxygen exchange during water diffusion in SiO_2. J Appl Phys 52:777-784
Poe BT, McMillan PF, Rubie DC, Chakraborty S, Yarger J, Diefenbacher J (1997) Silicon and oxygen self-diffusivities in silicate liquids measured to 15 GPa and 2800 K. Science 276:1245-1248
Proussevitch AA, Sahagian DL (1996) Dynamics of coupled diffusive and decompressive bubble growth in magmatic systems. J Geophys Res 101:17447-17455
Proussevitch AA, Sahagian DL (1998) Dynamics and energetics of bubble growth in magmas: analytical formulation and numerical modeling. J Geophys Res 103:18223-18251
Reid JE, Poe BT, Rubie DC, Zotov N, Wiedenbeck M (2001) The self-diffusion of silicon and oxygen in diopside ($CaMgSi_2O_6$) liquid up to 15 GPa. Chem Geol 174:77-86
Riciputi LR, Elam JM, Anovitz LM, Cole DR (2002) Obsidian diffusion dating by secondary ion mass spectrometry: A test using results from Mound 65, Chalco, Mexico. J Arch Sci 29:1055-1075
Roberts GJ, Roberts JP (1964) Influence of thermal history on the solubility and diffusion of 'water' in silica glass. Phys Chem Glasses 5:26-32
Roberts GJ, Roberts JP (1966) An oxygen tracer investigation of the diffusion of 'water' in silica glass. Phys Chem Glasses 7:82-89
Rubie DC, Ross CR, Carroll MR, Elphick SC (1993) Oxygen self-diffuson in $Na_2Si_2O_9$ liquid up to 10 GPa and estimation of high-pressure melt viscosities. Am Mineral 78:574-582
Robie RA, Hemingway BS (1995) Thermodynamic properties of minerals and related substances at 298.15 K and 1 bar (10^5 Pascals) pressure and at high temperatures. USGS Bulletin, Report 1452
Saal AE, Hauri EH, Cascio ML, Van Orman JA, Rutherford MJ, Cooper RF (2008) Volatile content of lunar volcanic glasses and the presence of water in the Moon's interior. Nature 454:192-196
Schulze F, Behrens H, Holtz F, Roux J, Johannes W (1996) The influence of H_2O on the viscosity of a haplogranitic melt. Am Mineral 81:1155-1165
Shannon RD (1976) Revised effective ionic radii and systematic studies of interatomic distances in halides and chalcogenides. Acta Crystallogr A32:751-767
Shaw HR (1974) Diffusion of H_2O in granitic liquids, I: experimental data; II: mass transfer in magma chambers. *In:* Geochemical Transport and Kinetics. Hofmann AW, Giletti BJ, Yoder HS, Yund RA (eds) Carnegie Inst Wash Publ. 634 Washington, p 139-170
Shackelford JF, Studt PL, Fulrath RM (1972) Solubility of gases in glass. II. He, Ne, and H_2 in fused silica. J Appl Phys 43:1619-1626
Shang LB, Chou IM, Lu WJ, Burruss RC, Zhang Y (2009) Determination of diffusion coefficients of hydrogen in fused silica between 296 and 523 K by Raman spectroscopy and application of fused silica capilaries in studying redox reactions. Geochim Cosmochim Acta 73:5435-5443
Shelby JE (1977) Molecular diffusion and solubility of hydrogen isotopes in vitreous silica. J Appl Phys 48:3387-3394
Shelby JE (1994) Protonic species in vitreous silica. J Non-Cryst Solids 179:138-147
Shelby JE (2008) A limited review of water diffusivity and solubility in glasses and melts. J Am Ceram Soc 91:703-708
Shen A, Keppler H (1995) Infrared spectroscopy of hydrous silicate melts to 1000 °C and 10 kbar: direct observation of H_2O speciation in a diamond-anvil cell. Am Mineral 80:1335-1338
Shimizu N, Kushiro I (1984) Diffusivity of oxygen in jadeite and diopside melts at high pressures. Geochim Cosmochim Acta 48:1295-1303
Sierralta M, Nowak M, Keppler H (2002) The influence of bulk composition on the diffusivity of carbon dioxide in Na aluminosilicate melts. Am Mineral 87:1710-1716
Silver L, Ihinger PD, Stolper EM (1990) The influence of bulk composition on the speciation of water in silicate glasses. Contrib Mineral Petrol 104:142-162
Silver L, Stolper EM (1989) Water in albitic glasses. J Petrol 30:667-709
Smets J, Lommen TPA (1983) The role of molecular water in the leaching of glasses. Phys Chem Glasses 24:35-36
Sowerby JR, Keppler H (1999) Water speciation in rhyolitic melt determined by in-situ infrared spectroscopy. Am Mineral 84:1843-1849
Sparks RSJ, Tait SR, Yanev Y (1999) Dense welding caused by volatile resorption. J Geol Soc 156:217-225
Stanton TR, Holloway JR, Hervig RL, Stolper EM (1985) Isotopic effect on water diffusivity in silicic melts. Eos 66:1131

Stolper EM (1982a) Water in silicate glasses: an infrared spectroscopic study. Contrib Mineral Petrol 81:1-17
Stolper EM (1982b) The speciation of water in silicate melts. Geochim Cosmochim Acta 46:2609-2620
Stolper EM (1989) Temperature dependence of the speciation of water in rhyolitic melts and glasses. Am Mineral 74:1247-1257
Stolper EM, and Newman S (1994) The role of water in the petrogenesis of Mariana Trough magmas. Earth Planet Sci Lett 121:293-325
Susa M, Shinohara H, Nagata K, Goto KS (1990) Diffusion of oxygen molecules in amorphous silica thin films (in Japanese). J Metal Soc Japan 54:193-200
Swets DE, Lee RW, Frank RC (1961) Diffusion coefficients of helium in fused quartz. J Chem Phys 34:17-22
Tinker D, Lesher CE (2001) Self diffusion of Si and O in dacitic liquid at high pressures. Am Mineral 86:1-13
Tinker D, Lesher CE, Baxter GM, Uchida T, Wang Y (2004) High-pressure viscometry of polymerized silicate melts and limitations of the Eyring equation. Am Mineral 89:1701-1708
Tinker D, Lesher CE, Hucheon ID (2003) Self-diffusion of Si and O in diopside-anorthite melt at high pressures. Geochim Cosmochim Acta 67:133-142
Tomozawa M (1985) Concentration dependence of the diffusion coefficient of water in SiO_2 glass. Am Ceram Soc 68:C251-252
Tsong IST, Houser CA, Tong, SSC (1980) Depth profiles of interdiffusing species in hydrated glasses. Phys Chem Glasses 21:197-198
Van der Laan SR, Zhang Y, Kennedy A, Wylie PJ (1994) Comparison of element and isotope diffusion of K and Ca in multicomponent silicate melts. Earth Planet Sci Lett 123:155-166
Vetere F, Behrens H, Holtz F, Neuville DR (2006) Viscosity of andesitic melts - new experimental data and a revised calculation model. Chem Geol 228:233-245
Wallace PJ (2005) Volatiles in subduction zone magmas: concentrations and fluxes based on melt inclusion and volcanic gas data. J Volcanol Geotherm Res 140:217-240
Wallace PJ, Dufek J, Anderson AT, Zhang Y (2003) Cooling rates of Plinian-fall and pyroclastic-flow deposits in the Bishop Tuff: inferences from water speciation in quartz-hosted glass inclusions. Bull Volcanol 65:105-123
Wang L, Essene EJ, Zhang Y (1999) Mineral inclusions in pyrope crystals from Garnet Ridge, Arizona, USA: implications for processes in the upper mantle. Contrib Mineral Petrol 135:164-178
Wang H, Xu Z, Behrens H, Zhang Y (2009) Water diffusion in Mount Changbai peralkaline rhyolitic melt. Contrib Mineral Pertrol 158:471-484
Wang L, Zhang Y, Essene EJ (1996) Diffusion of the hydrous component in pyrope. Am Mineral 81:706-718
Wasserburg GJ (1988) Diffusion of water in silicate melts. J Geol 96:363-367
Watson EB (1991) Diffusion of dissolved CO_2 and Cl in hydrous silicic to intermediate magmas. Geochim Cosmochim Acta 55:1897-1902
Watson EB, Sneeringer MA, Ross A (1982) Diffusion of dissolved carbonate in magmas: experimental results and applications. Earth Planet Sci Lett 61:346-358
Wendlandt RF (1991) Oxygen diffusion in basalt and andesite melts: experimental results and discussion of chemical versus tracer diffusion. Contrib Mineral Pertrol 108:463-471
Whittington AG, Hellwig BM, Behrens H, Joachim B, Stechern A, Vetere F (2009) The viscosity of hydrous dacitic liquids: implications for the rheology of evolving silicic magmas. Bull Volcanol 71:185-199
Withers AC, Behrens H (1999) Temperature-induced changes in the NIR spectra of hydrous albitic and rhyolitic glasses between 300 and 100 K. Phys Chem Minerals 27:119-132
Withers AC, Zhang Y, Behrens H (1999) Reconciliation of experimental results on H_2O speciation in rhyolitic glass using *in situ* and quenching techniques. Earth Planet Sci Lett 173:343-349
Workman RK, Hauri EH, Hart SR, Wang J, Blusztajin J (2006) Volatile and trace elements in basaltic glass from Samoa: implications for water distribution in the mantle. Earth Planet Sci Lett 241:932-951
Zhang Y (1993) A modified effective binary diffusion model. J Geophys Res 98:11901-11920
Zhang Y (1994) Reaction kinetics, geospeedometry, and relaxation theory. Earth Planet Sci Lett 122:373-391
Zhang Y (1999a) A criterion for the fragmentation of bubbly magma based on brittle failure theory. Nature 402:648-650
Zhang Y (1999b) H_2O in rhyolitic glasses and melts: measurement, speciation, solubility, and diffusion. Rev Geophys 37:493-516
Zhang Y (2008) Geochemical Kinetics. Princeton University Press NJ
Zhang Y (2009) Degassing of lunar basalts. Geochim Cosmochim Acta 73:A1514 (abstr)
Zhang Y (2010) Diffusion in minerals and melts: theoretical background. Rev Mineral Geochem 72:5-59
Zhang Y, Behrens H (1998) Resolving the controversy between quenched and *in situ* H_2O speciation in silicate melts and glasses. Eos Abstr 79:W123-W124
Zhang Y, Behrens H (2000) H_2O diffusion in rhyolitic melts and glasses. Chem Geol 169:243-262
Zhang Y, Belcher R, Ihinger PD, Wang L, Xu Z, Newman S (1997a) New calibration of infrared measurement of water in rhyolitic glasses. Geochim Cosmochim Acta 61:3089-3100

Zhang Y, Jenkins J, Xu Z (1997b) Kinetics of the reaction $H_2O + O = 2OH$ in rhyolitic glasses upon cooling: geospeedometry and comparison with glass transition. Geochim Cosmochim Acta 61:2167-2173

Zhang Y, Stolper EM (1991) Water diffusion in basaltic melts. Nature 351:306-309

Zhang Y, Stolper EM, Ihinger PD (1995) Kinetics of reaction $H_2O + O = 2OH$ in rhyolitic glasses: preliminary results. Am Mineral 80:593-612

Zhang Y, Stolper EM, Wasserburg GJ (1991a) Diffusion of water in rhyolitic glasses. Geochim Cosmochim Acta 55:441-456

Zhang Y, Stolper EM, Wasserburg GJ (1991b) Diffusion of a multi-species component and its role in the diffusion of water and oxygen in silicates. Earth Planet Sci Lett 103:228-240

Zhang Y, Xu Z (1995) Atomic radii of noble gas elements in condensed phases. Am Mineral 80:670-675

Zhang Y, Xu Z, Behrens H (2000) Hydrous species geospeedometer in rhyolite: improved calibration and application. Geochim Cosmochim Acta 64:3347-3355

Zhang Y, Xu Z, Liu Y (2003) Viscosity of hydrous rhyolitic melts inferred from kinetic experiments, and a new viscosity model. Am Mineral 88:1741-1752

Zhang Y, Xu Z, Zhu M, Wang H (2007) Silicate melt properties and volcanic eruptions. Rev Geophys 45:RG4004, doi:10.1029/2006RG000216

Zhang Y, Ni H, Chen Y (2010) Diffusion data in silicate melts. Rev Mineral Geochem 72:311-408